NASA Technical Paper 3104

October 1991

Annoyance Caused by Advanced Turboprop Aircraft Flyover Noise

Comparison of Different Propeller Configurations

David A. McCurdy

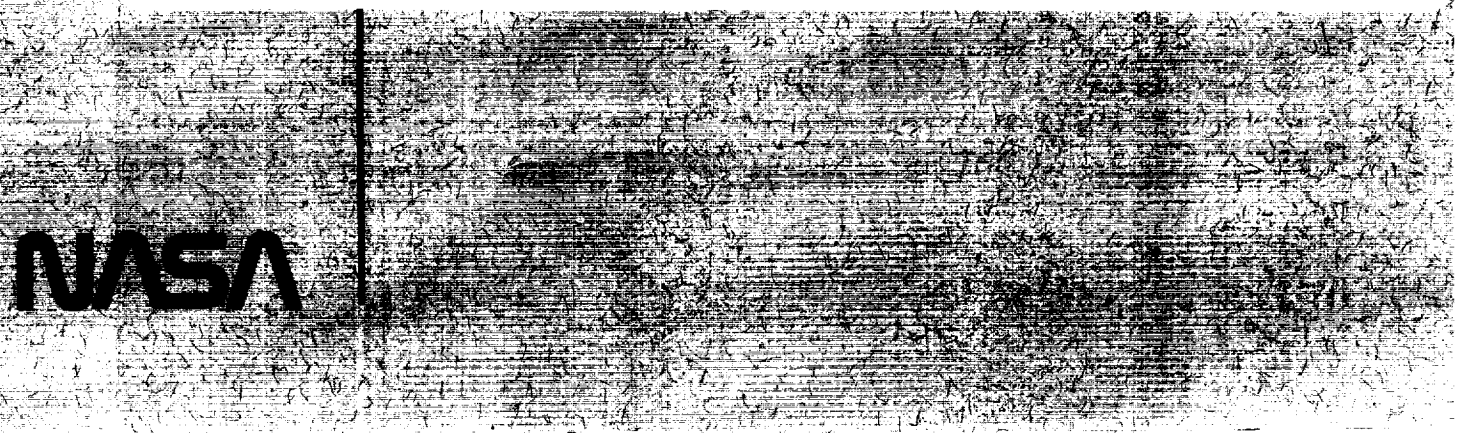

NASA Technical Paper 3104

1991

Annoyance Caused by Advanced Turboprop Aircraft Flyover Noise

Comparison of Different Propeller Configurations

David A. McCurdy
Langley Research Center
Hampton, Virginia

National Aeronautics and Space Administration
Office of Management
Scientific and Technical Information Program

Summary

A laboratory experiment was conducted to quantify the annoyance response of people to the flyover noise of advanced turboprop aircraft having different propeller configurations. The propeller configurations were single-rotating, counter-rotating with an equal number of blades, and counter-rotating with an unequal number of blades. The specific objectives were to (1) compare annoyance responses to the distinctive noises produced by the three propeller configurations of advanced turboprop aircraft, (2) compare annoyance responses to the advanced turboprop aircraft with annoyance responses to conventional turboprop and turbofan aircraft, (3) determine the effects on annoyance of fundamental frequency (blade passage frequency) and tone-to-broadband noise ratio, and (4) determine the ability of aircraft noise measurement procedures and corrections to predict annoyance. Analyses of the data obtained from the experiment are presented in this report.

A computer synthesis system was used to generate 40 realistic, time-varying simulations of advanced turboprop takeoff noise. Of the 40 noises, 8 represented single-rotating propeller configurations, 12 represented counter-rotating propeller configurations with an equal number of blades on each rotor, and 20 represented counter-rotating propeller configurations with an unequal number of blades on each rotor. In the experiment, 64 subjects judged the annoyance of the synthesized advanced turboprop takeoffs along with recordings of 5 conventional turboprop takeoffs and 5 conventional turbofan takeoffs. Each of the noises was presented at three sound pressure levels to the subjects in an anechoic listening room.

Analyses of the judgments found that advanced turboprops with single-rotating propellers were, on average, slightly less annoying than the other aircraft. Fundamental frequency and tone-to-broadband noise ratio affected annoyance response to advanced turboprops, but the effects varied with propeller configuration and noise metric. The addition of duration corrections and corrections for tones above 500 Hz to the noise measurement procedures improved annoyance prediction ability. Duration-corrected A-weighted sound pressure level, either with or without tone corrections, provided the most accurate annoyance prediction.

Introduction

The return of the propeller to long-haul commercial service may be rapidly approaching in the form of the advanced turboprop aircraft, as illustrated in figures 1 and 2. The advanced turboprop propeller is vastly different from conventional propellers in shape and number of blades. Also, it will most likely be a counter-rotating propeller (CRP) instead of the conventional single-rotating propeller (SRP) configuration found on almost all of today's propeller-driven aircraft. The counter-rotating propeller, shown in figure 3, consists of two rotors (or rows) of blades rotating in opposite directions around the same axis. The number of blades in each rotor can be equal ($n \times n$) or unequal ($n \times m$). The advanced turboprop aircraft offers substantial savings in operating costs through improved energy efficiency. However, such an aircraft will come into general usage only if its noise, which has unique spectral characteristics, especially in the two counter-rotating configurations, meets standards of community acceptability currently applied to existing aircraft. Much research has been directed towards understanding and quantifying the annoyance caused by jet aircraft flyover noise, but relatively little research has been conducted for conventional propeller noise. References 1 and 2 report studies which examined annoyance response to the different configurations of advanced turboprop aircraft one at a time. The present paper extends that work by examining the different configurations within the same experiment. A laboratory experiment was conducted to compare the annoyance responses of people to the flyover noise of advanced turboprop aircraft with different propeller configurations (SRP, $n \times n$ CRP, $n \times m$ CRP), conventional turboprop aircraft, and conventional turbofan aircraft.

The primary concern in quantifying advanced turboprop noise annoyance is the unique spectral characteristics of the noise. In general, propeller noise consists of a number of harmonically related pure tone components which are superimposed on broadband noise, as illustrated in figure 4. The fundamental frequency of these tones, which can dominate the total noise produced by the aircraft, occurs at the propeller blade passage frequency. The frequency envelope shape is described in terms of the sound pressure levels of the harmonics relative to the fundamental. The tone-to-broadband noise ratio is usually described in terms of a difference in level between the fundamental tone and the broadband noise. The fundamental frequency ranges from 50 Hz to about 150 Hz for conventional propeller aircraft. For advanced turboprop aircraft, the fundamental frequency is expected to range from 150 Hz to as high as 300 Hz. Figure 5(a) illustrates the tonal content and frequency envelope shape characteristic of the single-rotating propeller configuration. The

counter-rotating propeller configuration produces a second set of harmonically related pure tone components and a set of interaction pure tone components. For the counter-rotating configuration in which the number of blades on each rotor is equal, the second set of harmonic tones and the interaction tones are produced at the same frequencies as the first set of harmonic tones (assuming both rotors rotate at the same speed). This can affect the frequency envelope shape, as illustrated in figure 5(b). For the counter-rotating configuration in which the number of blades on each rotor is unequal, the second set of harmonic tones occurs at frequencies different from the first set, as shown in figure 5(c). In addition, the interaction tones occur at combinations of the frequencies of the two sets of harmonic tones. Thus the tonal content is increased and the frequency envelope shape affected, as shown in the example presented in figure 5(d). The directivity patterns of interaction tones also differ significantly from those of harmonic tones (refs. 3 and 4), as illustrated in figure 6. (As used in this report, the directivity angle is the angle about the aircraft pitch axis from the upstream flight path (0°) under the aircraft to the downstream flight path (180°).)

The annoyance caused by noise sources with strong tonal components has historically been more difficult to quantify than the annoyance caused by broadband noise (refs. 5–8). The uncertainty in accounting for tonal content is increased in this case because less basic psychoacoustic research has been conducted in the lower frequency ranges of tones from conventional and advanced turboprop propellers than in the higher frequency range of tones from jet aircraft.

The primary objective of the laboratory experiment was to compare the annoyance responses to the distinctive noises produced by the three propeller configurations of advanced turboprop aircraft: single-rotating, counter-rotating with an equal number of blades, and counter-rotating with an unequal number of blades. The second objective was to compare the annoyance responses to the advanced turboprop aircraft noise with the annoyance responses to conventional turboprop and turbofan noises. The experiment also examined effects on annoyance of fundamental (blade passage) frequencies and tone-to-broadband noise ratios. The final objective was to determine the ability of aircraft noise measurement procedures and corrections to predict annoyance response to the combined set of aircraft types.

Noise Metrics, Symbols, and Abbreviations

Noise Metrics

EPNL	effective perceived noise level, dB
L_A	A-weighted sound pressure level, dB
L_D	D-weighted sound pressure level, dB
L_E	E-weighted sound pressure level, dB
L_1	weighted sound pressure level based on modified frequency weighting from reference 9 (see "Acoustic Data Analyses" section), dB
LL	loudness level (Stevens Mark VI procedure), dB
LL_Z	Zwicker loudness level, dB
PL	perceived level (Stevens Mark VII procedure), dB
PNL	perceived noise level, dB
PNL_K, PNL_M, PNL_W	perceived noise level with critical-band corrections (see "Acoustic Data Analyses" section), dB

Detailed descriptions of the noise metrics used in this report can be found in references 9, 10, and 11.

Symbols and Abbreviations

ATP	advanced turboprop
CRP	counter-rotating propeller
F_o	fundamental frequency (blade passage frequency), Hz
F_{oa}	fundamental frequency (blade passage frequency) of aft rotor, Hz
F_{of}	fundamental frequency (blade passage frequency) of forward rotor, Hz
FAR	Federal Aviation Regulation
L_S	subjective noise level, dB
$n \times m$	unequal number of blades in each rotor of a counter-rotating propeller: n blades in forward rotor, m blades in aft rotor

$n \times n$	equal number of blades in each rotor of a counter-rotating propeller: n blades in forward rotor and in aft rotor
p	probability
SPL	sound pressure level, dB
SRP	single-rotating propeller
T_1	EPNL tone correction method (ref. 11)
T_2	tone correction method identical to T_1 except that no corrections are applied for tones below the 500-Hz 1/3-octave band
T/N	tone-to-broadband noise ratio, dB (In this report, the ratio is defined to be the difference between the 1/3-octave-band sound pressure level of the fundamental tone, measured separately, and the sound pressure level of the highest 1/3-octave band of broadband noise. The aft rotor fundamental tone is used for the $n \times m$ CRP propeller configuration.)

Experimental Method

Test Facility

The Anechoic Listening Room of the Langley Acoustics Research Laboratory (fig. 7) was used as the test facility in the experiment. This room, which has a volume of 20 m^3 and an A-weighted ambient noise level of 15 dB, provides an essentially echo-free environment. This eliminates any possibility of standing waves affecting the data. The monophonic recordings of the aircraft noise stimuli were played on a studio-quality tape recorder using a noise reduction system to reduce tape hiss. The noise reduction system provided a nominal 30-dB increase in signal-to-noise ratio and reduced tape hiss to inaudible levels. The stimuli were presented to the subjects using a speaker system consisting of one unit with a usable frequency range of 40 to 10 000 Hz.

Test Subjects

Sixty-four subjects were randomly selected from a pool of local residents with a wide range of socio-economic backgrounds and were paid to participate in the experiment. All test subjects were given audiograms prior to the experiment to verify normal hearing. Table I gives the sex and age data for the subjects.

Noise Stimuli

Advanced turboprop stimuli. A recently developed Aircraft Noise Synthesis System, described in reference 12, was used to generate the advanced turboprop noise stimuli used in this experiment. The computer-based system generates realistic, time-varying, audio simulations of aircraft flyover noise at a specified observer location on the ground. The synthesis takes into account the time-varying aircraft position relative to the observer; specified reference spectra consisting of broadband, narrowband, and pure tone components; directivity patterns; Doppler shift; atmospheric effects; and ground effects. These parameters can be specified and controlled in such a way as to generate stimuli in which certain noise characteristics such as fundamental frequency or duration are independently varied while the remaining characteristics such as broadband content are held constant. The synthesis system was used to generate 40 simulations of advanced turboprop aircraft takeoff noise in which the tonal content was systematically varied to represent several versions of each of the 3 propeller configurations.

The first step in generating the simulations was to define a synthesis system input data set for each of the 40 flyovers. A literature review was conducted to determine typical characteristics of advanced turboprop aircraft and expected ranges of the tonal characteristics (refs. 13–27). Because of testing time constraints, the simulations were limited to one takeoff flight profile, one observer location, one broadband noise spectrum, and one broadband noise directivity pattern. Each of these parameters was the same for each simulation. Aircraft speed was 70 m/sec (Mach number = 0.2). The selected takeoff flight profile resulted in an altitude at closest approach to the observer of 380 m, about the altitude expected at the FAR 36 takeoff noise measurement location (ref. 11). The observer was located on the centerline of the ground track. Since predictions of advanced turboprop broadband noise were not available, the broadband spectral content was based on measurements of an existing, large, turboprop aircraft, the Lockheed P-3. The broadband 1/3-octave spectrum and the broadband directivity pattern are given in figures 8 and 9, respectively.

The 40 simulations of advanced turboprop noise represented 8 SRP, 12 $n \times n$ CRP, and 20 $n \times m$ CRP

configurations. The eight SRP simulations represented a wing-mounted, tractor, single-rotating propeller configuration. The simulations consisted of the factorial combinations of four fundamental frequencies and two tone-to-broadband noise ratios. The tonal components, frequency envelope shape, and tone directivity patterns for each of the SRP simulations were determined using a computer program that calculates the discrete frequency noise of SRP propellers (ref. 28). This information was then used in the synthesis system input data sets. The numbers of blades chosen were 8, 10, and 13. When combined with the assumed rotation speed of 1350 rpm, the blade numbers yielded the following fundamental frequencies: 180, 225, and 292.5 Hz. Based on the results of previous studies, an additional fundamental frequency of 260 Hz was added for a total of four fundamental frequencies (ref. 1). The frequency envelope shape had an approximately linear roll-off rate of 6.2 dB per 100 Hz. Only harmonics below 1000 Hz were included, since the levels of harmonics above 1000 Hz were at least 20 dB below the broadband level at the frequency of the harmonic. The desired tone-to-broadband noise ratios of 15 and 30 dB were obtained by specifying the relative levels of the tonal content and the broadband noise in the synthesis system input data sets. The L_A time history and the 1/3-octave-band spectrum at peak L_A of the highest level presentation of each SRP flyover noise are given in figure 10. The narrowband spectrum of the 30-dB tone-to-broadband noise ratio condition for each fundamental frequency is given in figure 11.

The 12 $n \times m$ CRP simulations represented an aft-mounted, pusher, counter-rotating propeller configuration with an equal number of blades on each rotor. The simulations consisted of the factorial combinations of six fundamental frequencies and two tone-to-broadband noise ratios. The tonal components, frequency envelope shape, and tone directivity patterns for each of the 12 simulations were chosen based on a review of the available literature (refs. 3, 4, and 29–45), since no prediction program was available for CRP propellers. This information was then used in the synthesis system input data sets. The numbers of blades chosen for each rotor were 7, 8, 9, 10, 11, and 12. When combined with the assumed rotation speed of 1350 rpm, the blade numbers yielded the following fundamental frequencies: 157.5, 180, 202.5, 225, 247.5, and 270 Hz. The frequency envelope shape used for the simulations is shown in figure 12. The fundamental and 21 harmonic tones were included in each simulation. The directivity patterns for the fundamental and each harmonic tone are given in figure 13. The desired tone-to-broadband noise ratios of 15 and 30 dB were obtained by specifying the relative levels of the tonal content and the broadband noise in the synthesis system input data sets. The L_A time history and the 1/3-octave-band spectrum at peak L_A of the highest level presentation of each $n \times n$ CRP flyover noise are given in figure 14. The narrowband spectrum of the 30-dB tone-to-broadband noise ratio condition for each fundamental frequency is given in figure 15.

The 20 $n \times m$ CRP simulations represented an aft-mounted, pusher, counter-rotating propeller configuration having a different number of blades on each rotor. The aft rotor had either one or two blades less than the forward rotor. The simulations consisted of the factorial combinations of 10 fundamental frequency pairs and 2 tone-to-broadband noise ratios. As for the $n \times m$ CRP simulations, the tonal components, frequency envelope shape, and tone directivity patterns for each of the 20 simulations were chosen based on a review of the available literature (refs. 3, 4, and 29–45). The blade combinations chosen for the rotors were 8×6, 8×7, 9×7, 9×8, 10×8, 10×9, 11×9, 11×10, 12×10, and 12×11. When combined with the assumed rotation speed of 1350 rpm, the blade numbers yielded the following fundamental frequency combinations: 180×135, 180×157.5, 202.5×157.5, 202.5×180, 225×180, 225×202.5, 247.5×202.5, 247.5×225, 270×225, and 270×247.5 Hz. The frequency envelope shape used for the simulation is shown in figure 16. The frequency envelope shape included the 20 fundamental, harmonic, and interaction tones through the fourth harmonic range and the next 10 highest level tones (all interaction tones) through the ninth harmonic range. The directivity patterns for the fundamentals and each higher tone are given in figure 17. The desired tone-to-broadband noise ratios of 15 and 30 dB were obtained by specifying the relative levels of the tonal content and the broadband noise in the synthesis system input data sets. The L_A time history and the 1/3-octave-band spectrum at peak L_A of the highest level presentation of each $n \times m$ CRP flyover noise are given in figure 18. The narrowband spectrum of the 30-dB tone-to-broadband noise ratio condition for each fundamental frequency combination is given in figure 19.

For each of the 40 input data sets, the synthesis system generated an audio simulation which was recorded on tape. Each of these recordings was presented to the test subjects at peak D-weighted sound pressure levels of 70, 80, and 90 dB. The factorial combinations of 20 sets of fundamental frequencies, 2 tone-to-broadband noise ratios, and 3 levels

resulted in 120 advanced turboprop aircraft flyover noise stimuli.

Conventional turboprop and turbofan stimuli. Recordings of five conventional turboprop aircraft takeoffs and five conventional turbofan aircraft takeoffs were included in the experiment for comparison with the advanced turboprop noise stimuli. The types of aircraft used and some specifications of each are given in table II. The recordings of the turbofan aircraft were made on the extended runway centerline approximately 5000 m from the brake release point. The turboprop aircraft recordings were made at several airports, and the distances from brake release varied. At each location, the turboprop aircraft recordings were made on or near the extended runway centerline. Because of the higher flight profiles and lower source noise levels of the turboprop aircraft, the recording sites for the turboprop aircraft were located closer to the brake release point than those for the turbofan aircraft. Each takeoff was presented to the test subjects at peak D-weighted sound pressure levels of 70, 80, and 90 dB for a total of 15 conventional turboprop noise stimuli and 15 conventional turbofan noise stimuli. The L_A time histories and 1/3-octave-band spectra at peak L_A of the highest level presentations of the conventional turboprop and turbofan takeoffs are given in figure 20.

Other stimuli. Boeing 727 takeoff noise stimuli were included in the experiment as a reference noise for converting subjective responses to subjective decibel levels in the analyses of the experiment. In addition to the three presentations made as part of the conventional turbofan stimuli, the Boeing 727 takeoff recording was also presented at peak L_D levels of 61, 65, 75, 85, 95, and 99 dB. This resulted in a total of nine Boeing 727 stimuli being presented to the test subjects in the experiment. The test subjects were presented a total of 156 stimuli in the experiment.

Experiment Design

Numerical category scaling was chosen as the psychophysical method for the experiment. The choice was made to maximize the number of stimuli that could be judged in the fixed amount of time available. The scale selected was a unipolar, 11-point scale from 0 to 10. The end points of the scale were labeled "EXTREMELY ANNOYING" and "NOT ANNOYING AT ALL." The term "ANNOYING" was defined in the subject instructions as "UNWANTED, OBJECTIONABLE, DISTURBING, OR UNPLEASANT."

For the experiment, the stimuli were divided into two sets of four tapes. The first set of four tapes contained all the stimuli in the experiment. The second set contained the same stimuli as the first but in reverse order. There were 39 stimuli per tape. The stimuli were divided between tapes so that each blade count, tone-to-broadband noise ratio, level, propeller configuration, and/or aircraft type were about equally represented on each tape. The order of the stimuli on the tape was then randomly selected. The orders for each tape are given in table III. A period of approximately 10 sec was provided after each stimulus for the subjects to make and record their judgments. Each tape served as one of four test sessions for the subjects and required approximately 40 min for playback.

The 64 test subjects in the experiment were divided into 32 groups of 2 subjects. The first 4 tapes were presented to 16 groups of subjects, and the second 4 tapes were presented to the other 16 groups of subjects. To prevent subject fatigue and other temporal effects from unduly influencing the results, the order in which the tapes were presented was varied to provide a balanced presentation. Table IV gives the order of presentation used for the tapes.

Procedure

Upon arrival at the laboratory, the subjects were seated in the test facility and each was given a set of instructions and a consent form. Copies of these items are given in the appendix. After reading the instructions and completing the consent form, the subjects were given a brief verbal explanation of the cards used for recording judgments and were asked if they had any questions. Three practice stimuli were then presented to the subjects while the test conductor remained in the test facility. In order for the subjects to gain experience in scoring the sounds, they were instructed to make and record judgments of the practice stimuli. After asking again for any questions about the test, the test conductor issued scoring cards for the first session and left the facility. Then, the first of four test sessions began. After the conclusion of each session, the test conductor reentered the test facility, collected the scoring cards, and issued new scoring cards for the next session. Between the second and third sessions, the subjects were given a 15 min rest period outside the test facility.

Results and Discussions

Acoustic Data Analyses

Each noise stimulus was analyzed to provide 1/3-octave-band sound pressure levels from 20 Hz to 20 kHz for use in computing a selected group of noise metrics. The measurements were made with a

1.27-cm-diameter condenser microphone and a real-time, 1/3-octave analysis system which used digital filtering. The microphone was located at ear level midway between the two seats. No subjects were present during the measurements. A total of 11 noise metrics were computed in the analyses. They included the simple weighting procedures L_A, L_D, L_E, and L_1 and the more complex calculation procedures LL, LL_Z, PL, and PNL. In addition, three types of critical band corrections were applied to PNL.

The noise metric L_1 is based on a modified frequency weighting developed in a study of annoyance response to simulated helicopter rotor noise (ref. 9). That study found that annoyance prediction error was more correlated with the logarithm of the subjectively dominant frequency (approximated by the 1/3-octave-band center frequency with the greatest D-weighted energy) than with impulsiveness measures. Based on this result, a modified frequency weighting was developed which provided improved annoyance prediction when implemented as the L_1 noise metric. For 1/3-octave bands with center frequencies less than or equal to 1000 Hz, the modified frequency weighting falls between the A and D weightings. D-weighting values are used for bands above 1000 Hz. The L_1 metric uses the same energy summation method used for L_A, L_D, and L_E.

The first critical band correction procedure applied to PNL was suggested by Kryter (ref. 46). In this procedure, the increased bandwidths of critical bands below 400 Hz are approximated by groups of 1/3-octave bands. The groups are the bands with the following center frequencies: 315 and 250 Hz; 200, 160, and 125 Hz; and 100, 80, 63, and 50 Hz. Within each group the band levels are summed on an energy basis. The summed band levels are assigned to the band center frequency having the greatest intensity within the group. The PNL calculation procedure then uses these "critical bands" instead of the 1/3-octave bands below 400 Hz. The metric using this procedure is designated as PNL_K in further discussions in this report.

The second critical band correction procedure used the same groups for summing the 1/3-octave bands. The summed band levels, however, were assigned to the band center frequency responsible for the greatest "noy" value within the group before summing. The metric using this procedure is designated as PNL_M.

The third critical band correction procedure also used the same groups of 1/3-octave bands. In this case, the noy values of the 1/3-octave-band levels were added on an energy basis within each group. The resultant noy values for all critical bands were then summed using the PNL procedure. The metric using this procedure is designated as PNL_W.

Six variations of each of the 11 previously described noise metrics were calculated. The first was the peak or maximum level occurring during the flyover noise. Two other variations were calculated by applying two different tone corrections. Three more variations were attained by applying duration corrections to the non-tone-corrected level and the two tone-corrected levels. The duration correction and the first tone correction T_1 are identical to those used in the effective perceived noise level procedure defined in the Federal Aviation Administration FAR 36 regulation (ref. 11). The second tone correction T_2 is identical to the first except that no corrections are applied for tones identified in bands with center frequencies less than 500 Hz.

Subjective Data Analyses

The means (across subjects) of the judgments were calculated for each stimulus in the experiment. In order to obtain a subjective scale with meaningful units of measure, these mean annoyance scores were converted to subjective noise levels L_S having decibel-like properties through the following process. Included in the experiment for the purpose of converting the mean annoyance scores to L_S values were nine presentations of a Boeing 727 takeoff recording. The L_D levels of the nine presentations were 61, 65, 70, 75, 80, 85, 90, 95, and 99 dB. A third-order polynomial regression analysis was performed using data obtained for these nine stimuli. The dependent variable was the calculated PNL, and the independent variable was the mean annoyance score for each of the nine stimuli. Figure 21 presents the data set and the resulting best fit curve. The regression equation was then used to predict the level of the Boeing 727 takeoff noise which would produce the same mean annoyance score as each of the other noise stimuli in the experiment. These levels were then considered as the subjective noise level for each stimulus. Comparisons in previous studies indicate that analyses using subjective noise levels yield the same results as analyses using mean annoyance scores.

Comparison of Noise Metrics

In order to investigate the prediction ability of the noise measurement procedures and corrections, the differences between the subjective noise level L_S and the calculated noise level for each of the six variations of the measurement procedures and corrections were determined for each stimulus. These differences were considered to be the "prediction error" for each

stimulus and noise metric variation. The standard deviation of the prediction errors for each noise metric variation is a measurement of how accurately the variation predicts annoyance. The smaller the standard deviation is, the greater the prediction accuracy. Table V gives the standard deviations of prediction error for each noise metric variation examined for the combined set of 150 advanced turboprop, conventional turboprop, and conventional turbofan stimuli.

It should be noted that, because of interrelationships between the data cases, statistical tests for significance of differences in the standard deviations of prediction error are not straightforward. The following results are based primarily on the consistent trends found in the data. Statistical comparisons of the correlation coefficients between the different noise metrics and the subjective noise level (ref. 47) indicate that differences as small as 0.09 dB in the standard deviations in table V could be significant ($p \leq 0.05$).

Comparisons of the standard deviations in table V indicate that annoyance prediction ability was improved by the addition of duration corrections. The T_2 tone correction improved prediction ability in all but two cases. However, the results for the T_1 tone correction were mixed. When the T_1 tone correction was applied to the noise metric variations without duration corrections, it usually degraded prediction ability. When the T_1 correction was applied to the noise metric variations with duration corrections, it improved prediction ability in most cases, but not as much as the T_2 tone correction. The L_A with duration corrections and T_2 tone corrections had the smallest standard deviation of prediction error. Duration-corrected L_A without tone corrections and L_A with duration corrections and T_1 tone corrections had the second and third smallest standard deviations of prediction error. The difference between the standard deviations for the three noise metric variations was not significant. The addition of critical band corrections to PNL did not significantly improve its prediction ability. Comparisons of the standard deviations of prediction error in table V clearly indicate that duration-corrected L_A, either with or without tone corrections, most accurately predicted the annoyance caused by the combined set of aircraft types.

The following analyses of the advanced turboprop stimuli will be presented in terms of L_A, PNL, and $\mathrm{LL_Z}$. The L_A and PNL are used because they are the two most commonly used procedures. The $\mathrm{LL_Z}$ is included because, in some cases, the results using $\mathrm{LL_Z}$ differ somewhat from the results using the other noise measurement procedures.

Effects of Advanced Turboprop Tone Characteristics

Figures 22, 23, and 24 illustrate the effects of fundamental frequency and tone-to-broadband noise ratio on annoyance prediction for the SRP, $n \times n$ CRP, and $n \times m$ CRP configurations of advanced turboprop stimuli, respectively. In each figure, the effects on annoyance are presented for each combination of duration and tone corrections applied to L_A, PNL, and $\mathrm{LL_Z}$. Annoyance relative to the noise metric prediction is plotted versus fundamental frequency for each of the two tone-to-broadband noise ratios. "Annoyance relative to noise metric prediction" is the prediction error (subjective noise level minus the calculated level of the metric) normalized by subtracting the average (across the stimuli group) prediction error for the metric. When defined in this manner, a positive number represents annoyance greater than that predicted by the metric, and results for different metrics can be directly compared. The results for the SRP advanced turboprop stimuli are generally similar across different metrics; however, for the two CRP configurations, the magnitudes of the effects and interaction of the two tone characteristics vary between the different combinations of noise measurement procedures and corrections. The most consistent trend for all three propeller configurations is the difference in annoyance between the 15- and 30-dB tone-to-broadband noise ratios. However, the effect is opposite between the SRP and CRP configurations. For the SRP stimuli, annoyance was less at the higher tone-to-broadband noise ratio. For both groups of CRP stimuli, annoyance was greater at the higher tone-to-broadband noise ratio. These results are consistent with previous studies that examined the different propeller configurations separately (refs. 1 and 2).

Effect of Blade Number Difference

The $n \times m$ CRP advanced turboprop aircraft were divided into two groups based on the blade number difference between the front and aft rotors. The blade combinations in the first group (8×7, 9×8, 10×9, 11×10, and 12×11) had a blade number difference of one. The blade combinations in the second group (8×6, 9×7, 10×8, 11×9, and 12×10) had a blade number difference of two. The two groups of stimuli were compared by using indicator (dummy) variable analyses (ref. 48). The results, which are consistent across noise metrics, indicated no difference in annoyance response to the two groups of $n \times m$ CRP advanced turboprop stimuli. These results are consistent with a previous study that examined the $n \times m$ CRP configuration separately

(ref. 2). Blade number difference did not affect annoyance response.

Comparison of Aircraft Types

Figure 25 compares the annoyance responses to conventional turboprop and conventional turbofan aircraft flyover noises with the annoyance responses to the flyover noises of advanced turboprop aircraft in each of the three propeller configurations. The figure plots subjective noise level versus duration-corrected L_A for each of the five categories of aircraft. Simple linear regression lines for each of the aircraft types are also shown. Indicator (dummy) variable analyses for the duration-corrected L_A metric found no statistically significant differences in slope or intercept between the appropriate regressions for the $n \times n$ CRP advanced turboprop, $n \times m$ CRP advanced turboprop, conventional turboprop, and conventional turbofan aircraft types. The indicator variable analyses did show a statistically significant difference in slope and intercept between the appropriate regressions for the SRP advanced turboprops and the combined set of other aircraft types. Figure 26 shows similar results using EPNL (EPNL is duration-corrected PNL with T_1 tone corrections). For all the metrics considered, the only statistically significant difference found between the annoyance responses to the five aircraft types was a significant difference in slope and intercept between the appropriate regressions for the SRP advanced turboprops and the combined set of $n \times n$ CRP advanced turboprops, $n \times m$ CRP advanced turboprops, conventional turboprops, and conventional turbofans.

Further examination of figures 25 and 26 reveals the reason for this difference in annoyance response between the SRP advanced turboprop stimuli and the other stimuli. Several data points for the SRP advanced turboprops lie well below the other data points and corresponding regression lines. These low-lying data points represent SRP advanced turboprop stimuli with 30-dB tone-to-broadband noise ratios. This finding agrees with the previous finding, illustrated in figure 22, that the annoyance response to the SRP advanced turboprop stimuli with the high tone-to-broadband noise ratio is less than the annoyance response to the other SRP advanced turboprop stimuli. This difference is responsible for the SRP advanced turboprop noises being, on average, slightly less annoying than the noises of other aircraft types in figures 25 and 26.

These results are generally consistent with previous studies that examined the different propeller configurations separately (refs. 1 and 2). The important outcome of the comparisons in figures 25 and 26 is that, for a given level, the advanced turboprop aircraft flyover noise is not more annoying than the flyover noise of current aircraft.

Conclusions

A laboratory experiment was conducted to provide information on quantifying the annoyance response of people to the flyover noise of advanced turboprop aircraft having different propeller configurations. Three advanced turboprop propeller configurations were considered: single-rotating propeller, counter-rotating propellers with an equal number of blades on each rotor, and counter-rotating propellers with an unequal number of blades on each rotor. The experiment compared the annoyance response to flyover noise from advanced turboprop aircraft having the three different propeller configurations with the annoyance response to conventional turboprop and conventional turbofan aircraft flyover noise. A computer synthesis system was used to generate 40 realistic simulations of advanced turboprop aircraft takeoff noise. Of the 40 noises, 8 represented single-rotating propeller configurations, 12 represented counter-rotating propeller configurations with an equal number of blades on each rotor, and 20 represented counter-rotating propeller configurations with an unequal number of blades on each rotor. The simulations for each propeller configuration represented different combinations of fundamental frequency and tone-to-broadband noise ratio. The advanced turboprop simulations along with recordings of 5 conventional turboprop takeoffs and 5 conventional turbofan takeoffs were presented at 3 sound pressure levels to 64 subjects in an anechoic listening room. Analyses of the annoyance responses were conducted in terms of several variations of seven conventional noise metrics (A-, D-, and E-weighted sound pressure level, loudness level (Stevens Mark VI procedure), Zwicker loudness level, perceived level (Stevens Mark VII procedure), and perceived noise level) and one other recently developed noise metric (L_1) based on a modified frequency weighting.

Based on the results presented in this paper, the following conclusions were noted:

1. The annoyance prediction ability of the noise metrics was improved by the addition of a duration correction.
2. The annoyance prediction ability of the noise metrics was improved by the addition of a tone correction similar to the one used in effective perceived noise level (EPNL) but limited to tones in 1/3-octave bands with center frequencies greater than or equal to 500 Hz. The addition of the effective perceived noise level (EPNL) tone correction

to the noise metrics did not achieve as much improvement and often degraded prediction ability.

3. Critical band corrections to perceived noise level (PNL) did not significantly improve annoyance prediction.

4. Duration-corrected A-weighted sound pressure level, either with or without tone corrections, provided the most accurate annoyance prediction.

5. Fundamental frequency and tone-to-broadband noise ratio did significantly affect annoyance response to the advanced turboprop aircraft noise. However, the direction and magnitude of the effects varied with propeller configuration and noise metric.

6. Annoyance was not significantly affected by the difference in number of blades between the front and aft rotors of the advanced turboprop aircraft with counter-rotating propellers having an unequal number of blades on each rotor.

7. No significant differences in annoyance response between the advanced turboprops with counter-rotating propellers and the conventional turboprops and turbofans were found. The advanced turboprops with single-rotating propellers were found, on average, to be, depending on noise level, from 0 to 5 dB less annoying than the other aircraft.

NASA Langley Research Center
Hampton, VA 23665-5225
July 8, 1991

Appendix

Instructions and Consent Form

The experiment in which you are participating will help us understand the characteristics of aircraft sounds which can cause annoyance in airport communities. We would like you to judge how ANNOYING some of these aircraft sounds are. By ANNOYING we mean - UNWANTED, OBJECTIONABLE, DISTURBING, OR UNPLEASANT.

The experiment consists of four 40 minute sessions. During each session 39 aircraft sounds will be presented for you to judge. You will record your judgments of the sounds on computer cards like the one below:

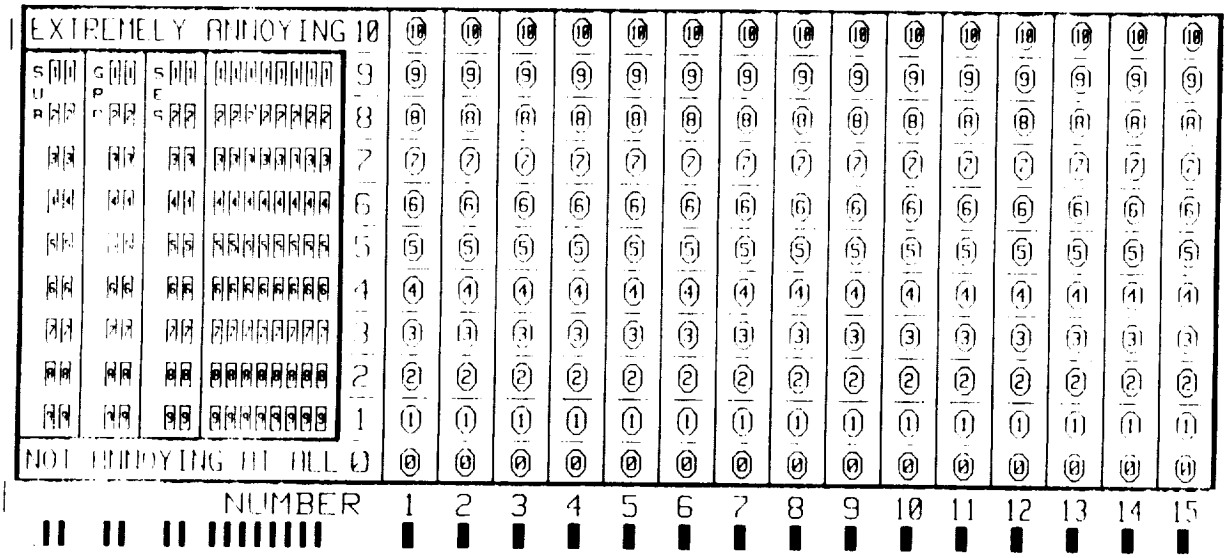

After each sound there will be a few seconds of silence. During this interval, please indicate how annoying you judge the sound to be by marking the appropriate numbered circle on the computer card. The number of each sound is indicated across the bottom of the card. If you judge a sound to be only slightly annoying, mark one of the numbered circles close to the NOT ANNOYING AT ALL end of the scale, that is a low numbered circle near the bottom of the card. Similarly, if you judge a sound to be very annoying, then mark one

of the numbered circles close to the EXTREMELY ANNOYING end of the scale, that is a high numbered circle near the top of the card. A moderately annoying judgment should be marked in the middle portion of the scale. In any case, make your mark so that the circle that most closely indicates your annoyance to the sound is completely filled in. There are no right or wrong answers; we are only interested in your judgment of each sound.

Before the first session begins you will be given a practice computer card and three sounds will be presented to familiarize you with making and recording judgments. I will remain in the testing room with you during the practice time to answer any questions you may have.

Thank you for your help in conducting the experiment.

VOLUNTARY CONSENT FORM FOR SUBJECTS

FOR HUMAN RESPONSE TO AIRCRAFT NOISE AND VIBRATION

I understand the purpose of the research and the technique to be used, including my participation in the research, as explained to me by the Principal Investigator (or qualified designee).

I do voluntarily consent to participate as a subject in the human response to aircraft noise experiment to be conducted at NASA Langley Research Center on _____.
date

I understand that I may at any time withdraw from the experiment and that I am under no obligation to give reasons for withdrawal or to attend again for experimentation.

I undertake to obey the regulations of the laboratory and instruction of the Principal Investigator regarding safety, subject only to my right to withdraw declared above.

I affirm that, to my knowledge, my state of health has not changed since the time at which I completed and signed the medical report form required for my participation as a test subject.

_____
PRINT NAME

_____
SIGNATURE

References

1. McCurdy, David A.: *Annoyance Caused by Advanced Turboprop Aircraft Flyover Noise—Single-Rotating Propeller Configuration.* NASA TP-2782, 1988.

2. McCurdy, David A.: *Annoyance Caused by Advanced Turboprop Aircraft Flyover Noise—Counter-Rotating Propeller Configuration.* NASA TP-3027, 1990.

3. Block, P. J. W.: Noise Radiation Patterns of Counter-Rotation and Unsteadily Loaded Single-Rotation Propellers. *J. Aircr.*, vol. 22, no. 9, Sept. 1985, pp. 776–783.

4. Woodward, Richard P.: *Noise of a Model High Speed Counterrotation Propeller at Simulated Takeoff/Approach Conditions (F7/A7).* NASA TM-100206, 1987. (Available as AIAA-87-2657.)

5. Pearsons, Karl S.: *Combination Effects of Tone and Duration Parameters on Perceived Noisiness.* NASA CR-1283, 1969.

6. Kryter, K. D.; Johnson, P. J.; and Young, J. R.: *Judgment Tests of Flyover Noise From Various Aircraft.* NASA CR-1635, 1970.

7. Scharf, B.; and Hellman, R.: *Comparison of Various Methods for Predicting the Loudness and Acceptability of Noise. Part 2: Effects of Spectral Pattern and Tonal Components.* Rep. EPA-550/9-79-102, U.S. Environmental Protection Agency, Nov. 1979. (Available from NTIS as PB82 138 702.)

8. Kryter, Karl D.: *Physiological, Psychological, and Social Effects of Noise.* NASA RP-1115, 1984.

9. Powell, Clemans A.; and McCurdy, David A.: *Effects of Repetition Rate and Impulsiveness of Simulated Helicopter Rotor Noise on Annoyance.* NASA TP-1969, 1982.

10. Pearsons, Karl S.; and Bennett, Ricarda L.: *Handbook of Noise Ratings.* NASA CR-2376, 1974.

11. *Noise Standards: Aircraft Type and Airworthiness Certification.* Part 36, Title 14 (Parts 1 to 59), Code of Federal Regulations, Federal Aviation Adm., Jan. 1, 1990.

12. McCurdy, David A.; and Grandle, Robert E.: *Aircraft Noise Synthesis System.* NASA TM-89040, 1987.

13. Stern, John A.: *Aircraft Propulsion—A Key to Fuel Conservation, An Aircraft Manufacturer's View.* SAE Paper 760538, May 1976.

14. Kraus, E. F.; and Van Abkoude, J. C.: *Cost/Benefit Tradeoffs for Reducing the Energy Consumption of the Commercial Air Transportation System—Summary Report.* NASA CR-137925, 1976.

15. Douglas Aircraft Co.: *Cost/Benefit Tradeoffs for Reducing the Energy Consumption of the Commercial Air Transportation System. Volume I: Technical Analysis.* NASA CR-137923, 1976.

16. Hanson, Donald B.: Near Field Noise of High Tip Speed Propellers in Forward Flight. AIAA Paper No. 76-565, July 1976.

17. Dugan, J. F.; Miller, B. A.; and Sagerser, D. A.: Status of Advanced Turboprop Technology. *CTOL Transport Technology—1978*, NASA CP-2036, Part I, 1978, pp. 139–166.

18. Dugan, James F., Jr.; Gatzen, Bernard S.; and Adamson, William M.: *Prop-Fan Propulsion—Its Status and Potential.* SAE Tech. Paper Ser. 780995, 1978.

19. Hanson, Donald B.: The Influence of Propeller Design Parameters on Far Field Harmonic Noise in Forward Flight. AIAA Paper 79-0609, Mar. 1979.

20. Dittmar, James H.; Jeracki, Robert J.; and Blaha, Bernard J.: *Tone Noise of Three Supersonic Helical Tip Speed Propellers in a Wind Tunnel.* NASA TM-79167, [1979].

21. Rennison, D. C.; Wilby, J. F.; Marsh, A. H.; and Wilby, E. G.: *Interior Noise Control Prediction Study for High-Speed Propeller-Driven Aircraft.* NASA CR-159200, 1979.

22. Brooks, Bennett M.; and Metzger, F. B.: *Acoustic Test and Analysis of Three Advanced Turboprop Models.* NASA CR-159667, 1980.

23. Revell, J. D.; Balena, F. J.; and Koval, L. R.: *Analytical Study of Interior Noise Control by Fuselage Design Techniques on High-Speed, Propeller-Driven Aircraft.* NASA CR-159222, 1980.

24. Dugan, James F.; Miller, Brent A.; Graber, Edwin J.; and Sagerser, David A.: *The NASA High-Speed Turboprop Program.* NASA TM-81561, [1980].

25. Muehlbauer, J. C.; Hewell, J. G., Jr.; Lindenbaum, S. P.; Randall, C. C.; Searle, N.; and Stone, F. R., Jr.: *Turboprop Cargo Aircraft Systems Study, Phase 1.* NASA CR-159355, 1980.

26. Muehlbauer, J. C.; Hewell, J. G., Jr.; Lindenbaum, S. P.; Randall, C. C.; Searle, N.; and Stone, F. R., Jr.: *Turboprop Cargo Aircraft Systems Study.* NASA CR-165813, 1981.

27. Arndt, William E.: Fuel Efficient and Mach 0.8, Too. *Lockheed Horiz.*, Issue 10, Spring 1982, pp. 27–34.

28. Martin, R. M.; and Farassat, F.: *Users' Manual for a Computer Program To Calculate Discrete Frequency Noise of Conventional and Advanced Propellers.* NASA TM-83135, 1981.

29. French-Developed Propfan Demonstrates Performance in Wind Tunnel Tests. *Aviation Week & Space Technol.*, vol. 124, no. 1, Jan. 1986, p. 67.

30. Allison Propfan Development Centers on Gearbox Design. *Aviation Week & Space Technol.*, vol. 123, no. 25, Dec. 1985, pp. 46–47.

31. Douglas Plans Continuing Upgrades to Maintain MD-80 Competitiveness. *Aviation Week & Space Technol.*, vol. 123, no. 19, Nov. 1985, pp. 52, 57, 59, 61, 65.

32. DeMeis, Richard: Propfans Gear Up. *Aerosp. America*, vol. 24, no. 10, Oct. 1985, pp. 22, 24.

33. Full-Power Tests on Propfan Progress at Wright-Patterson. *Aviation Week & Space Technol.*, vol. 123, no. 13, Sept. 1985, p. 55.

34. Rolls Royce Favoring Geared Propfan Design for New Development Program. *Aviation Week & Space Technol.*, vol. 122, no. 13, Apr. 1985, p. 64.

35. DeMeis, Richard.: Propfans: Fuel Saving but Ear Splitting. *Aerosp. Amercia*, vol. 22, no. 10, Oct. 1984, pp. 37, 40, 88.

36. Brown, David A.: Propfan Concepts Gain in Development. *Aviation Week & Space Technol.*, vol. 121, no. 12, Sept. 1984, pp. 54–55.

37. Brahney, James H.: Propfan Engine Designs Examined. *Aerosp. Eng.*, vol. 6, no. 2, Feb. 1986, pp. 17–22.

38. Holt, Daniel J.: Will 1990s Aircraft be Powered by Propfan or Advanced Turbofan? *Aerosp. Eng.*, vol. 6, no. 2, Feb. 1986, pp. 8–12.

39. Brown, David A.: Rolls Attacks Technical Obstacles in Propfan Development Program. *Aviation Week & Space Technol.*, vol. 122, no. 10, Mar. 1985, pp. 38–39.

40. Mordoff, Keith F.: NASA/Lockheed Propfan System Completes Ground Tests. *Aviation Week & Space Technol.*, vol. 125, no. 3, July 1986, pp. 93–95.

41. Mordoff, Keith F.: Douglas Studies MD-92X Production. *Aviation Week & Space Technol.*, vol. 125, no. 7, Aug. 1986, pp. 33–34.

42. Mordoff, Keith F.: General Electric Flies First Unducted Fan Demonstrator. *Aviation Week & Space Technol.*, vol. 125, no. 8, Aug. 1986, pp. 31–32.

43. Bradley, A. J.: A Study of the Rotor/Rotor Interaction Tones From a Contra-Rotating Propeller Driven Aircraft. AIAA-86-1894, July 1986.

44. Parzych, David; and Shattuck, Colman: Noise of the Fairey Gannet Counter Rotating Propeller. AIAA-86-1895, July 1986.

45. Hanson, D. B.: Noise of Counter Rotation Propellers. AIAA-84-2305, Oct. 1984.

46. Kryter, K. D.: *Possible Modifications to the Calculation of Perceived Noisiness.* NASA CR-1636, 1970.

47. Klugh, Henry E.: *Statistics - The Essentials for Research.* John Wiley & Sons, Inc., c.1970.

48. Canavos, George C.: *Applied Probability and Statistical Methods.* Little, Brown and Co., c.1984.

Table I. Data on Test Subjects

Sex	Number of participants	Mean age	Median age	Age range
Male	23	31	29	18–56
Female	41	41	41	18–69
All subjects	64	38	38	18–69

Table II. Conventional Turboprop and Turbofan Aircraft in the Experiment

Airplane	Number of engines	Engine type	Maximum takeoff weight, kg
de Havilland Canada DHC-7 Dash 7	4	Turboprop	20 000
Lockheed P-3	4	↓	61 200
NAMC YS-11	2	↓	24 500
Nord 262	2	↓	10 600
Shorts 330	2	↓	10 300
Airbus Industrie A-300	2	Turbofan	≥142 000
Boeing 707	4	↓	≥117 000
Boeing 727-200	3	↓	86 900
McDonnell Douglas DC-9	2	↓	≥41 100
McDonnell Douglas DC-10	3	↓	≥206 400

Table III. Presentation Order of Stimull on Tapes

Practice tape	Tape 1 ↓	Tape 2 ↓	Tape 3 ↓	Tape 4 ↓
1008 3 80	0260 3 80	0908 3 70	0908 2 90	DD-7 T 70
S330 T 70	1212 2 70	0260 3 90	DC-9 T 70	0807 2 80
0180 2 90	B727 T 80	B727 T 85	1210 2 70	1110 2 70
	DD-7 T 90	1111 2 90	0908 3 80	0907 3 90
	1109 2 90	1211 2 70	N262 T 90	B707 T 80
	0907 2 80	DD-7 T 80	0806 2 90	1210 3 90
	N262 T 70	1111 3 70	1010 2 70	0808 2 70
	1211 3 90	1008 2 80	1009 3 70	1110 3 90
	0808 2 90	DC-9 T 90	1211 3 80	1109 2 70
	DC-9 T 80	0909 3 70	B707 T 70	1210 2 80
	0707 3 70	1210 3 80	0808 3 90	B727 T 65
	1212 3 90	0806 2 70	1109 2 80	N262 T 80
	1009 2 70	1212 3 80	0292 2 80	1010 3 90
	0808 3 80	1110 2 90	0260 3 70	1111 2 70
	0225 3 90	YS11 T 80	0907 2 70	0260 2 80
	0908 2 80	0807 3 80	0707 3 90	A300 T 70
	A300 T 90	B727 T 70	0180 2 80	1009 3 90
	0807 2 70	0292 3 80	LP-3 T 70	0908 2 70
	1109 3 70	0707 2 90	0807 3 70	1212 2 80
	0909 2 80	0808 3 70	1110 3 80	B727 T 90
	0292 3 90	S330 T 70	0225 2 90	1008 3 80
	LP-3 T 80	0180 2 90	0806 3 80	0806 2 80
	0806 3 90	1109 3 80	S330 T 80	0225 2 70
	1010 3 70	0292 2 70	1008 2 70	S330 T 90
	1110 2 80	0909 2 90	A300 T 80	0180 3 90
	B727 T 99	B707 T 90	0260 2 90	1009 2 80
	0907 3 70	0907 3 80	1008 3 90	DC10 T 90
	1010 2 90	1210 2 90	0707 2 80	1211 3 70
	1009 3 80	1008 3 70	0225 3 70	0292 3 70
	0260 2 70	0907 2 90	1211 2 90	1010 2 80
	YS11 T 70	B727 T 61	YS11 T 90	0225 3 80
	1111 2 80	1010 3 80	DC10 T 80	0908 3 90
	0807 3 90	1009 2 90	1212 2 90	0707 2 70
	0180 2 70	0180 3 70	0909 2 70	B727 T 75
	1211 2 80	0225 2 80	1109 3 90	0909 3 90
	0180 3 80	0807 2 90	1212 3 70	0707 3 80
	1008 2 90	LP-3 T 90	B727 T 95	0292 2 90
	1210 3 70	1110 3 70	1111 3 80	0806 3 70
	DC10 T 70	0808 2 80	0909 3 80	1111 3 90
	Tape 5 ↑	Tape 6 ↑	Tape 7 ↑	Tape 8 ↑

Table III. Concluded

Stimuli key					
Aircraft type, blade passage frequency, and/or number of blades				Operation type or tone-to-broadband noise ratio	Nominal L_D
Advanced turboprop		Conventional turboprop	Conventional turbofan	T = Takeoff 2 = 15 dB 3 = 30 dB	61 = 61 dB 65 = 65 dB 70 = 70 dB 75 = 75 dB 80 = 80 dB 85 = 85 dB 90 = 90 dB 95 = 95 dB 99 = 99 dB
Single-rotating propeller (nnnn < 0300)	Counter-rotating propeller (nnnn > 0300)				
nnnn = blade passage frequency, Hz 0180 = 180 Hz 0225 = 225 Hz 0260 = 260 Hz 0292 = 292.5 Hz	nnnn = ffaa ff = # of forward blades aa = # of aft blades	DD-7 = Dash 7 LP-3 = P-3 YS11 = YS-11 N262 = Nord 262 S330 = Shorts 330	A300 = Airbus A-300 B707 = Boeing 707 B727 = Boeing 727 DC-9 = DC-9 DC10 = DC-10		

Table IV. Order of Tapes Presented to Test Subjects

Test subject group	Tapes presented during session—			
	1	2	3	4
1	1	2	3	4
2	2	4	1	3
3	3	1	4	2
4	4	3	2	1
5	5	6	7	8
6	6	8	5	7
7	7	5	8	6
8	8	7	6	5
9	2	1	4	3
10	1	3	2	4
11	4	2	3	1
12	3	4	1	2
13	6	5	8	7
14	5	7	6	8
15	8	6	7	5
16	7	8	5	6
17	3	2	1	4
18	2	4	3	1
19	1	3	4	2
20	4	1	2	3
21	7	6	5	8
22	6	8	7	5
23	5	7	8	6
24	8	5	6	7
25	3	1	2	4
26	1	4	3	2
27	2	3	4	1
28	4	2	1	3
29	7	5	6	8
30	5	8	7	6
31	6	7	8	5
32	8	6	5	7

Table V. Standard Deviations of Prediction Error for Advanced Turboprop, Conventional Turboprop, and Conventional Turbofan Stimuli

Metric	Standard deviation, dB, for—					
	No duration correction			Duration corrected		
	No tone correction	T_1	T_2	No tone correction	T_1	T_2
L_A	2.80	2.92	2.85	2.46	2.48	2.43
L_D	3.70	3.77	3.67	3.30	3.31	3.19
L_E	3.63	3.70	3.61	3.20	3.22	3.10
L_1	3.15	3.26	3.18	2.79	2.79	2.72
LL	3.73	3.73	3.63	3.41	3.30	3.21
LL_Z	3.20	3.18	3.09	2.94	2.81	2.76
PL	3.45	3.43	3.33	3.25	3.12	3.04
PNL	3.45	3.49	3.39	3.17	3.10	2.99
PNL_K	3.44	3.50	3.37	3.13	3.09	2.98
PNL_M	3.48	3.51	3.41	3.14	3.09	2.99
PNL_W	3.47	3.54	3.42	3.17	3.14	3.02

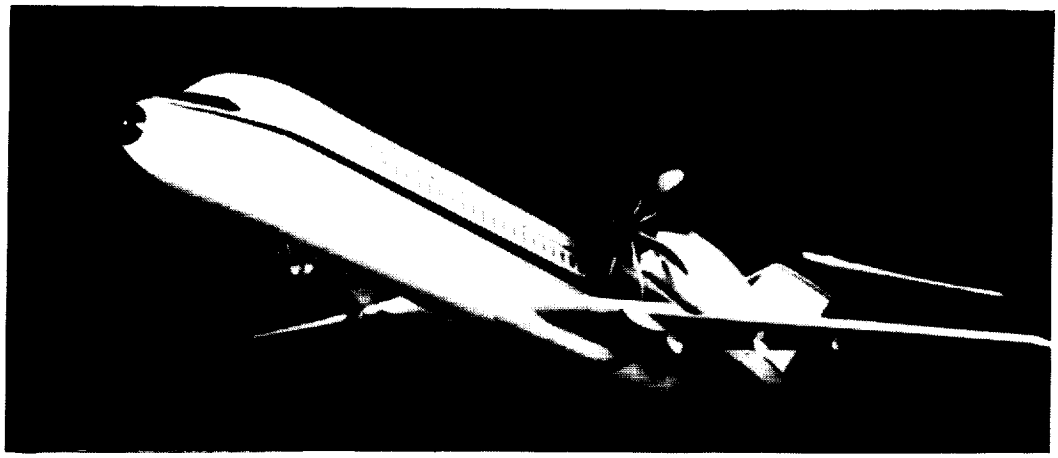

L-84-11,572

Figure 1. A wing-mounted, tractor, single-rotating propeller configuration of an advanced turboprop aircraft.

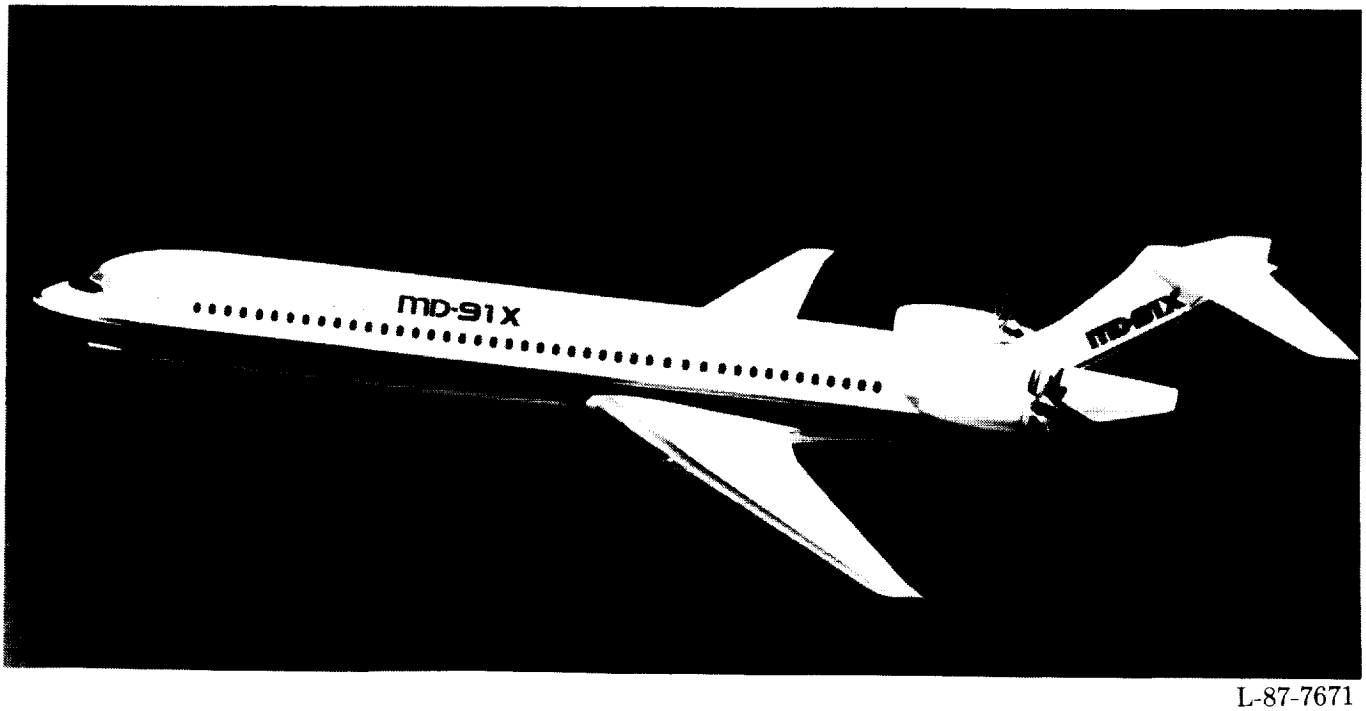

L-87-7671

Figure 2. An aft-mounted, pusher, counter-rotating propeller configuration of an advanced turboprop aircraft.

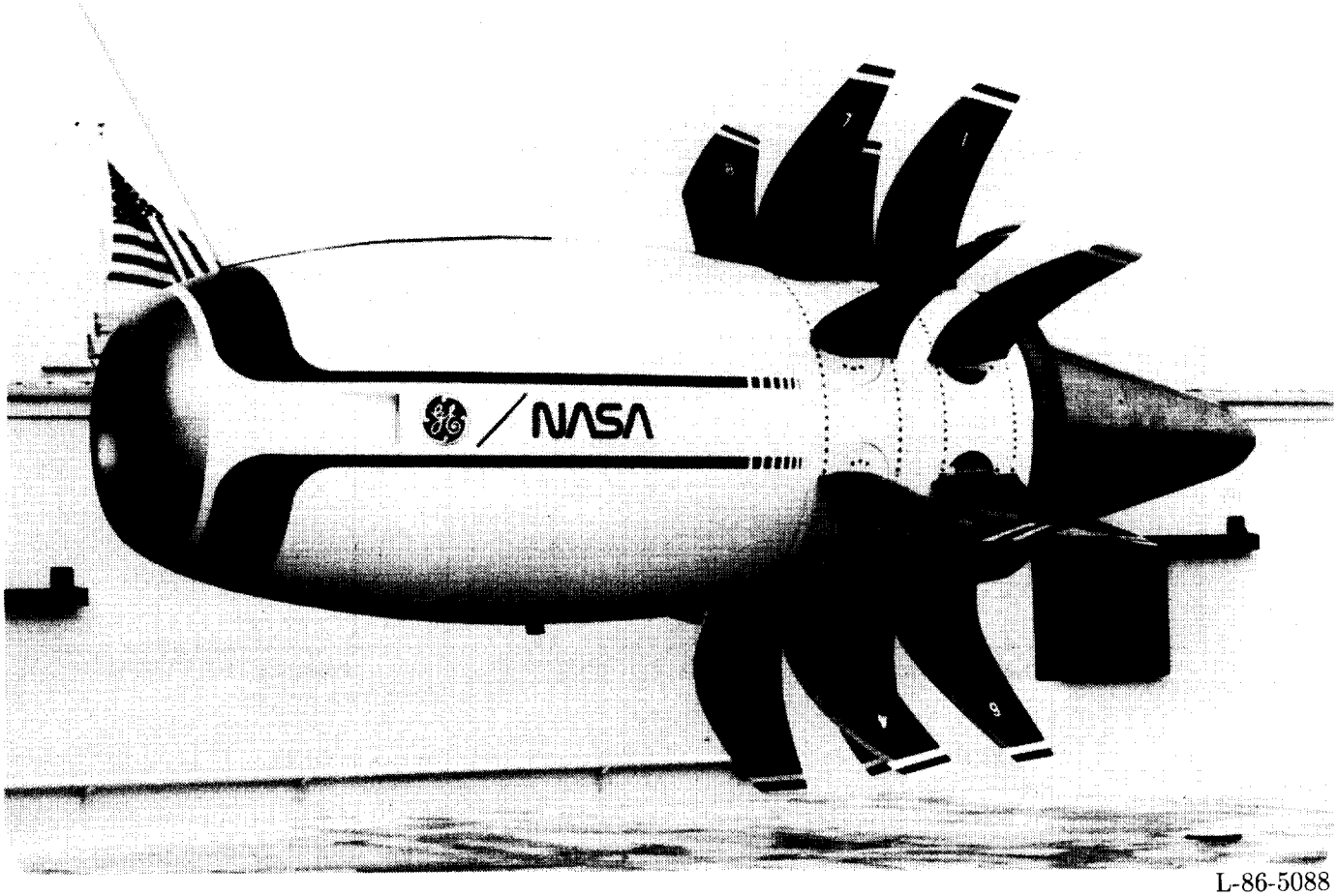

L-86-5088

Figure 3. Advanced turboprop engine with counter-rotating propeller.

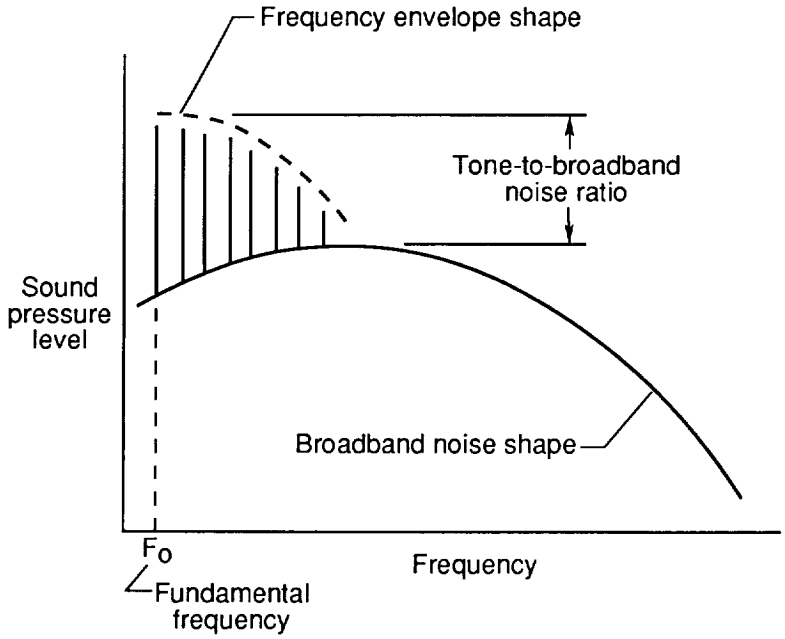

Figure 4. Propeller aircraft noise characteristics.

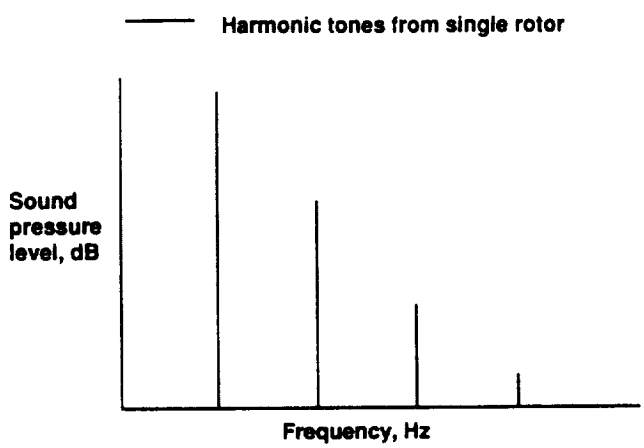

(a) SRP.

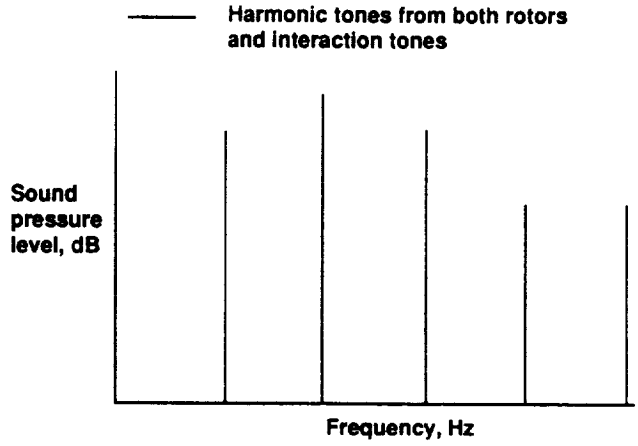

(b) $n \times n$ CRP.

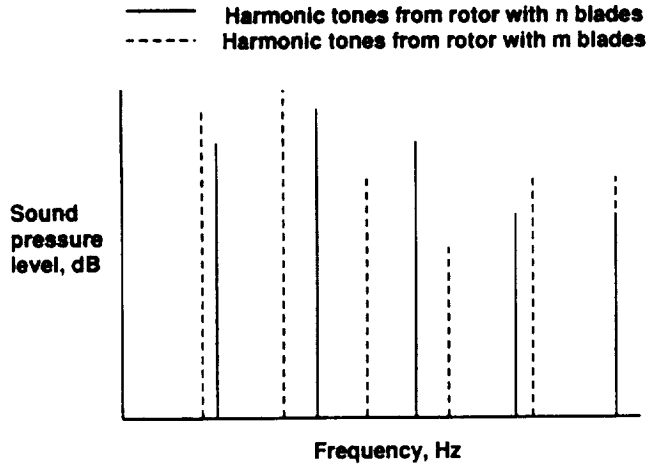

(c) $n \times m$ CRP (harmonic tones only).

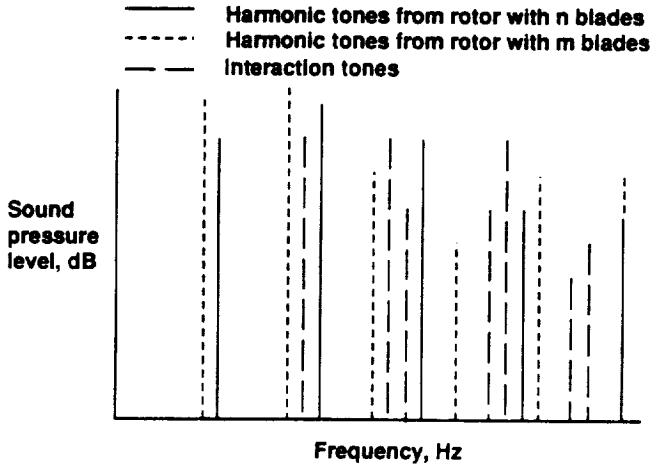

(d) $n \times m$ CRP (harmonic and interaction tones).

Figure 5. Examples of tonal content and frequency envelope shape for different advanced turboprop propeller configurations.

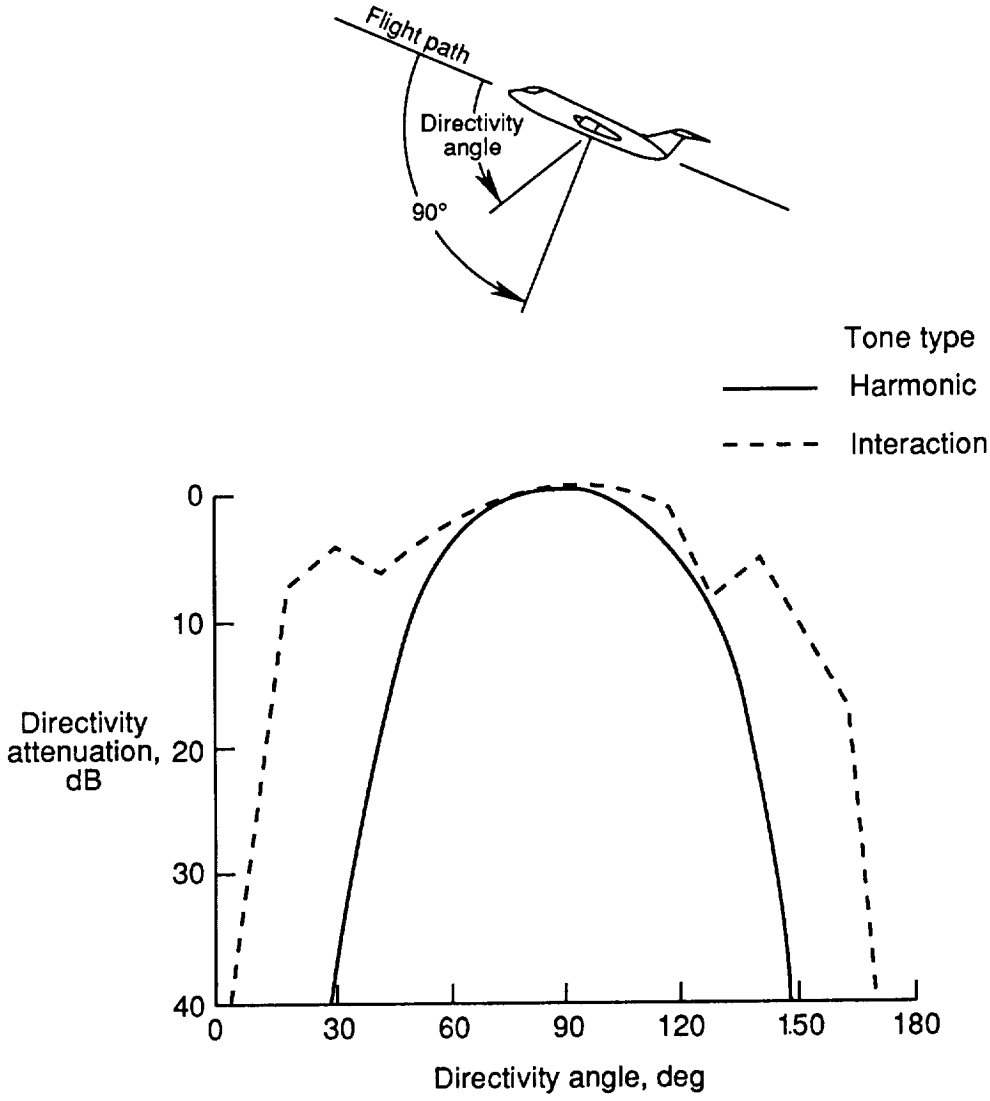

Figure 6. Examples of directivity patterns for different types of advanced turboprop propeller tones.

ORIGINAL PAGE
BLACK AND WHITE PHOTOGRAPH

L-80-6613

Figure 7. Subjects in the Anechoic Listening Room in the Langley Acoustics Research Laboratory.

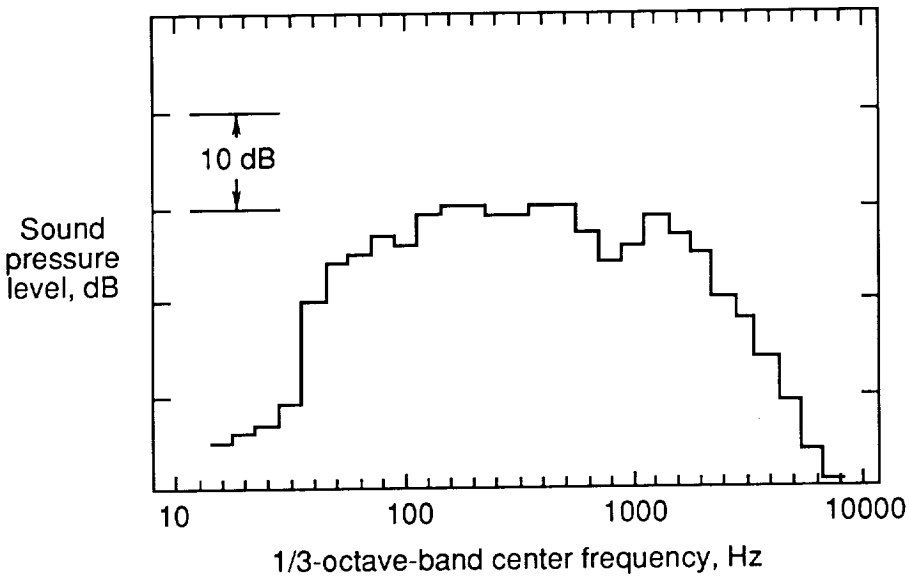

Figure 8. Broadband 1/3-octave spectrum used in synthesis of advanced turboprop aircraft flyover noise.

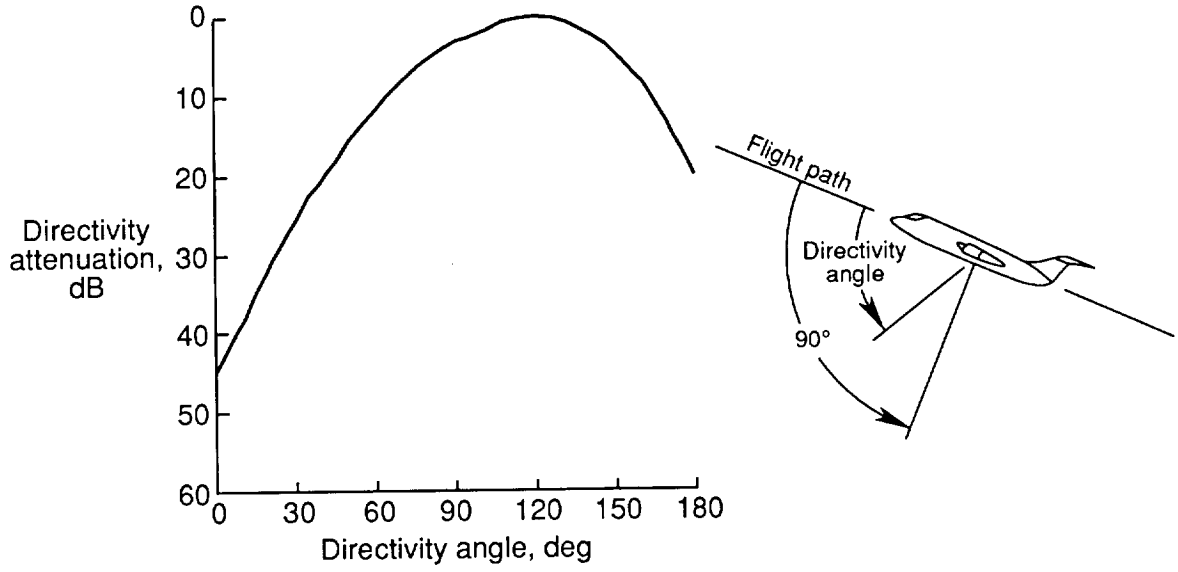

Figure 9. Directivity pattern of broadband 1/3-octave spectrum used in synthesis of advanced turboprop aircraft flyover noise.

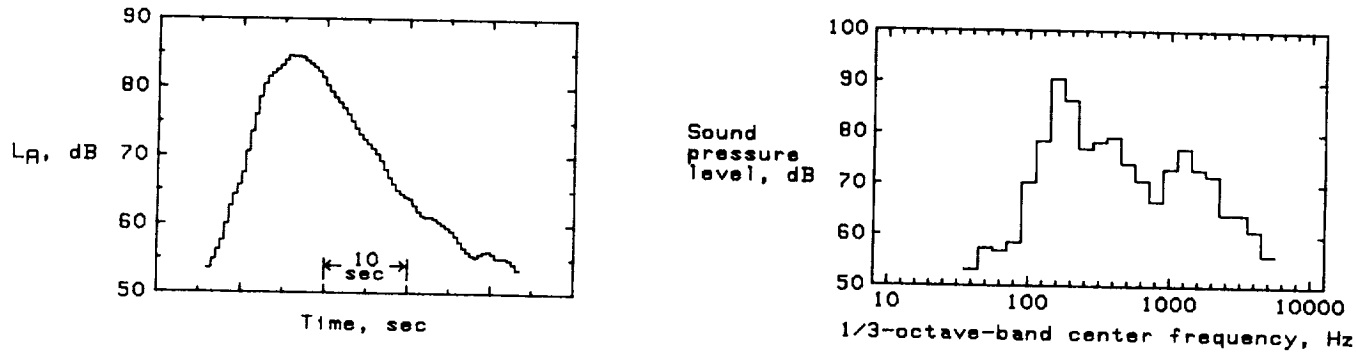

(a) $F_o = 180$ Hz; $T/N = 15$ dB.

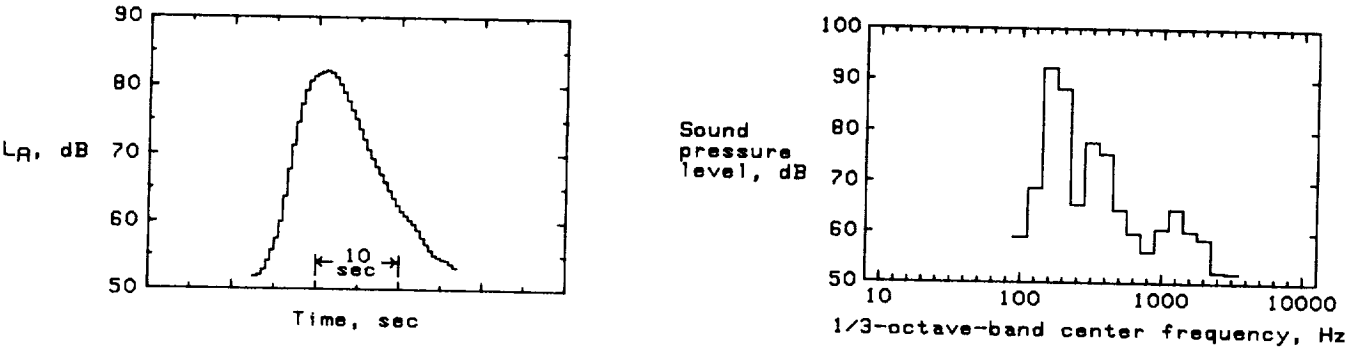

(b) $F_o = 180$ Hz; $T/N = 30$ dB.

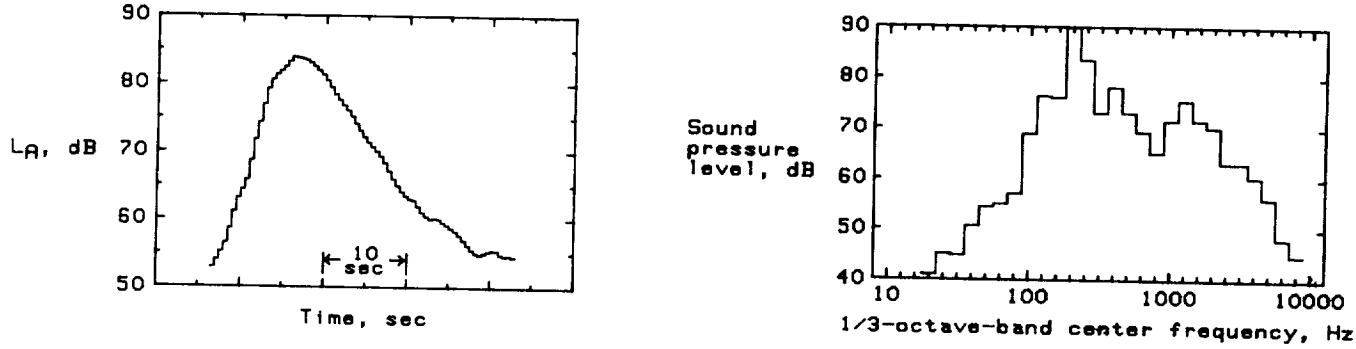

(c) $F_o = 225$ Hz; $T/N = 15$ dB.

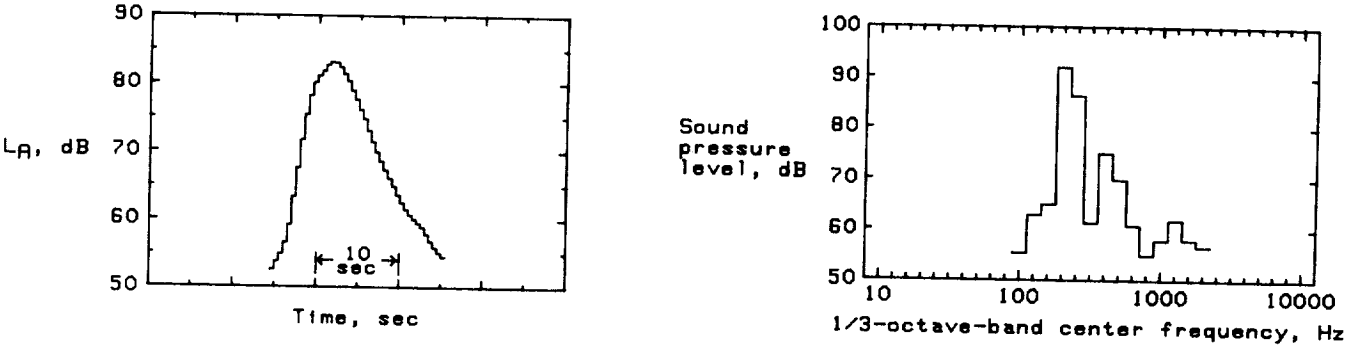

(d) $F_o = 225$ Hz; $T/N = 30$ dB.

Figure 10. L_A time history and 1/3-octave-band spectrum at peak L_A of the highest level presentation of each SRP advanced turboprop flyover noise.

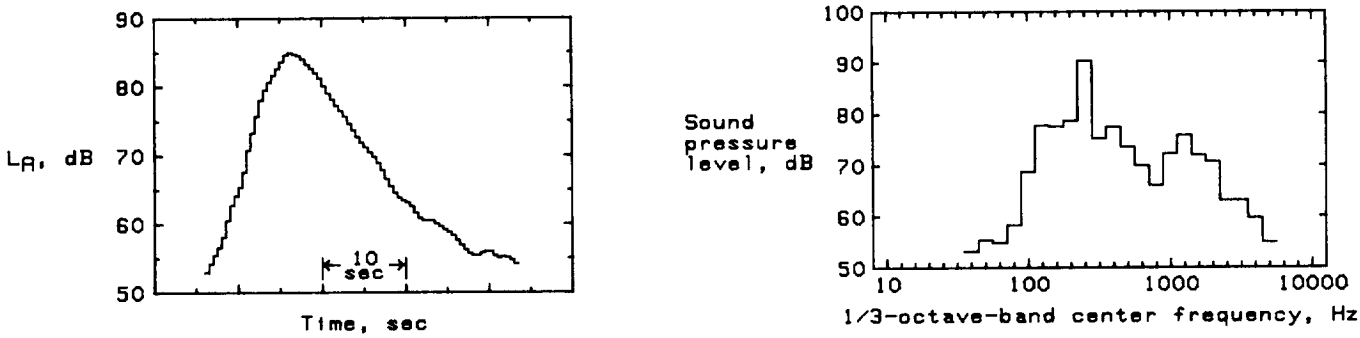

(e) $F_o = 260$ Hz; $T/N = 15$ dB.

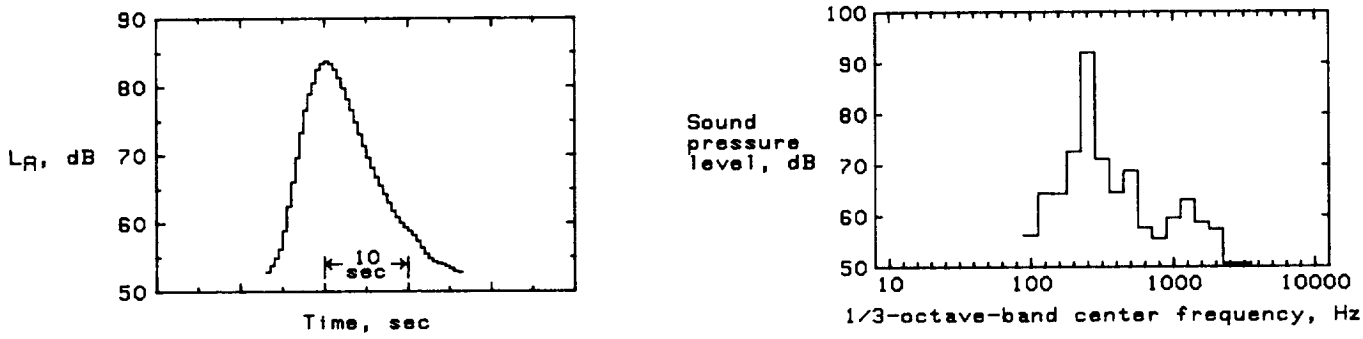

(f) $F_o = 260$ Hz; $T/N = 30$ dB.

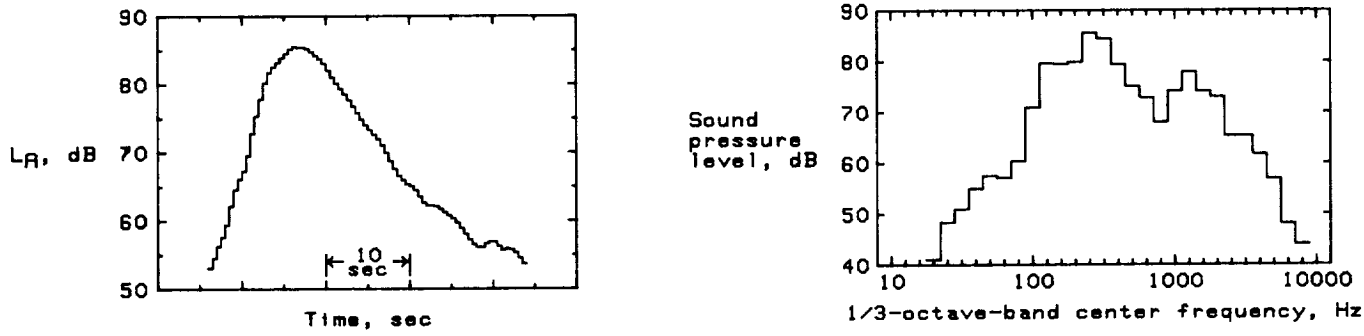

(g) $F_o = 292.5$ Hz; $T/N = 15$ dB.

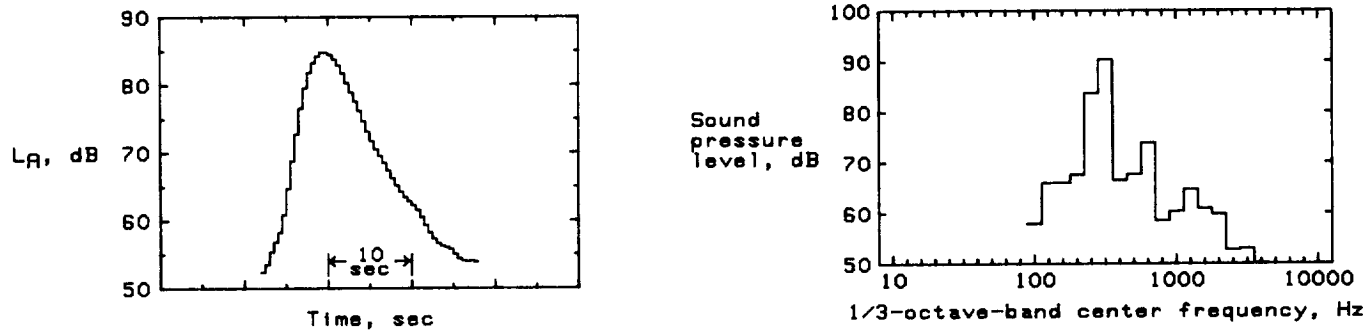

(h) $F_o = 292.5$ Hz; $T/N = 30$ dB.

Figure 10. Concluded.

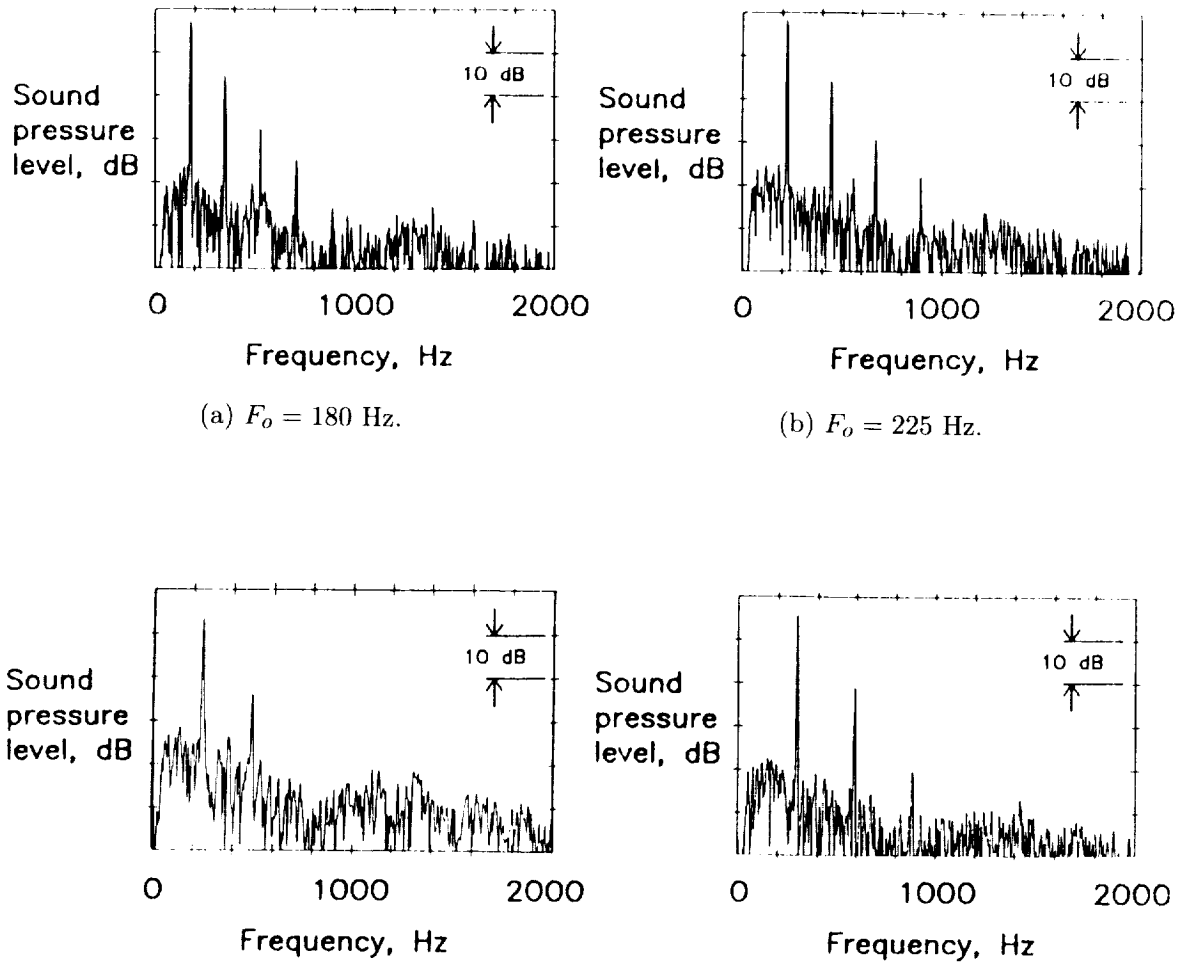

(a) $F_o = 180$ Hz.

(b) $F_o = 225$ Hz.

(c) $F_o = 260$ Hz.

(d) $F_o = 292.5$ Hz.

Figure 11. Narrowband spectrum of each SRP advanced turboprop flyover noise with 30-dB tone-to-broadband noise ratio. (Spectra measured at point in time history corresponding to no Doppler shift in frequency.)

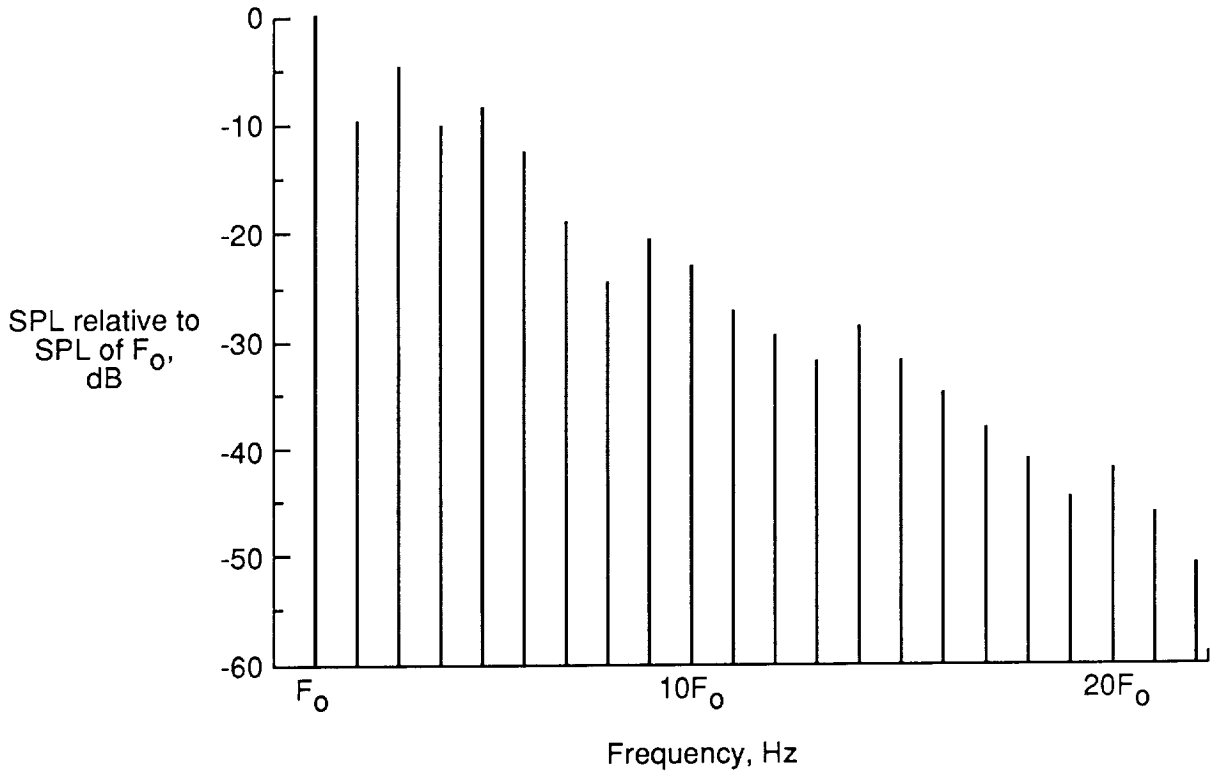

Figure 12. Tonal components used in synthesis of flyover noise from advanced turboprop aircraft with counter-rotating propellers having an equal number of blades on each rotor.

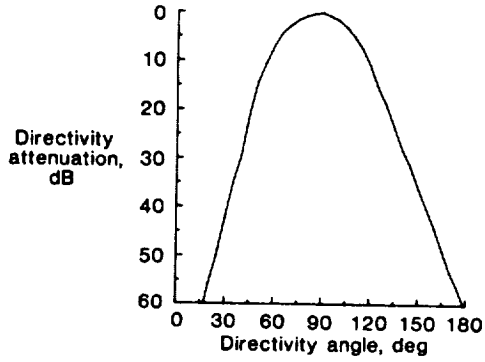

(a) F_o.

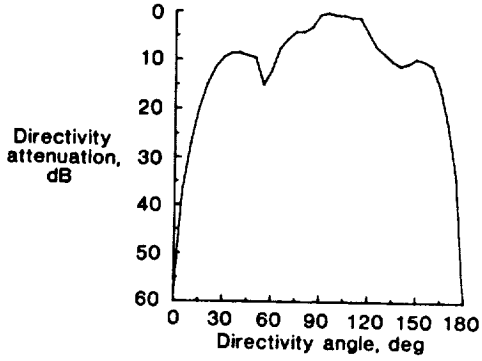

(b) $2F_o$.

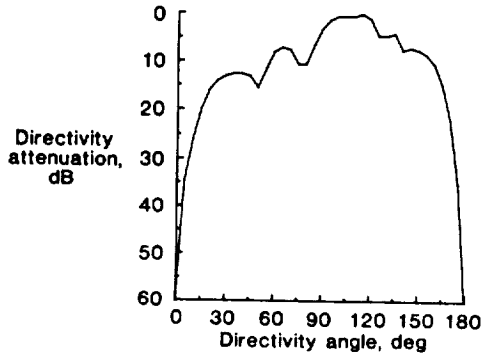

(c) $3F_o$.

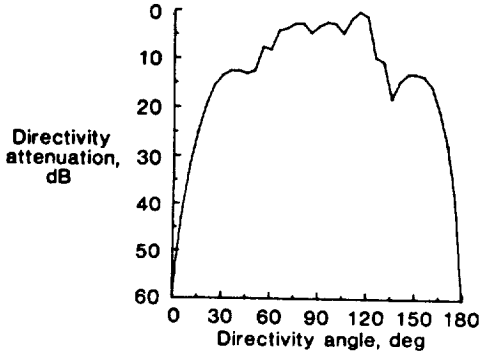

(d) $4F_o$.

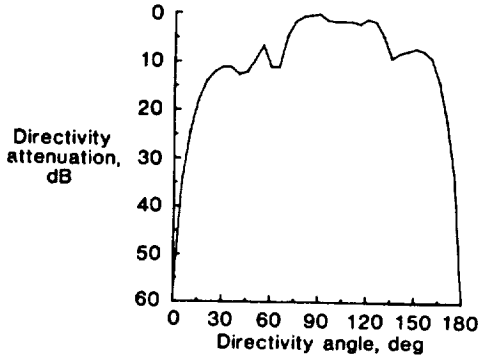

(e) $5F_o$.

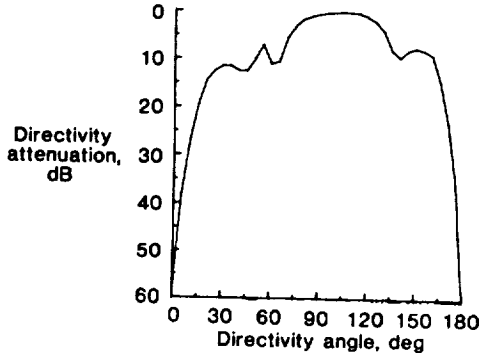

(f) nF_o, $n \geq 6$.

Figure 13. Directivity patterns of tonal components used in synthesis of flyover noise from advanced turboprop aircraft with counter-rotating propellers having an equal number of blades on each rotor.

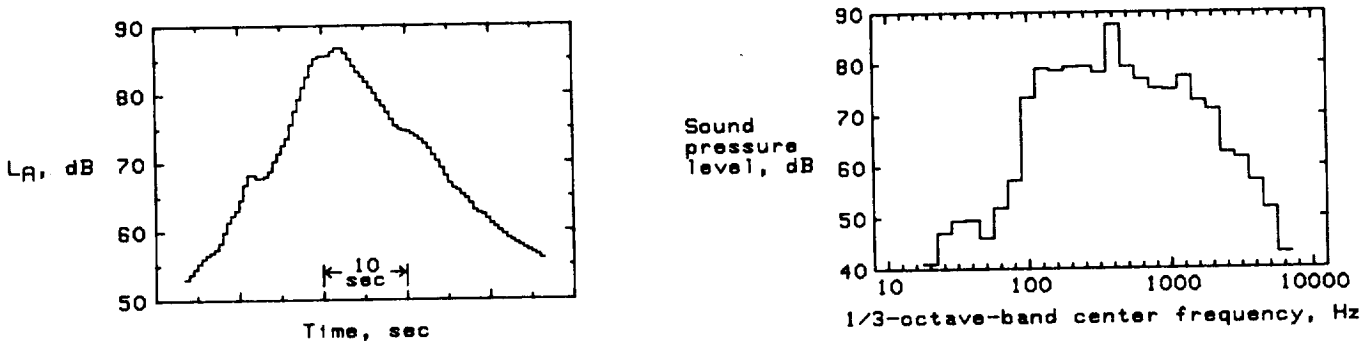

(a) $F_o = 157.5$ Hz; $T/N = 15$ dB.

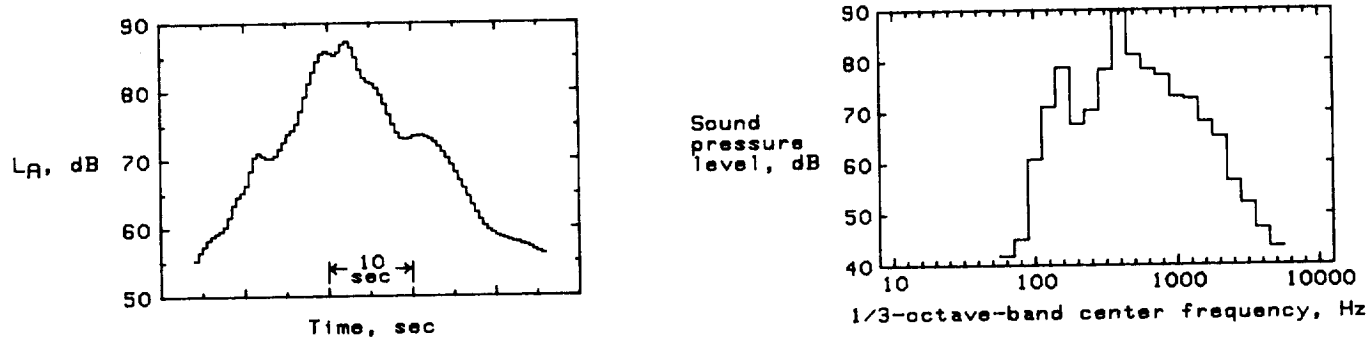

(b) $F_o = 157.5$ Hz; $T/N = 30$ dB.

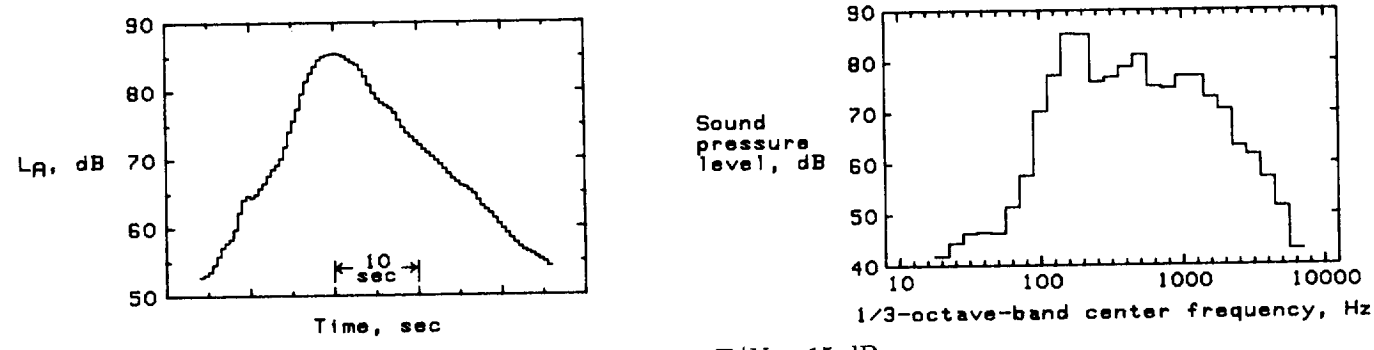

(c) $F_o = 180$ Hz; $T/N = 15$ dB.

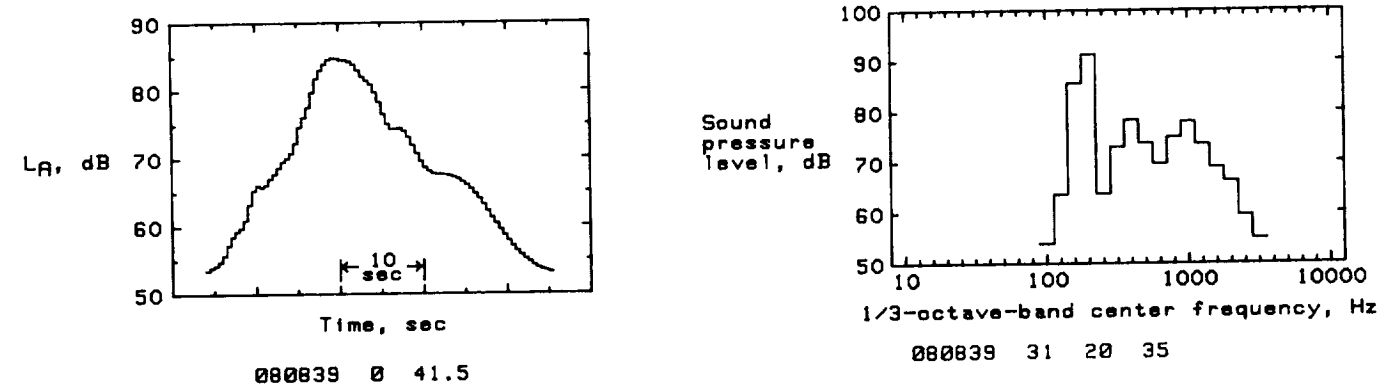

(d) $F_o = 180$ Hz; $T/N = 30$ dB.

Figure 14. L_A time history and 1/3-octave-band spectrum at peak L_A of the highest level presentation of each $n \times n$ CRP advanced turboprop flyover noise.

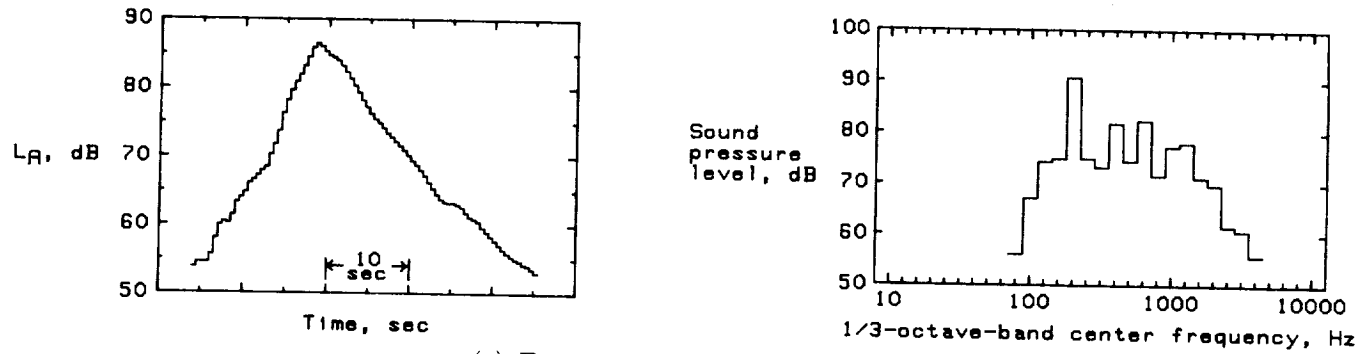

(e) $F_o = 202.5$ Hz; $T/N = 15$ dB.

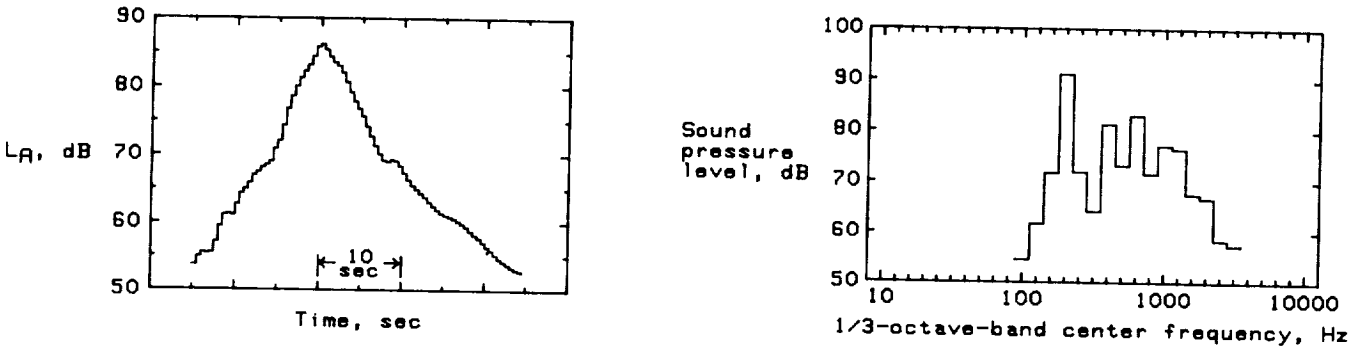

(f) $F_o = 202.5$ Hz; $T/N = 30$ dB.

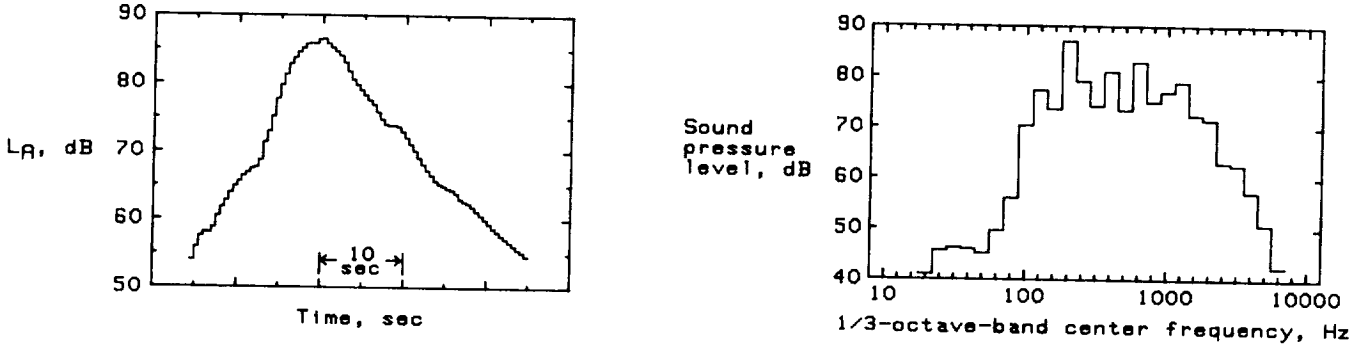

(g) $F_o = 225$ Hz; $T/N = 15$ dB.

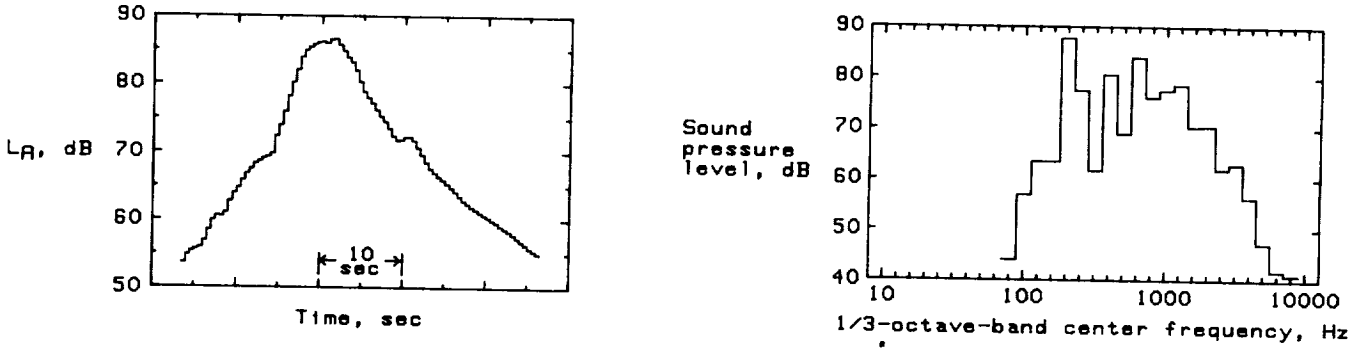

(h) $F_o = 225$ Hz; $T/N = 30$ dB.

Figure 14. Continued.

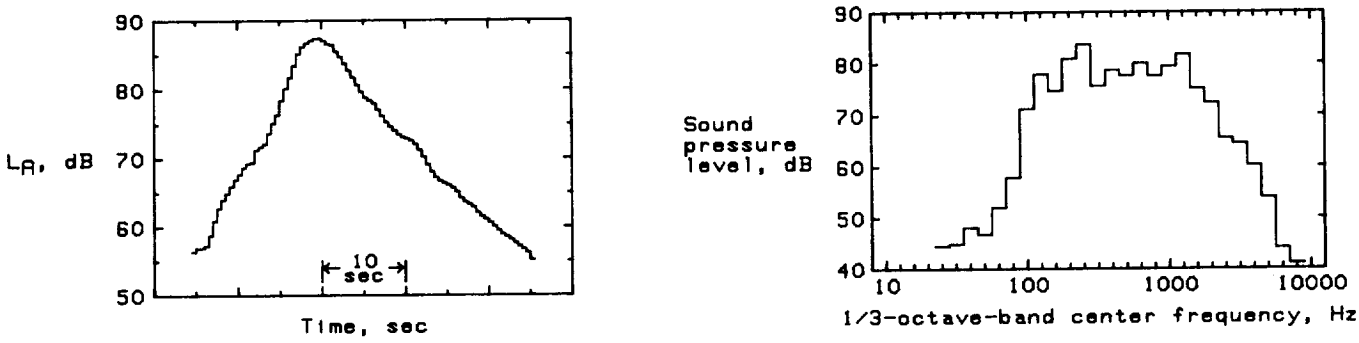

(i) $F_o = 247.5$ Hz; $T/N = 15$ dB.

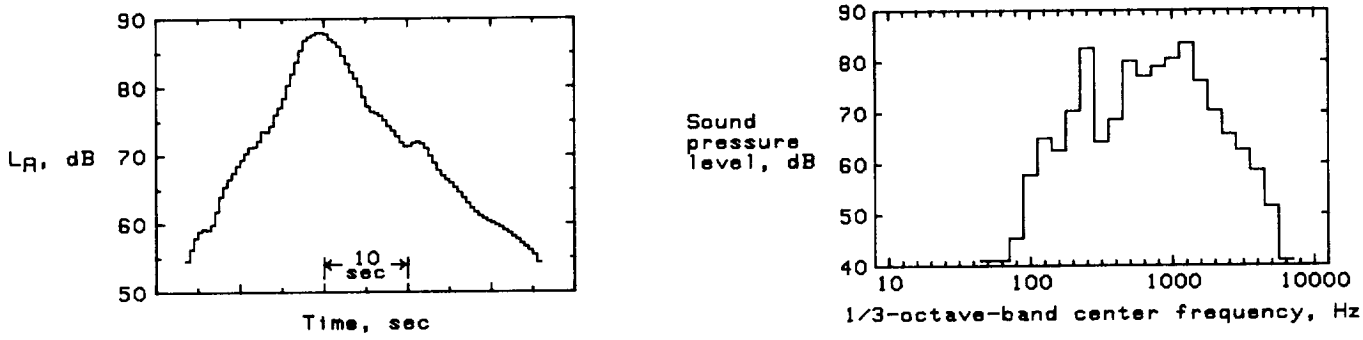

(j) $F_o = 247.5$ Hz; $T/N = 30$ dB.

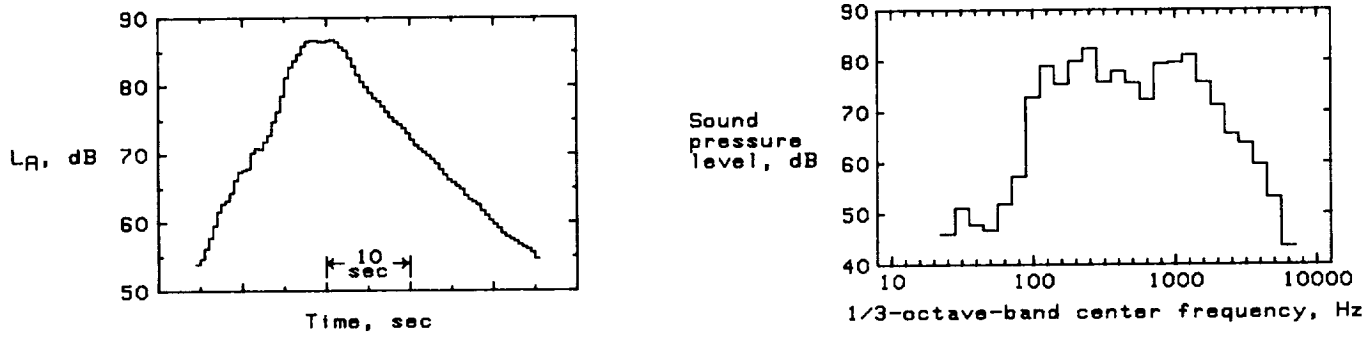

(k) $F_o = 270$ Hz; $T/N = 15$ dB.

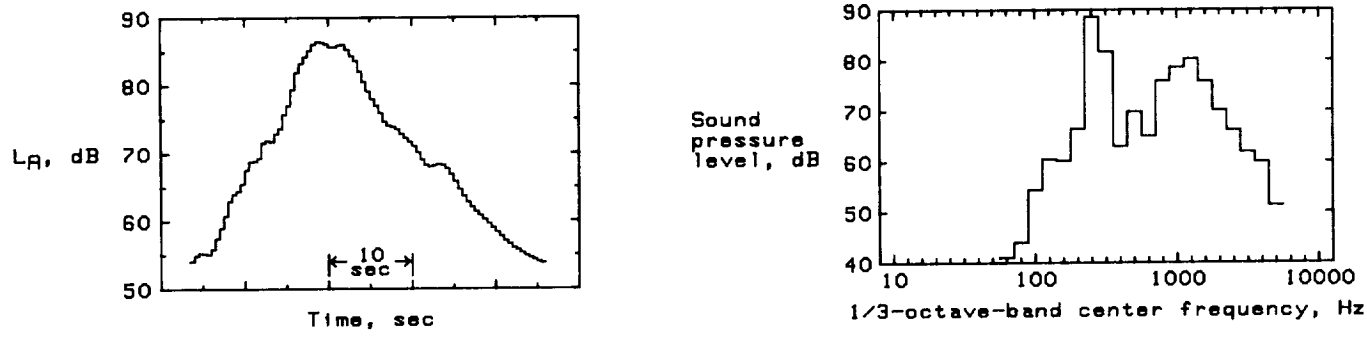

(l) $F_o = 270$ Hz; $T/N = 30$ dB.

Figure 14. Concluded.

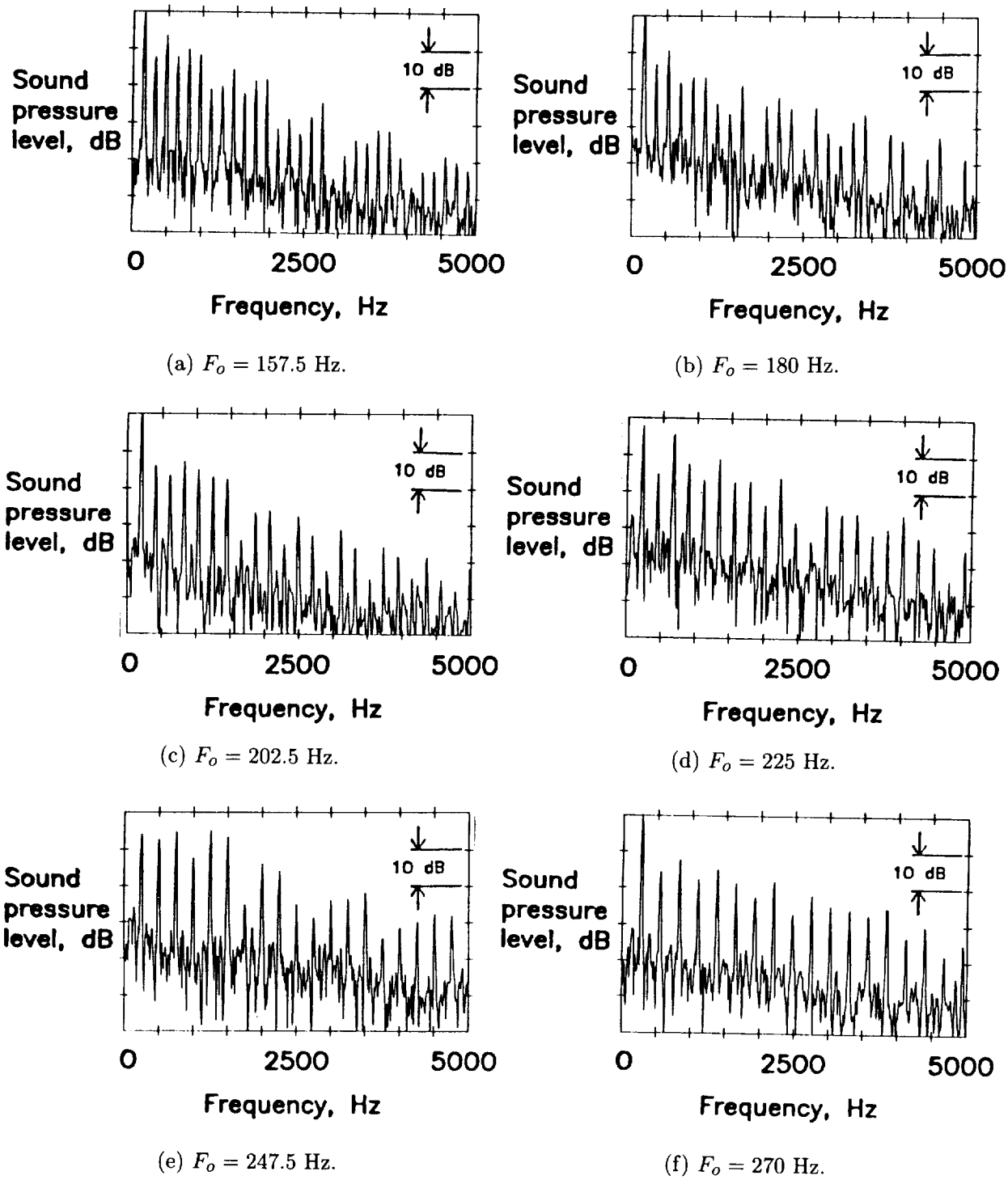

(a) $F_o = 157.5$ Hz.

(b) $F_o = 180$ Hz.

(c) $F_o = 202.5$ Hz.

(d) $F_o = 225$ Hz.

(e) $F_o = 247.5$ Hz.

(f) $F_o = 270$ Hz.

Figure 15. Narrowband spectrum of each $n \times n$ CRP advanced turboprop flyover noise with 30-dB tone-to-broadband noise ratio. (Spectra measured at point in time history corresponding to no Doppler shift in frequency.)

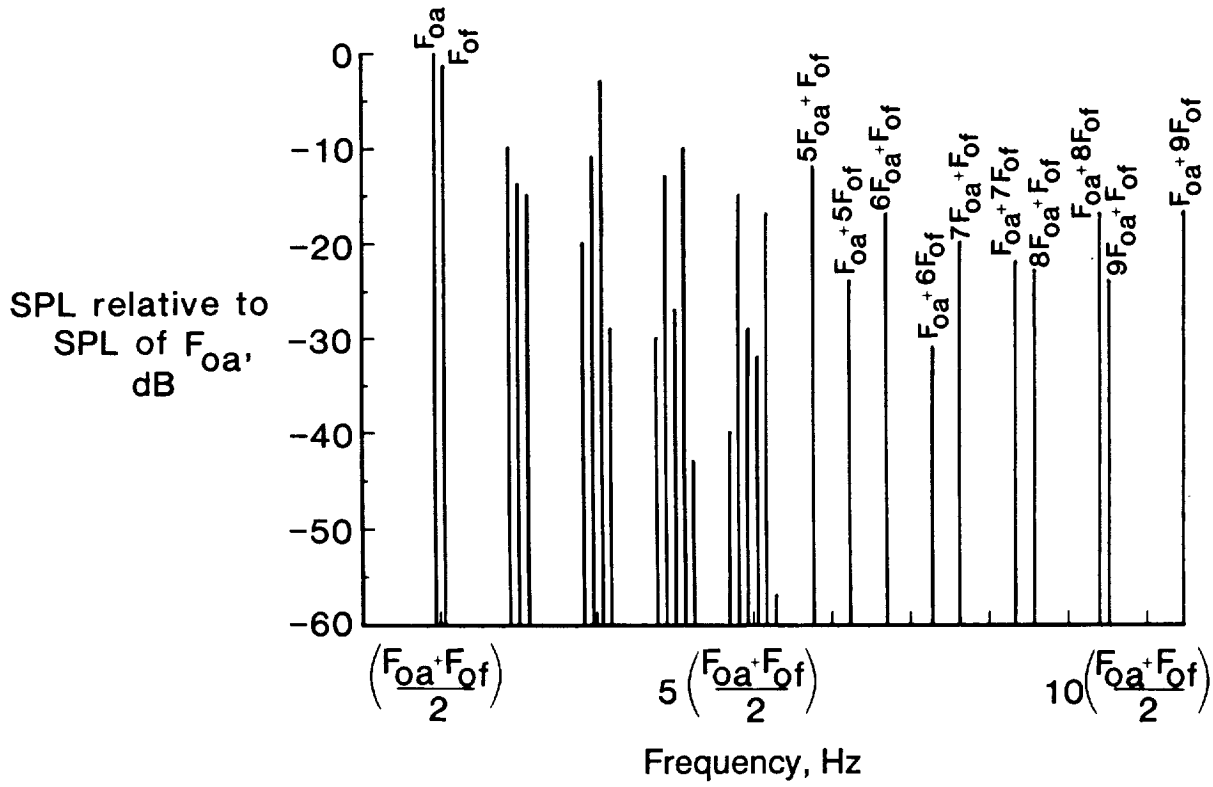

Figure 16. Tonal components used in synthesis of flyover noise from advanced turboprop aircraft with counter-rotating propellers having an unequal number of blades on each rotor.

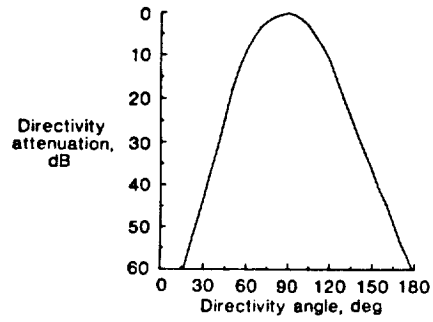

(a) F_{oa}.

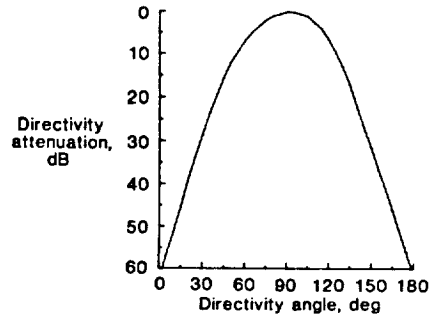

(b) F_{of}.

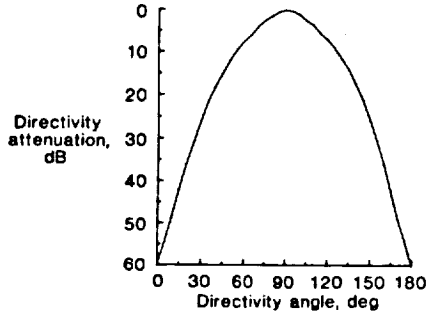

(c) nF_{oa}, nF_{of} for $n \geq 2$.

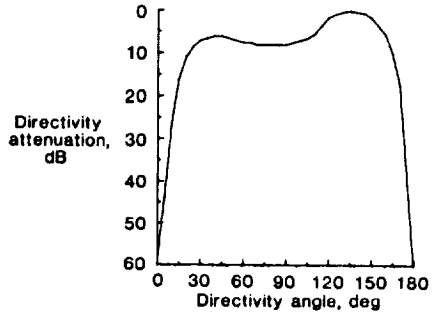

(d) $F_{oa} + F_{of}$.

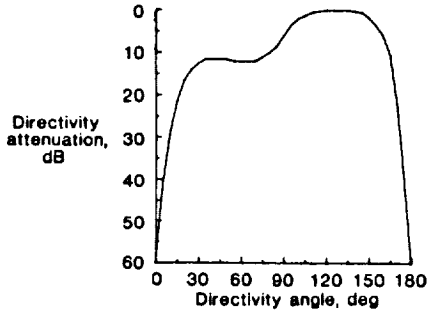

(e) $2F_{oa} + F_{of}$.

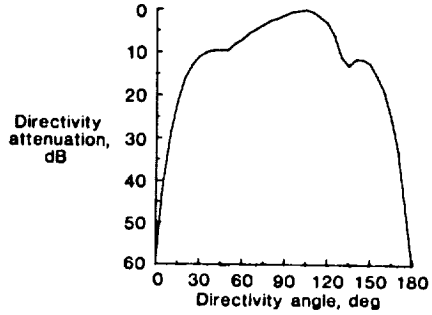

(f) $F_{oa} + 2F_{of}$.

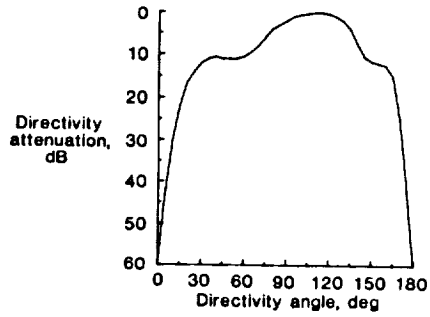

(g) $mF_{oa} + nF_{of}$ for $m \geq 1,\ n \geq 1,\ m + n \geq 4$.

Figure 17. Directivity patterns of tonal components used in synthesis of flyover noise from advanced turboprop aircraft with counter-rotating propellers having an unequal number of blades on each rotor.

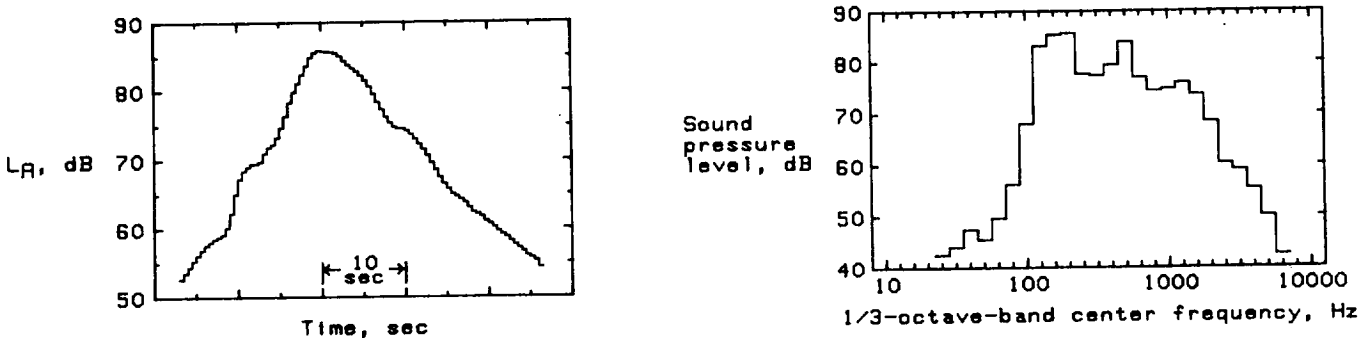

(a) $F_{of} = 180$ Hz; $F_{oa} = 135$ Hz; $T/N = 15$ dB.

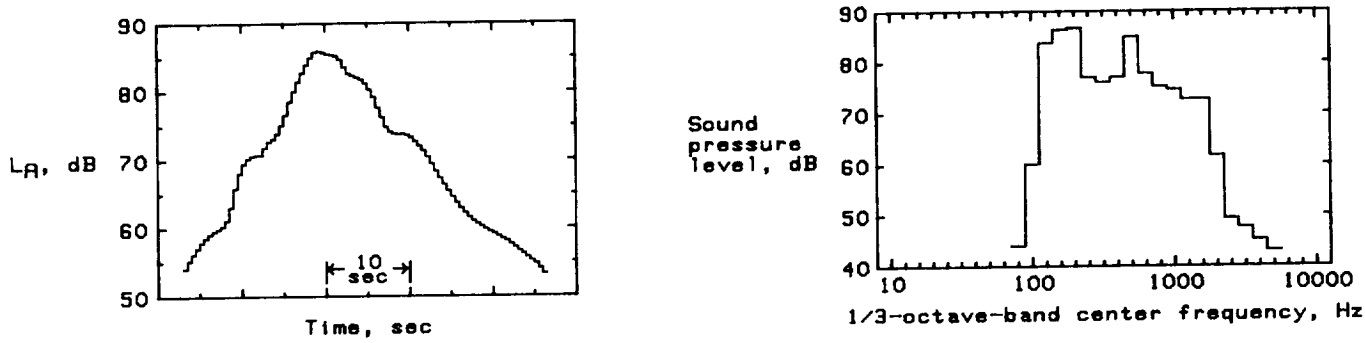

(b) $F_{of} = 180$ Hz; $F_{oa} = 135$ Hz; $T/N = 30$ dB.

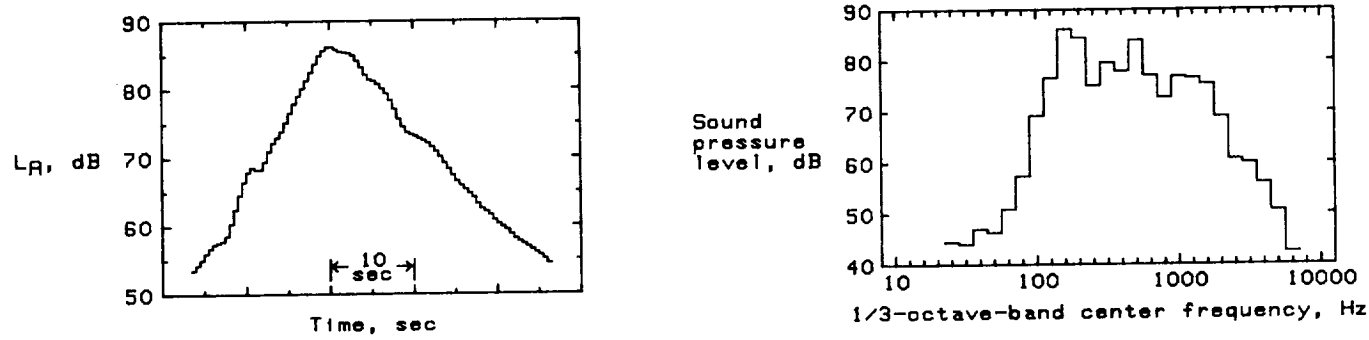

(c) $F_{of} = 180$ Hz; $F_{oa} = 157.5$ Hz; $T/N = 15$ dB.

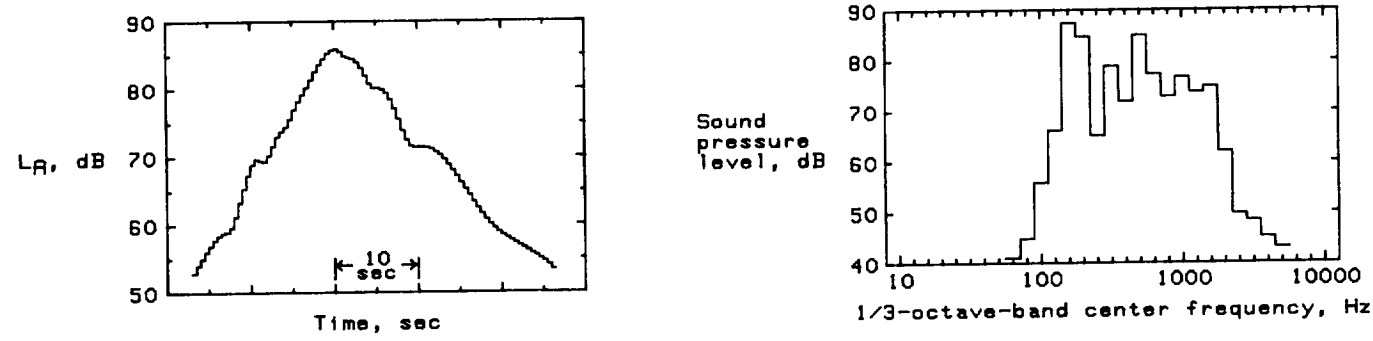

(d) $F_{of} = 180$ Hz; $F_{oa} = 157.5$ Hz; $T/N = 30$ dB.

Figure 18. L_A time history and 1/3-octave-band spectrum at peak L_A of the highest level presentation of each $n \times m$ CRP advanced turboprop flyover noise.

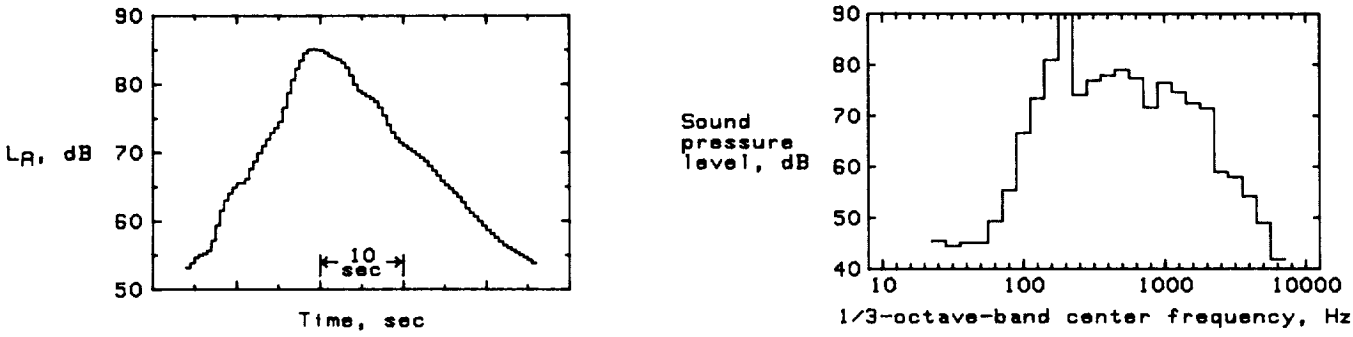

(e) $F_{of} = 202.5$ Hz; $F_{oa} = 157.5$ Hz; $T/N = 15$ dB.

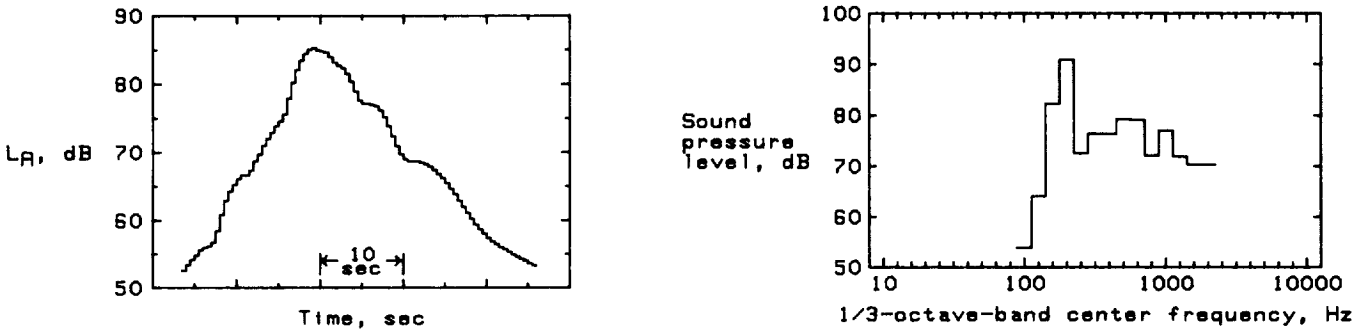

(f) $F_{of} = 202.5$ Hz; $F_{oa} = 157.5$ Hz; $T/N = 30$ dB.

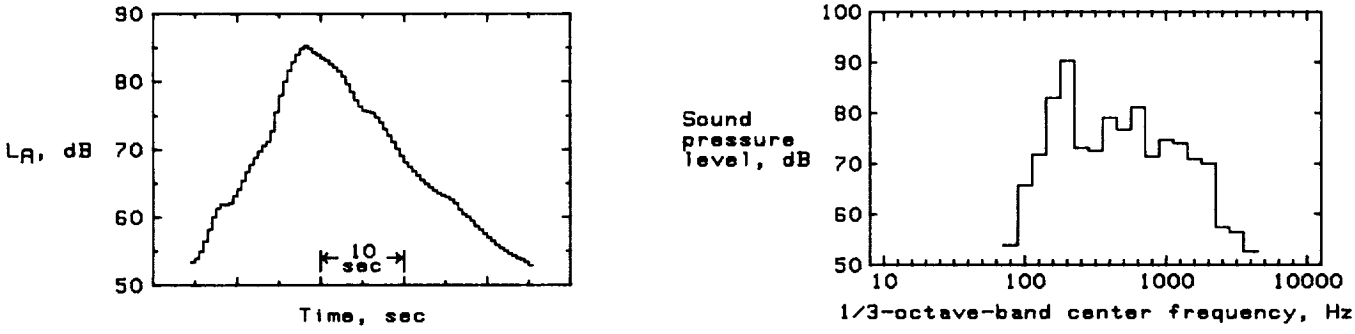

(g) $F_{of} = 202.5$ Hz; $F_{oa} = 180$ Hz; $T/N = 15$ dB.

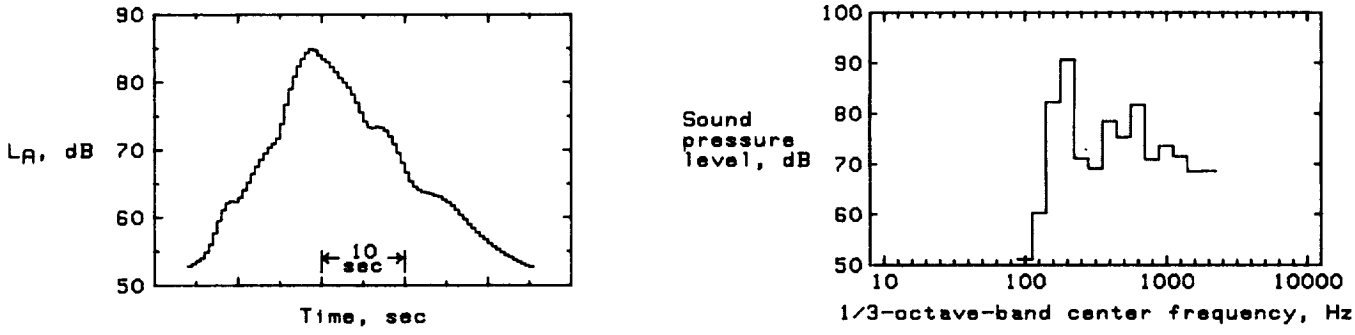

(h) $F_{of} = 202.5$ Hz; $F_{oa} = 180$ Hz; $T/N = 30$ dB.

Figure 18. Continued.

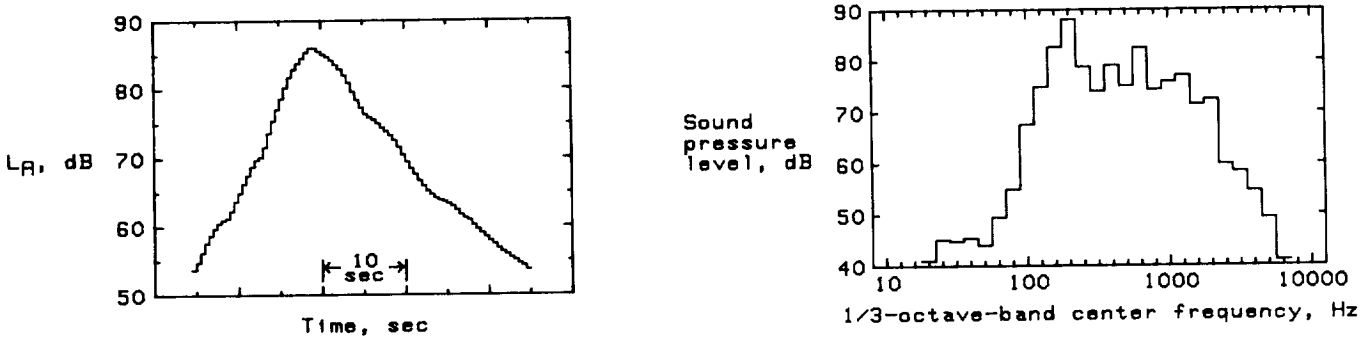

(i) $F_{of} = 225$ Hz; $F_{oa} = 180$ Hz; $T/N = 15$ dB.

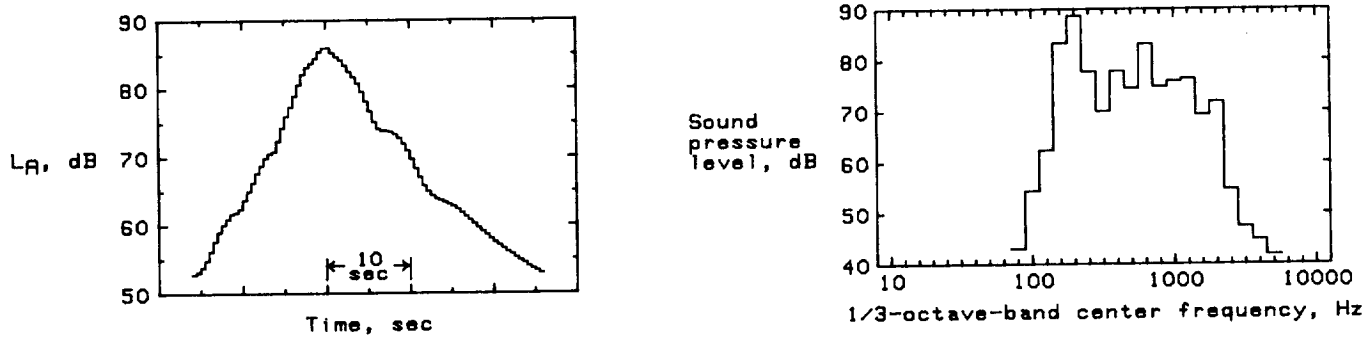

(j) $F_{of} = 225$ Hz; $F_{oa} = 180$ Hz; $T/N = 30$ dB.

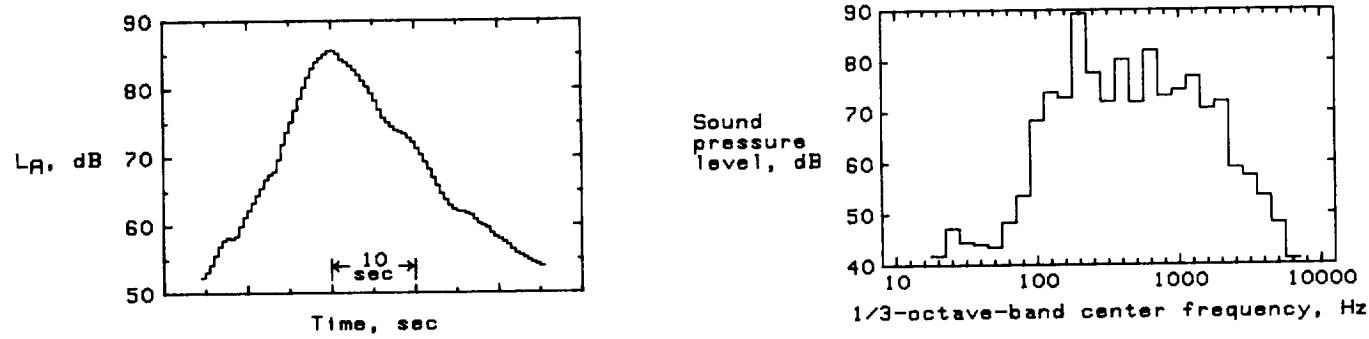

(k) $F_{of} = 225$ Hz; $F_{oa} = 202.5$ Hz; $T/N = 15$ dB.

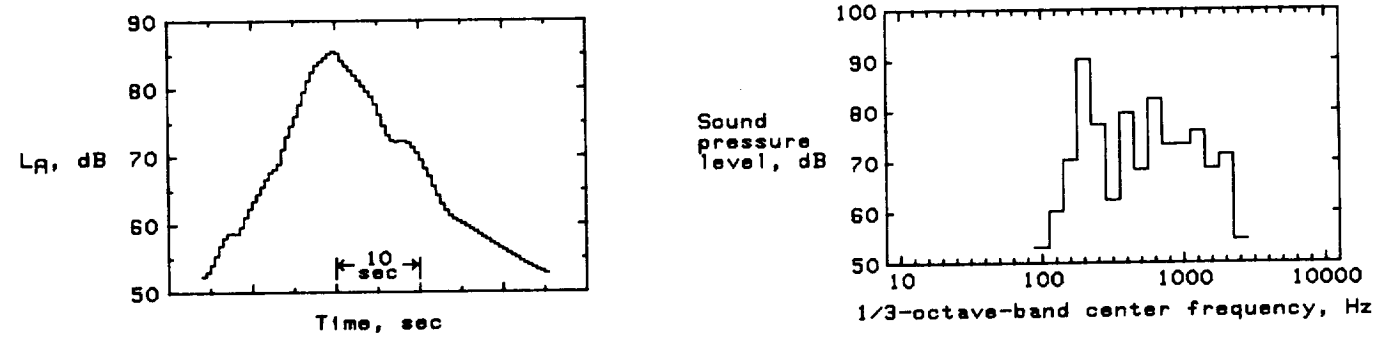

(l) $F_{of} = 225$ Hz; $F_{oa} = 202.5$ Hz; $T/N = 30$ dB.

Figure 18. Continued.

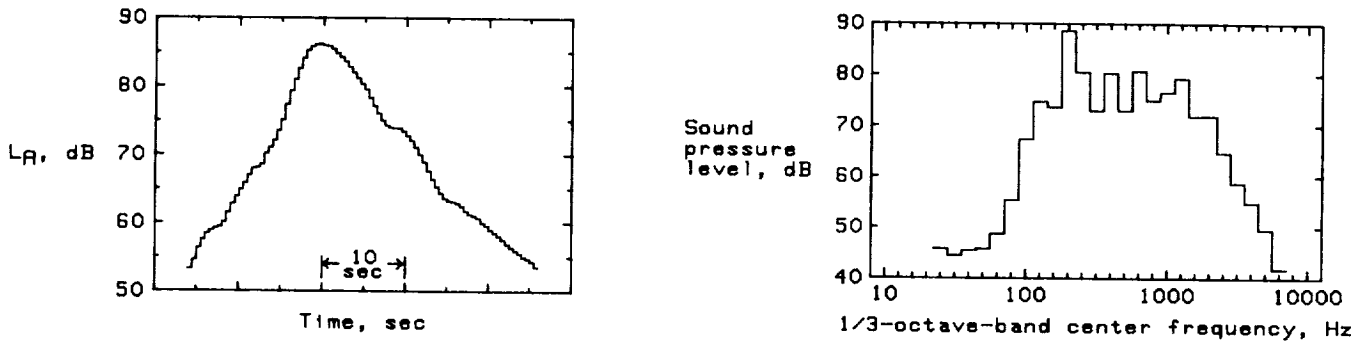

(m) $F_{of} = 247.5$ Hz; $F_{oa} = 202.5$ Hz; $T/N = 15$ dB.

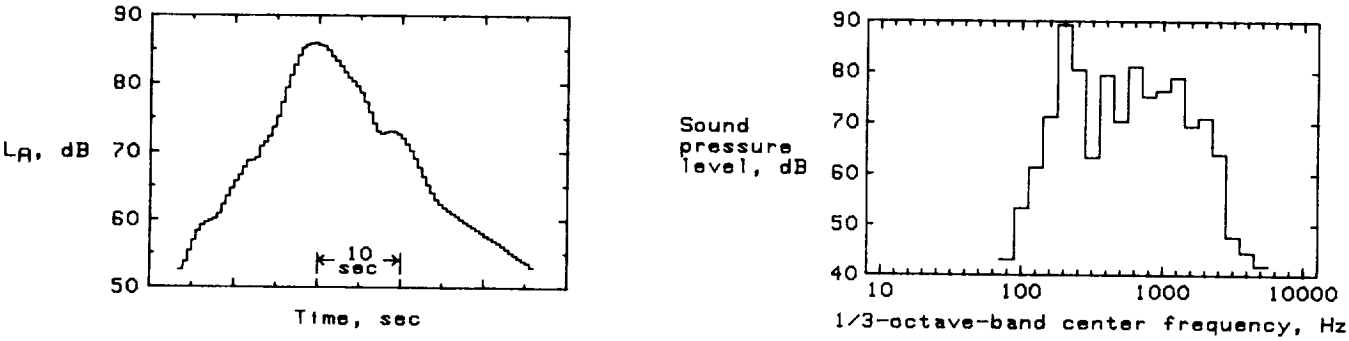

(n) $F_{of} = 247.5$ Hz; $F_{oa} = 202.5$ Hz; $T/N = 30$ dB.

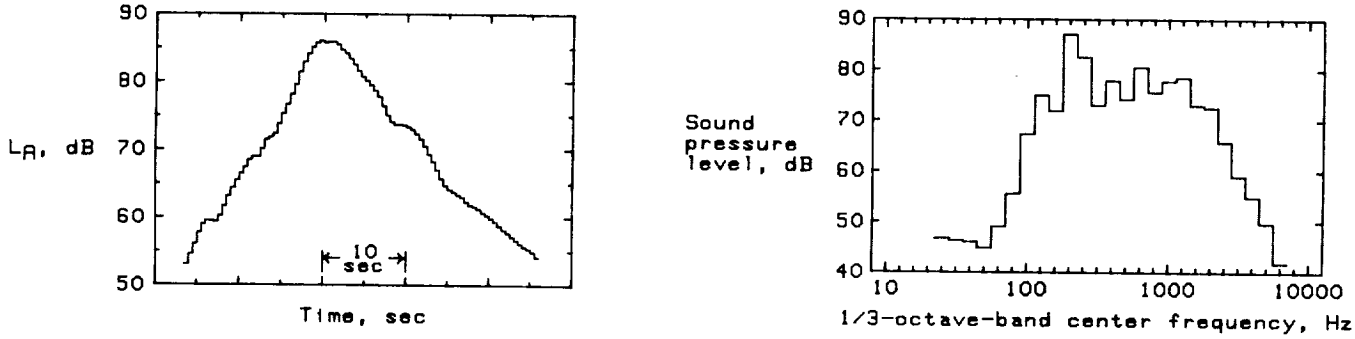

(o) $F_{of} = 247.5$ Hz; $F_{oa} = 225$ Hz; $T/N = 15$ dB.

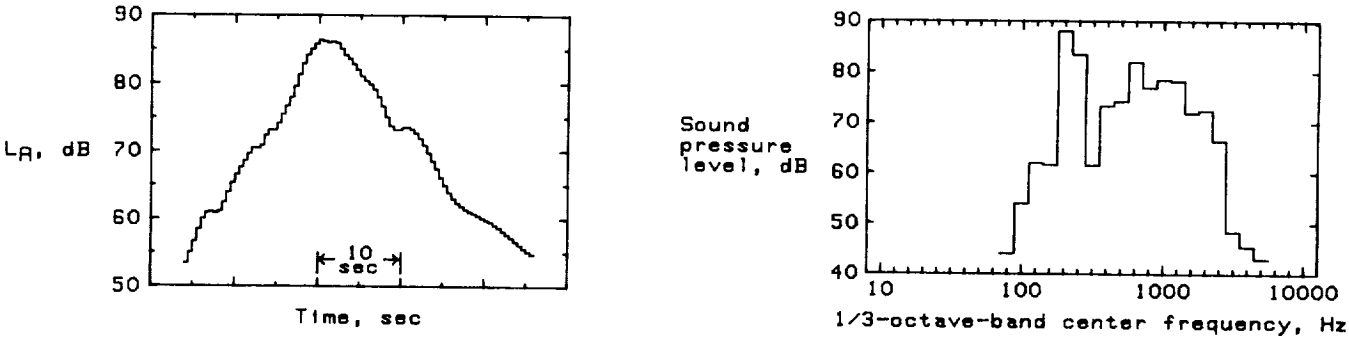

(p) $F_{of} = 247.5$ Hz; $F_{oa} = 225$ Hz; $T/N = 30$dB.

Figure 18. Continued.

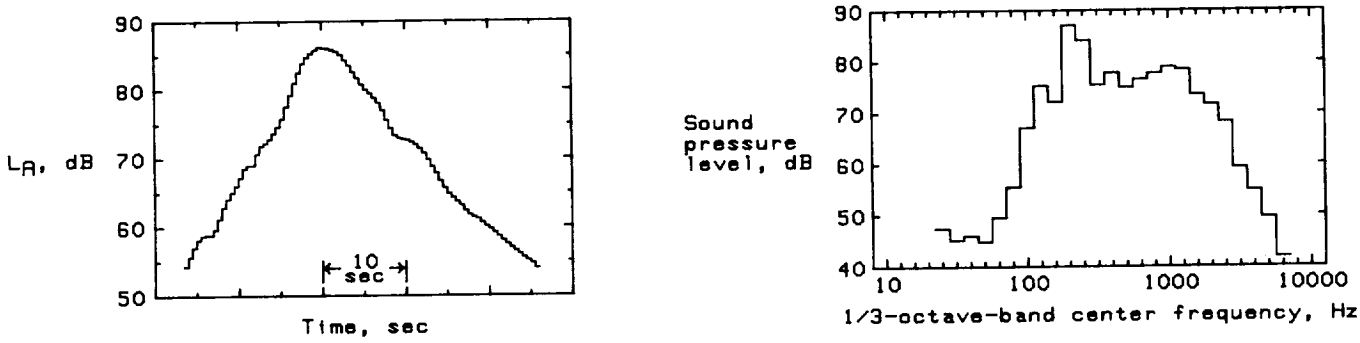

(q) $F_{of} = 270$ Hz; $F_{oa} = 225$ Hz; $T/N = 15$ dB.

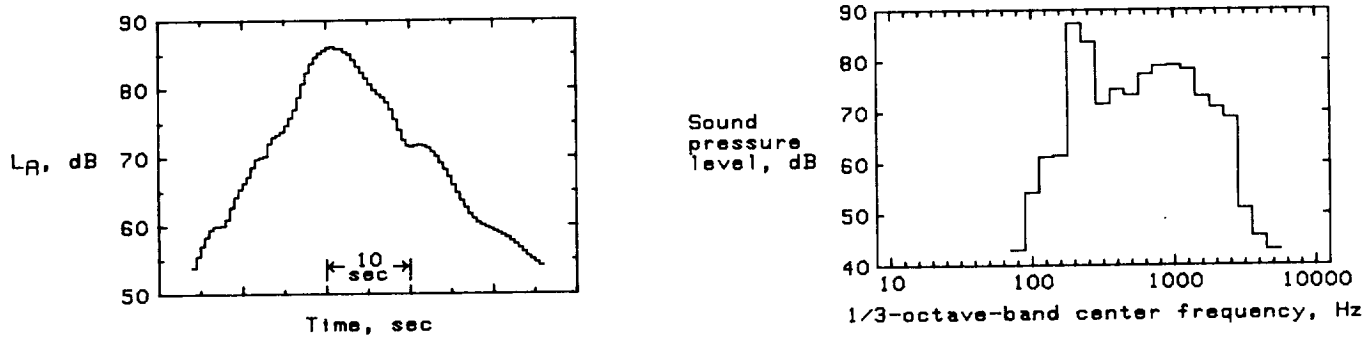

(r) $F_{of} = 270$ Hz; $F_{oa} = 225$ Hz, $T/N = 30$ dB.

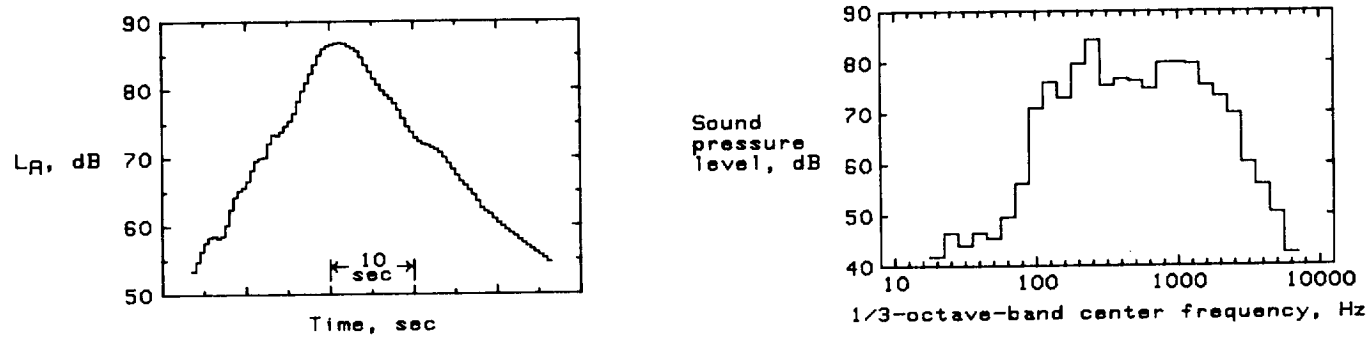

(s) $F_{of} = 270$ Hz; $F_{oa} = 247.5$ Hz; $T/N = 15$ dB.

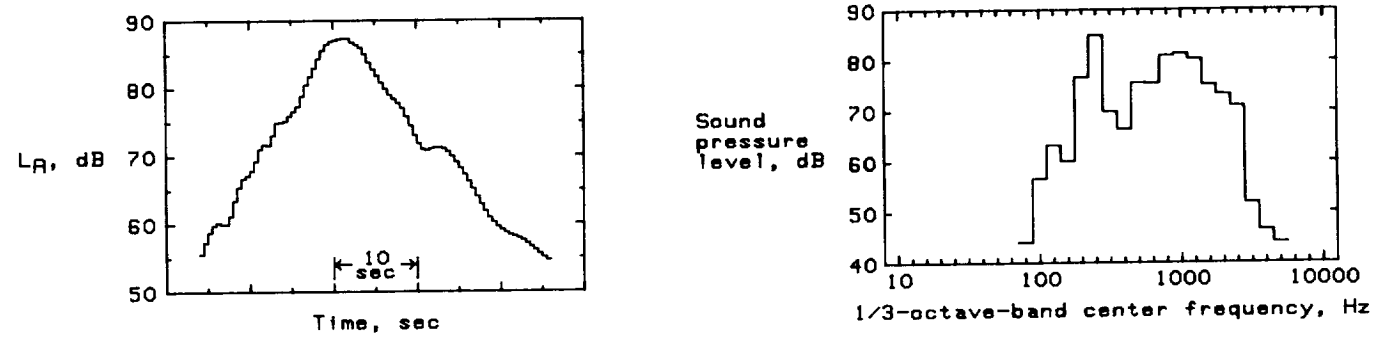

(t) $F_{of} = 270$ Hz; $F_{oa} = 247.5$ Hz; $T/N = 30$ dB.

Figure 18. Concluded.

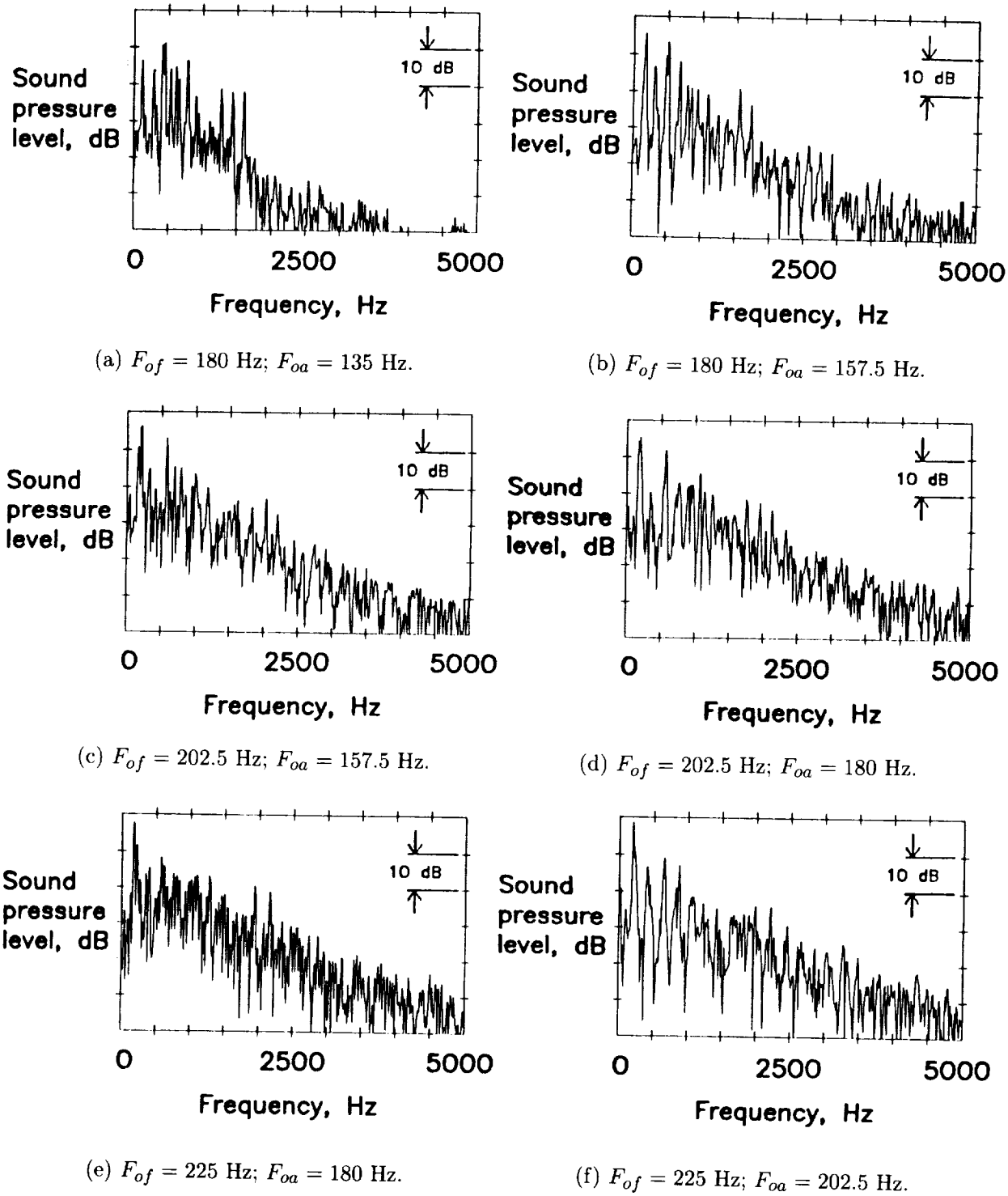

(a) F_{of} = 180 Hz; F_{oa} = 135 Hz.

(b) F_{of} = 180 Hz; F_{oa} = 157.5 Hz.

(c) F_{of} = 202.5 Hz; F_{oa} = 157.5 Hz.

(d) F_{of} = 202.5 Hz; F_{oa} = 180 Hz.

(e) F_{of} = 225 Hz; F_{oa} = 180 Hz.

(f) F_{of} = 225 Hz; F_{oa} = 202.5 Hz.

Figure 19. Narrowband spectrum of each $n \times m$ CRP advanced turboprop flyover noise with 30-dB tone-to-broadband noise ratio. (Spectra measured at point in time history corresponding to no Doppler shift in frequency.)

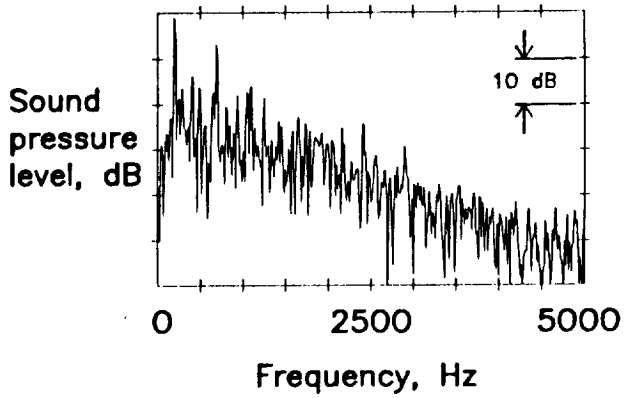

(g) $F_{of} = 247.5$ Hz; $F_{oa} = 202.5$ Hz.

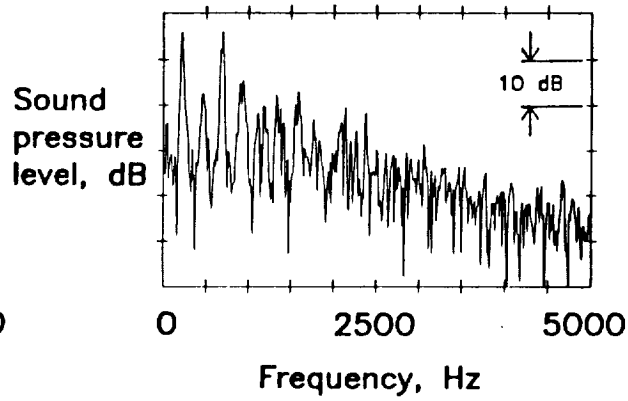

(h) $F_{of} = 247.5$ Hz; $F_{oa} = 225$ Hz.

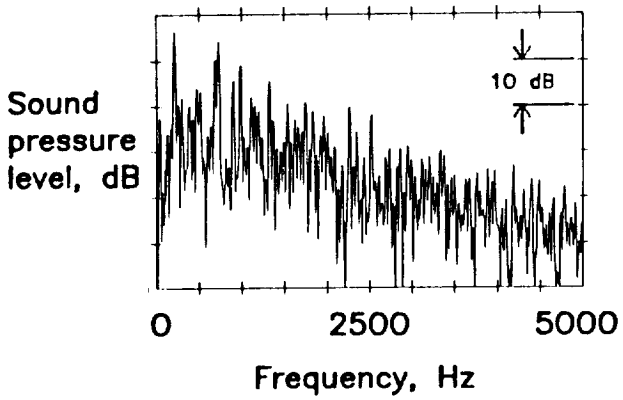

(i) $F_{of} = 270$ Hz; $F_{oa} = 225$ Hz.

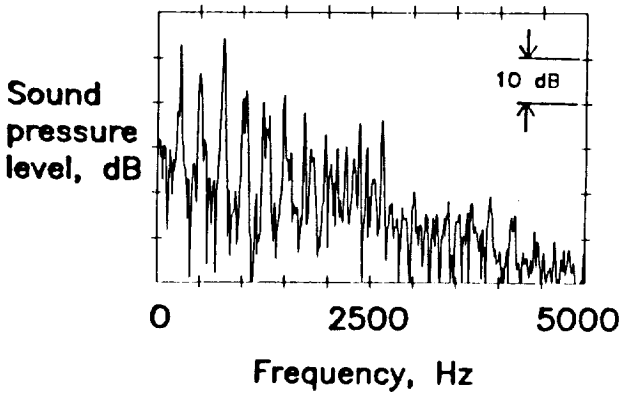

(j) $F_{of} = 270$ Hz; $F_{oa} = 247.5$ Hz.

Figure 19. Concluded.

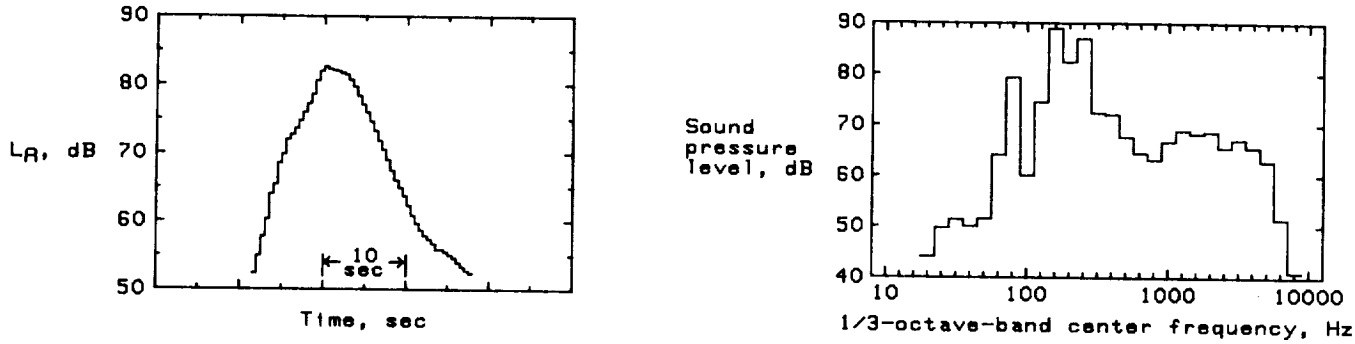

(a) Lockheed P-3 takeoff.

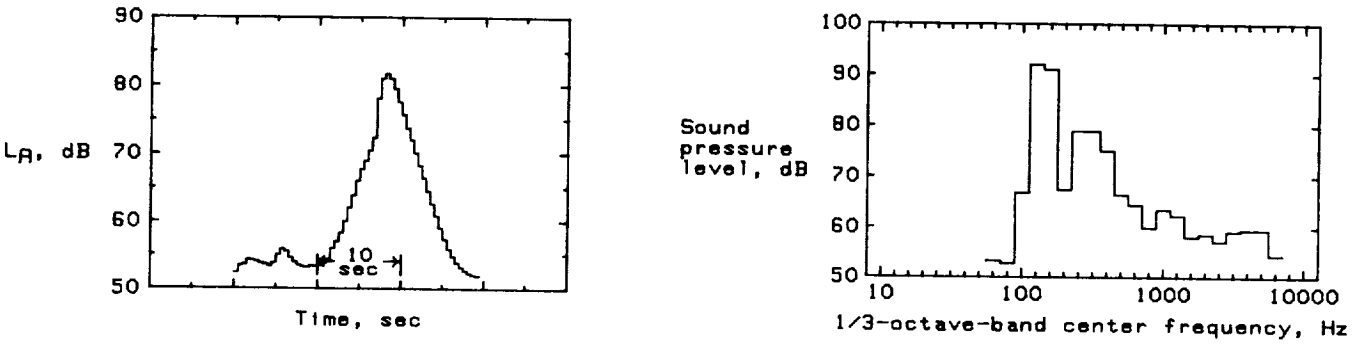

(b) Shorts 330 takeoff.

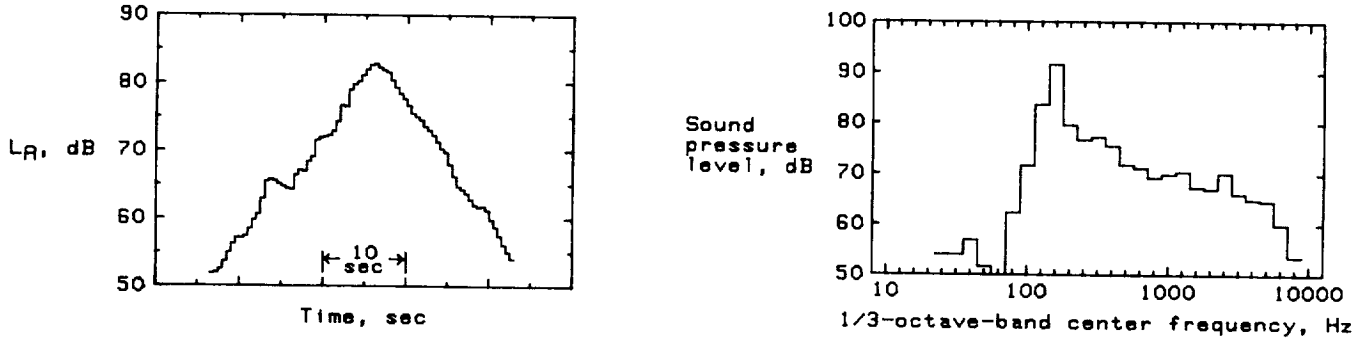

(c) de Havilland Canada DHC-7 Dash 7 takeoff.

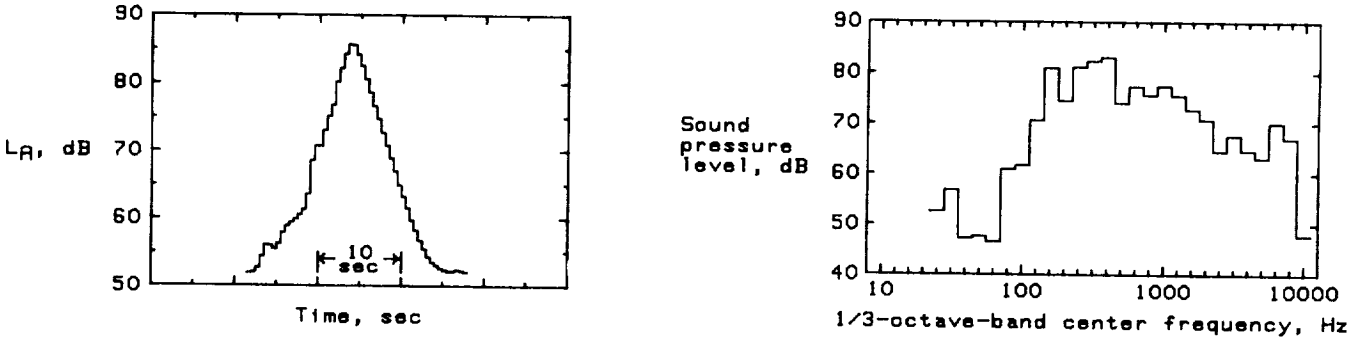

(d) Nord 262 takeoff.

Figure 20. L_A time histories and 1/3-octave-band spectra at peak L_A of the highest level presentations of takeoffs of conventional turboprop and turbofan aircraft.

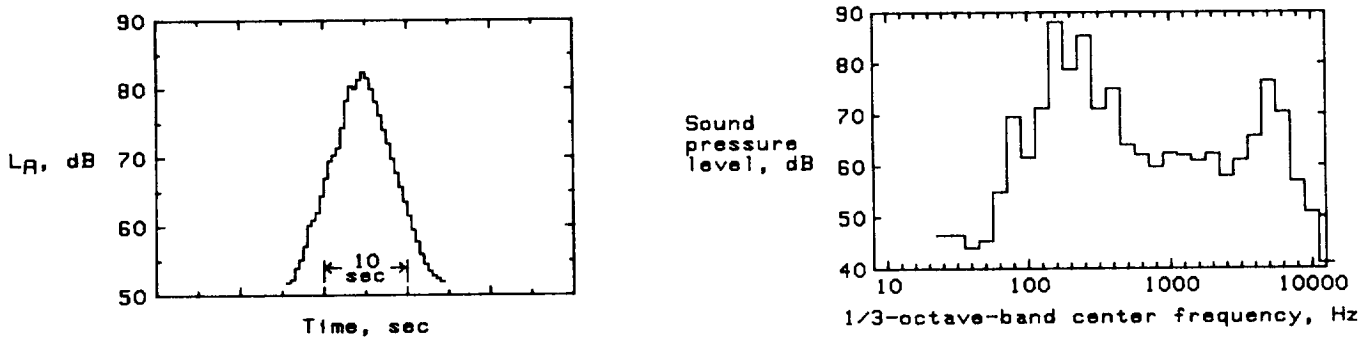

(e) NAMC YS-11 takeoff.

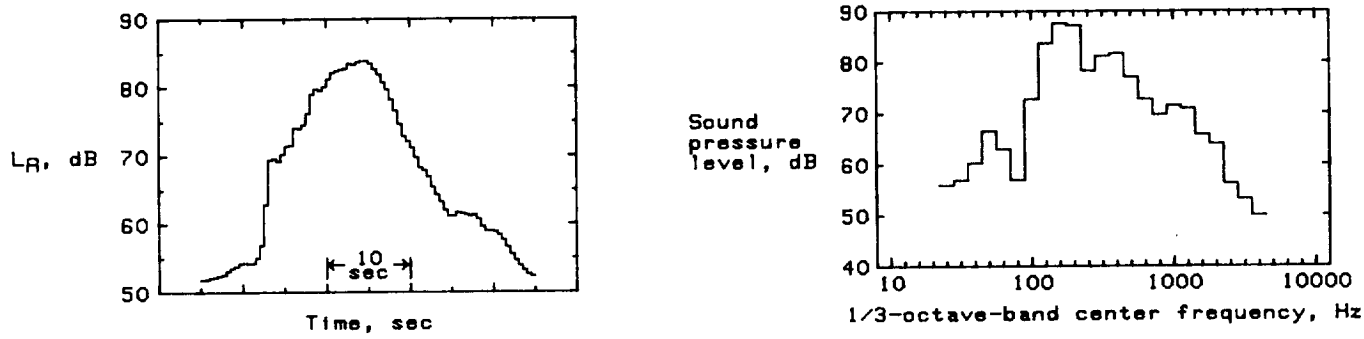

(f) Airbus Industrie A-300 takeoff.

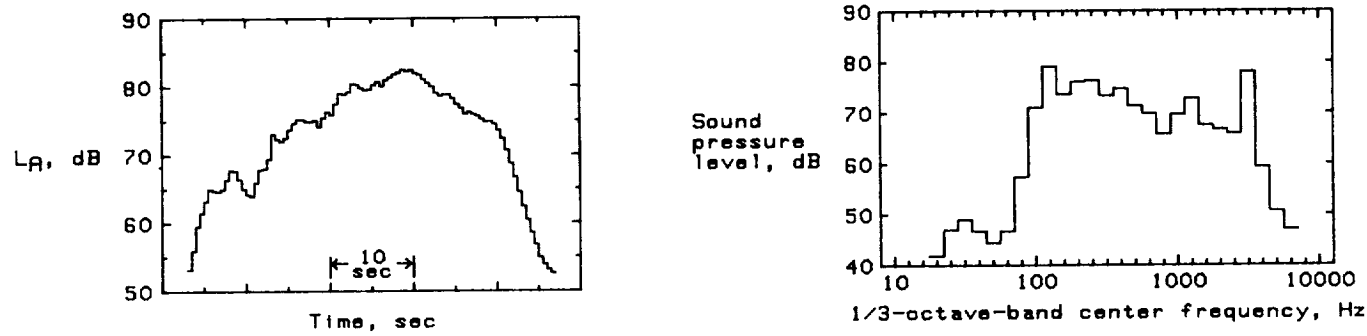

(g) Boeing 707 takeoff.

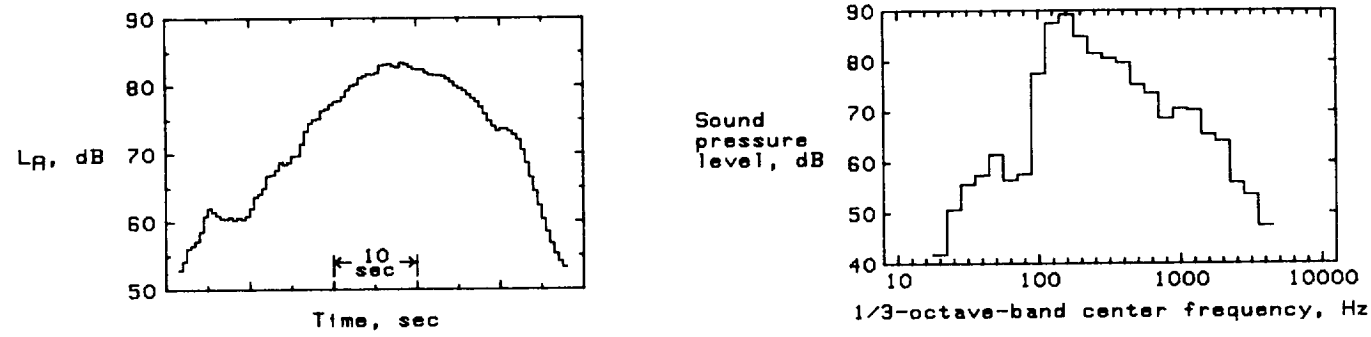

(h) Boeing 727-200 takeoff.

Figure 20. Continued.

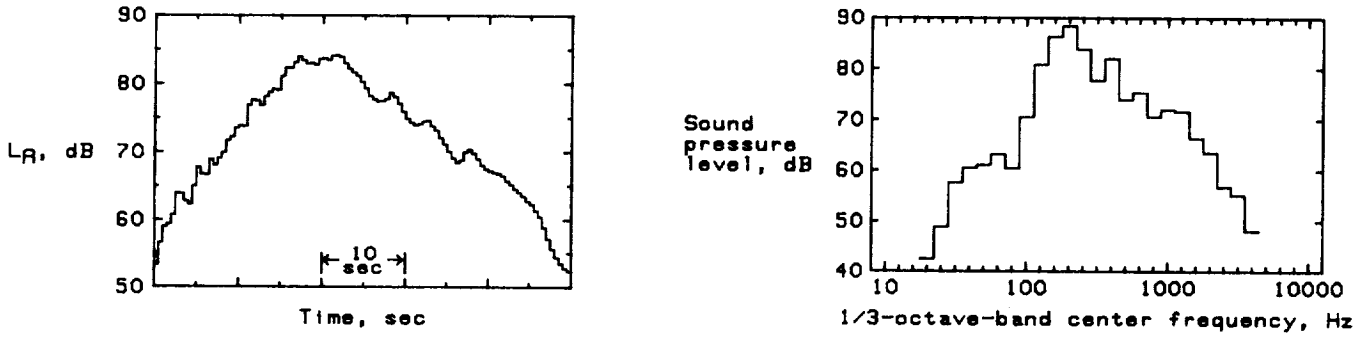

(i) McDonnell Douglas DC-9 takeoff.

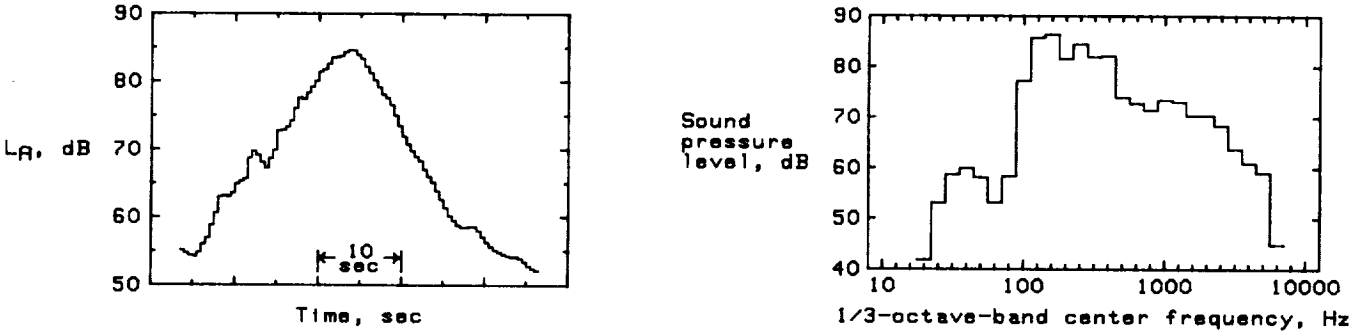

(j) McDonnell Douglas DC-10 takeoff.

Figure 20. Concluded.

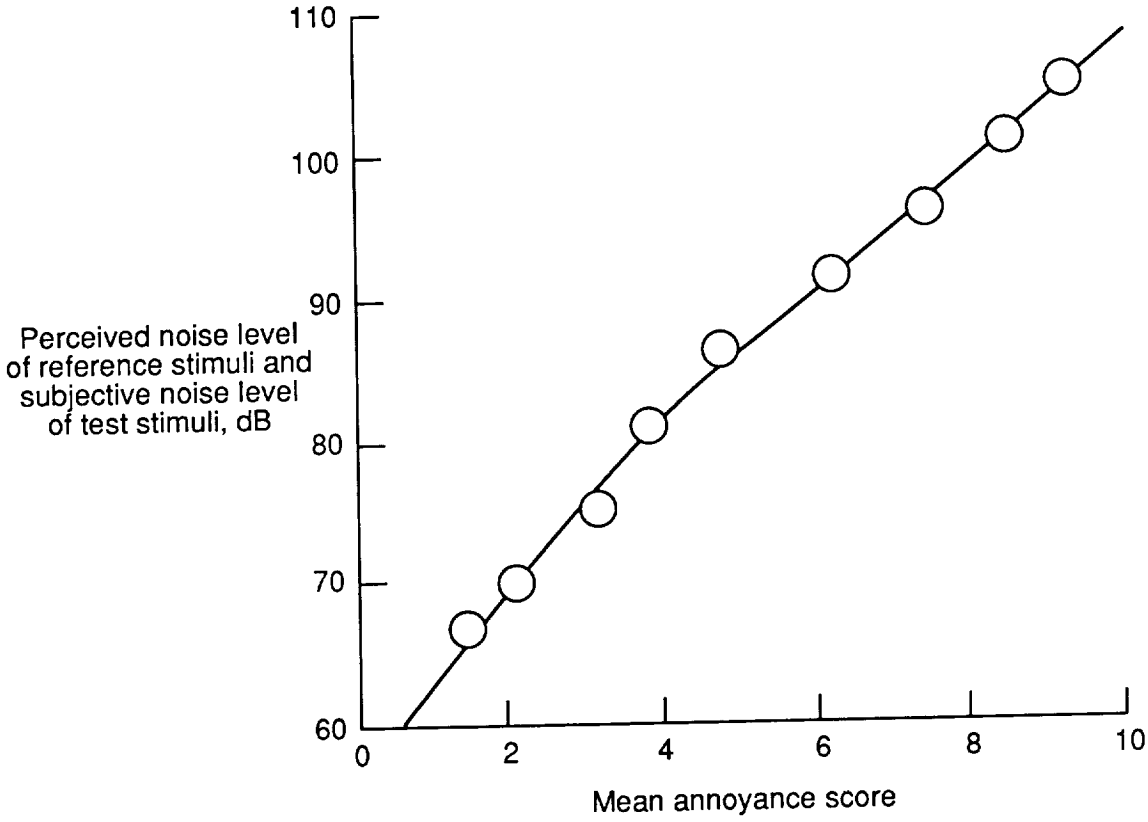

Figure 21. Regression analyses of PNL on mean annoyance scores for Boeing 727 takeoff stimuli used to convert annoyance judgments to subjective noise levels L_S.

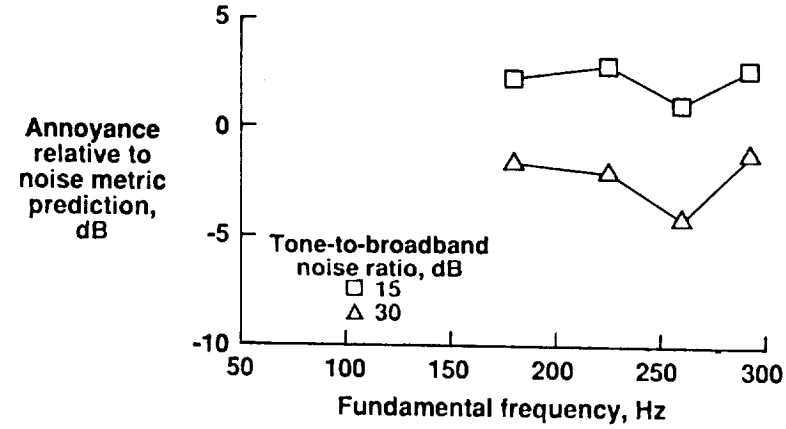

(a) L_A.

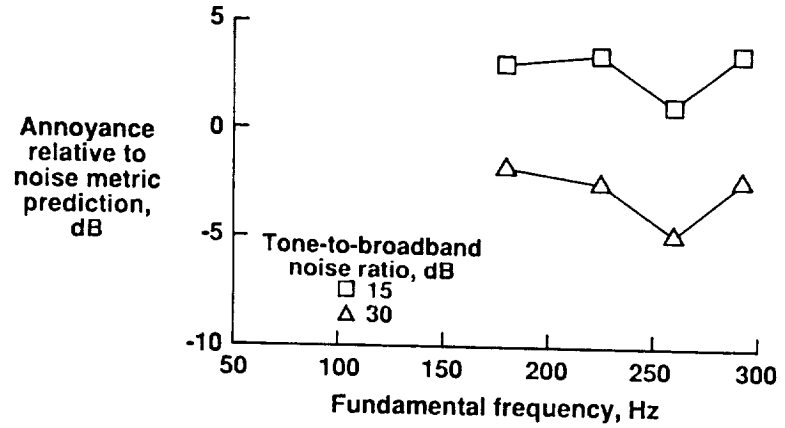

(b) L_A with T_1 tone correction.

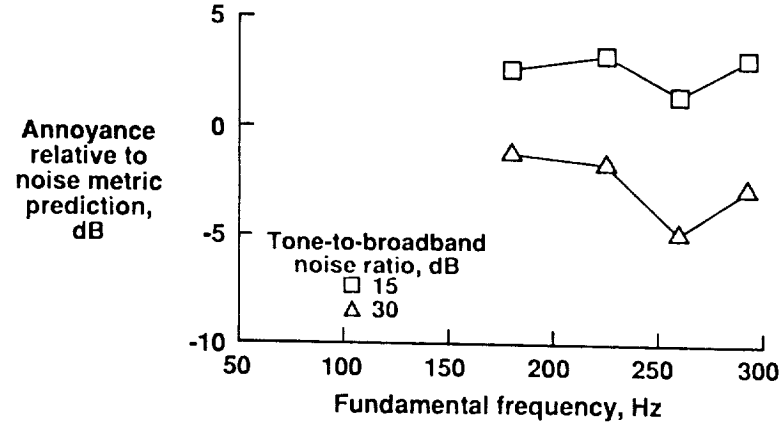

(c) L_A with T_2 tone correction.

Figure 22. Effect of interaction of fundamental frequency with tone-to-broadband noise ratio on annoyance prediction in terms of different noise metrics for SRP advanced turboprop stimuli.

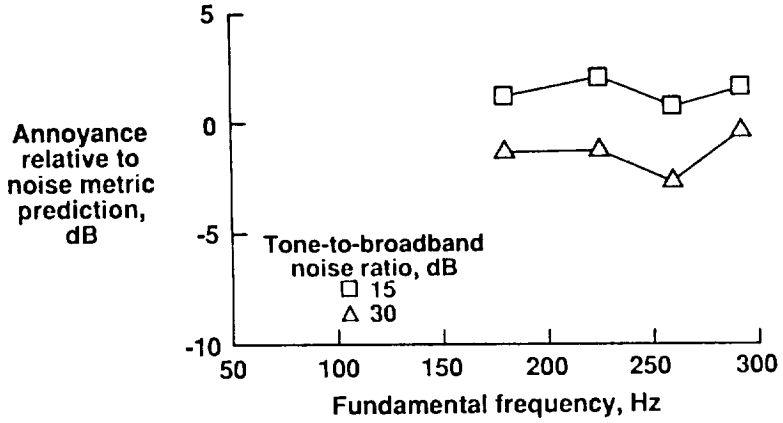

(d) Duration-corrected L_A.

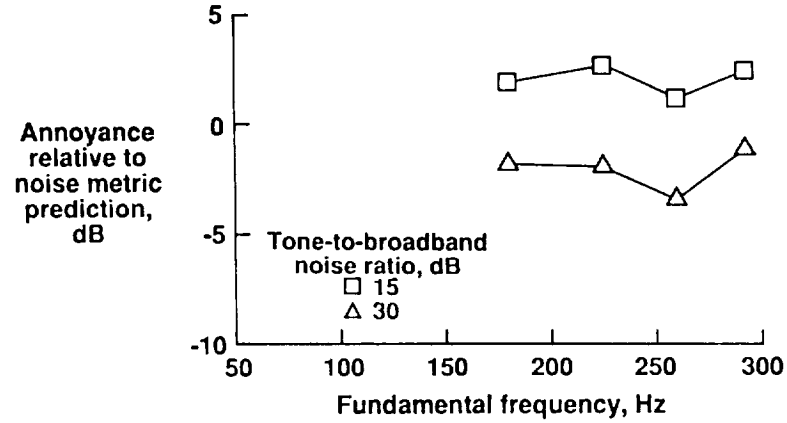

(e) Duration-corrected L_A with T_1 tone correction.

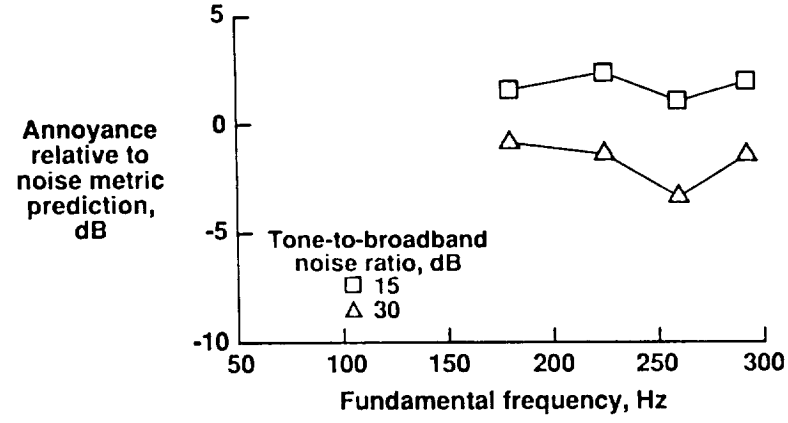

(f) Duration-corrected L_A with T_2 tone correction.

Figure 22. Continued.

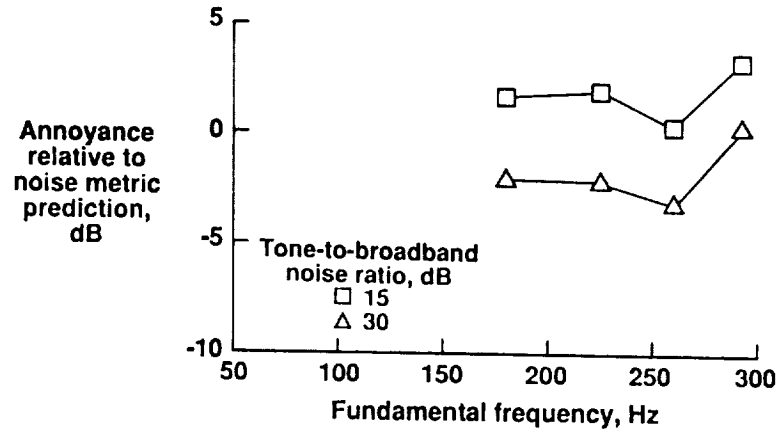

(g) PNL.

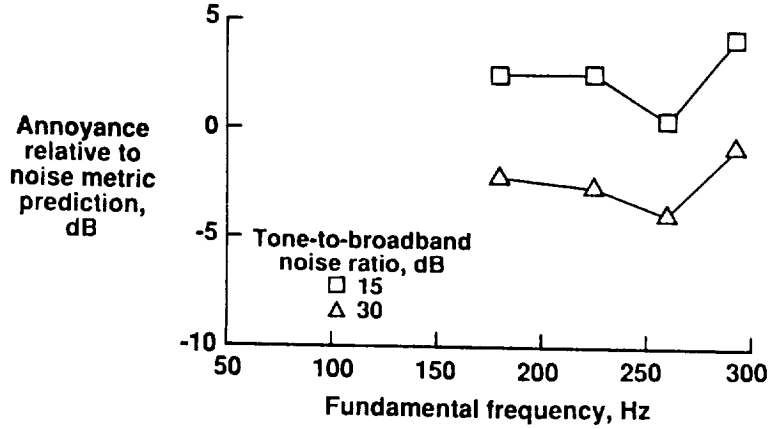

(h) PNL with T_1 tone correction.

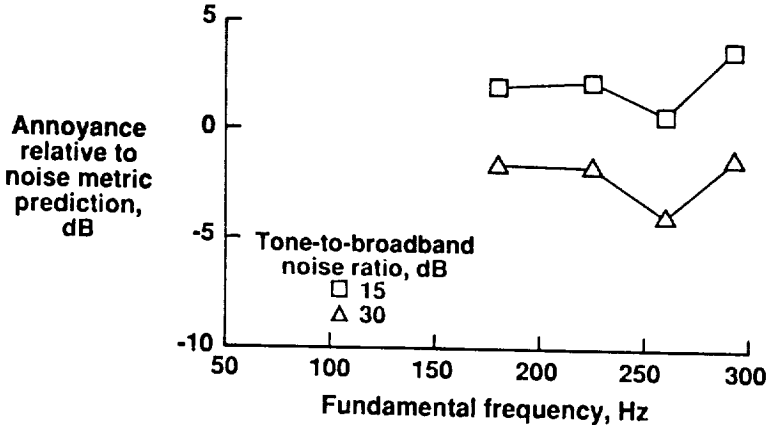

(i) PNL with T_2 tone correction.

Figure 22. Continued.

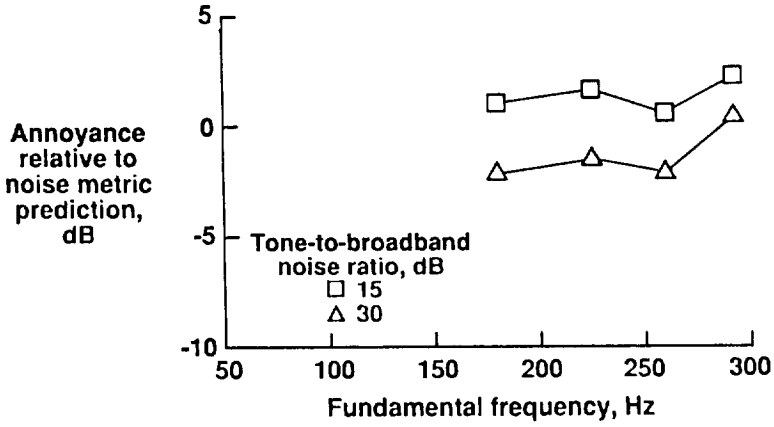

(j) Duration-corrected PNL.

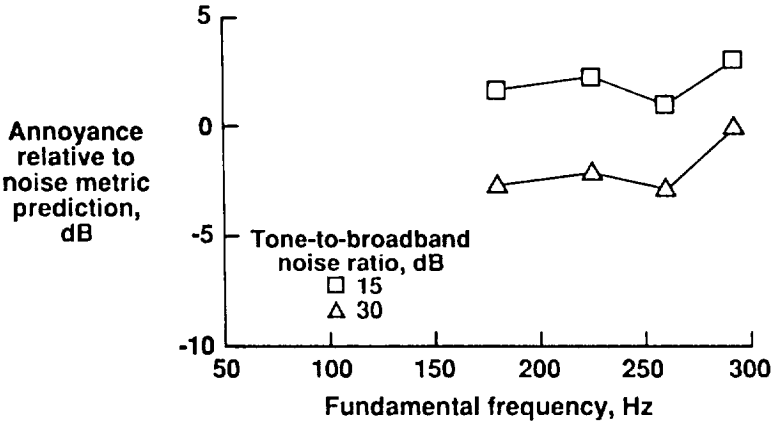

(k) Duration-corrected PNL with T_1 tone correction.

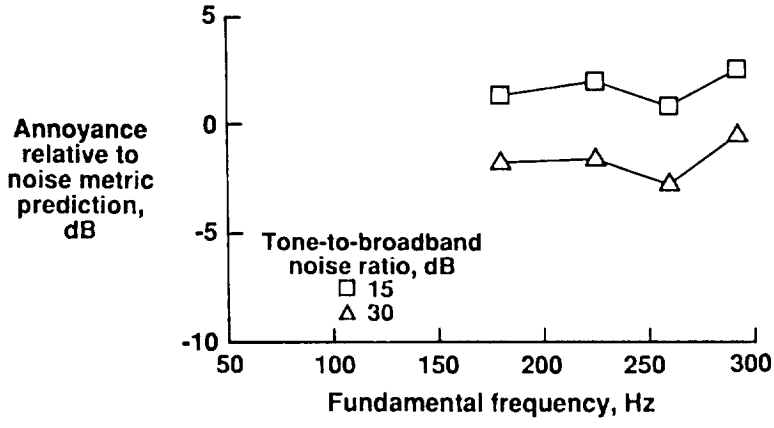

(l) Duration-corrected PNL with T_2 tone correction.

Figure 22. Continued.

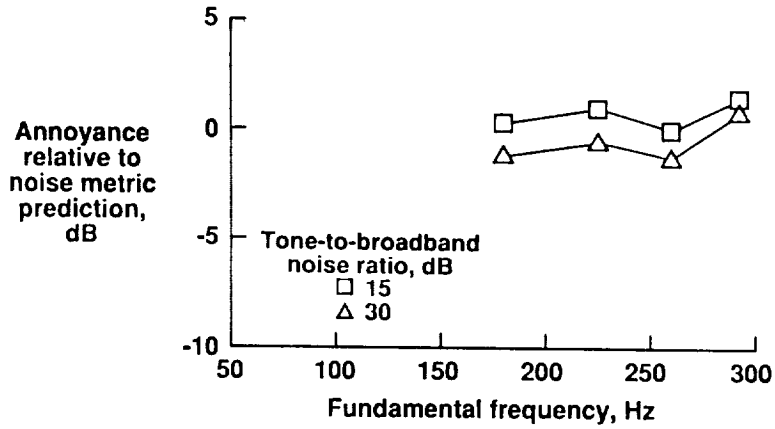

(m) LL_Z.

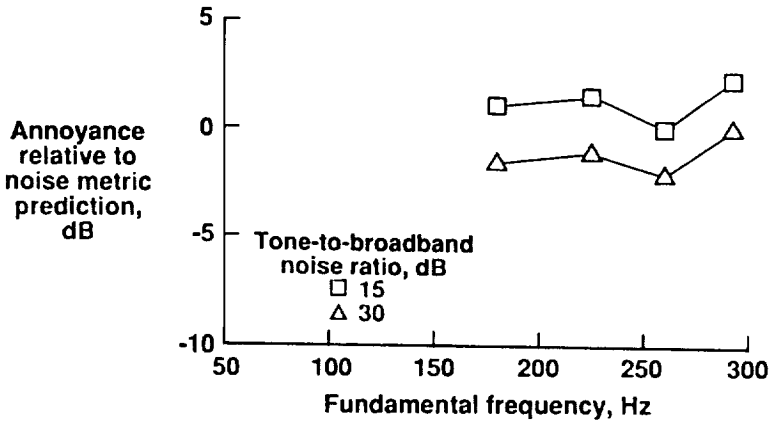

(n) LL_Z with T_1 tone correction.

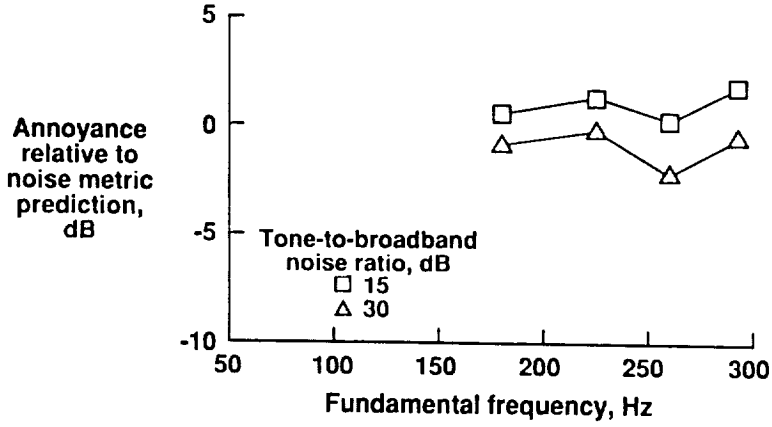

(o) LL_Z with T_2 tone correction.

Figure 22. Continued.

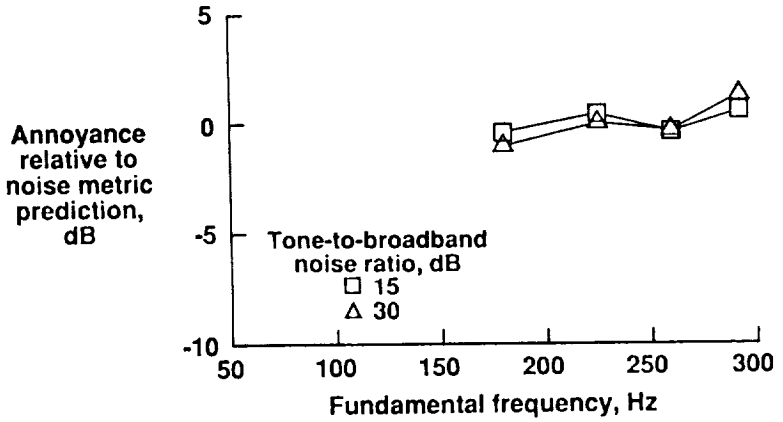

(p) Duration-corrected LL_Z.

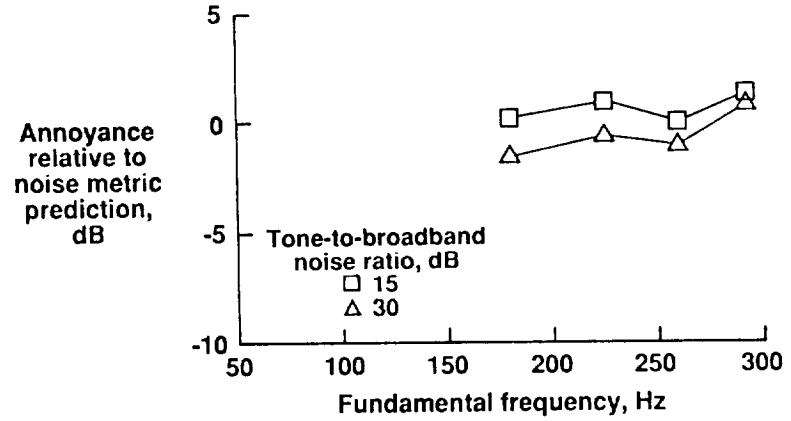

(q) Duration-corrected LL_Z with T_1 tone correction.

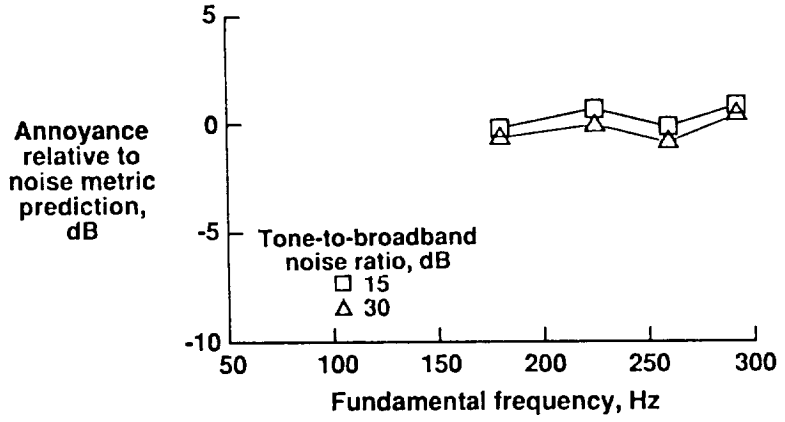

(r) Duration-corrected LL_Z with T_2 tone correction.

Figure 22. Concluded.

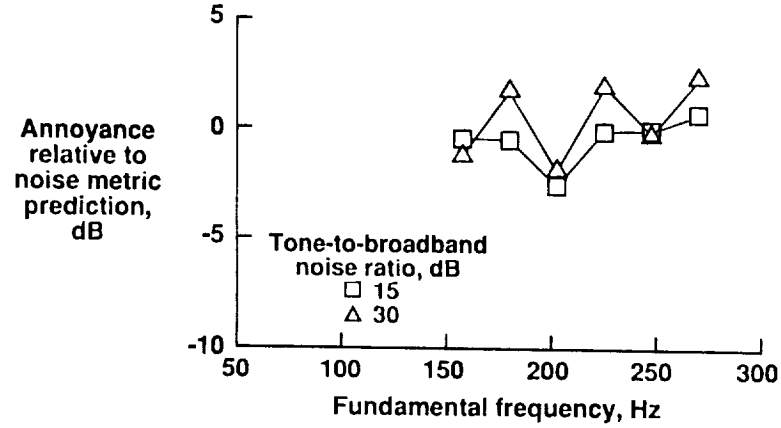

(a) L_A.

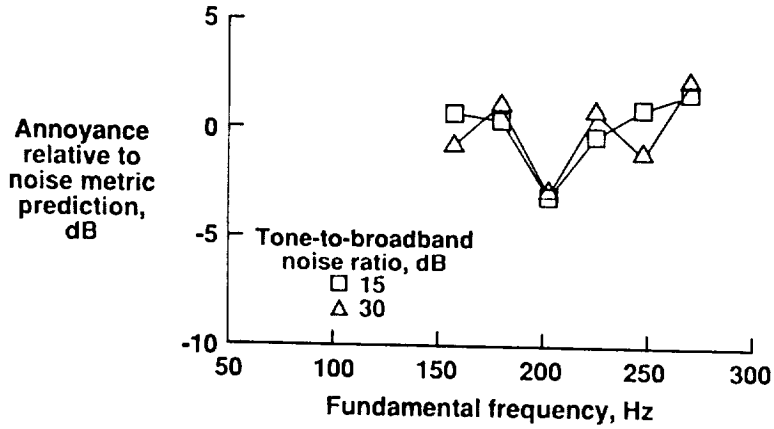

(b) L_A with T_1 tone correction.

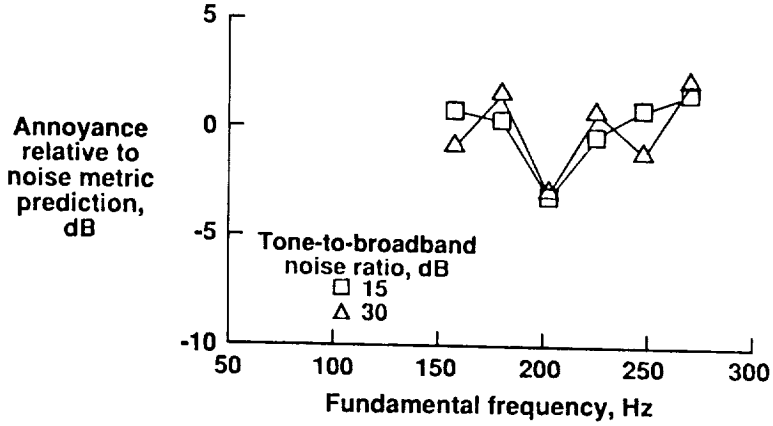

(c) L_A with T_2 tone correction.

Figure 23. Effect of interaction of fundamental frequency with tone-to-broadband noise ratio on annoyance prediction in terms of different noise metrics for $n \times n$ CRP advanced turboprop stimuli.

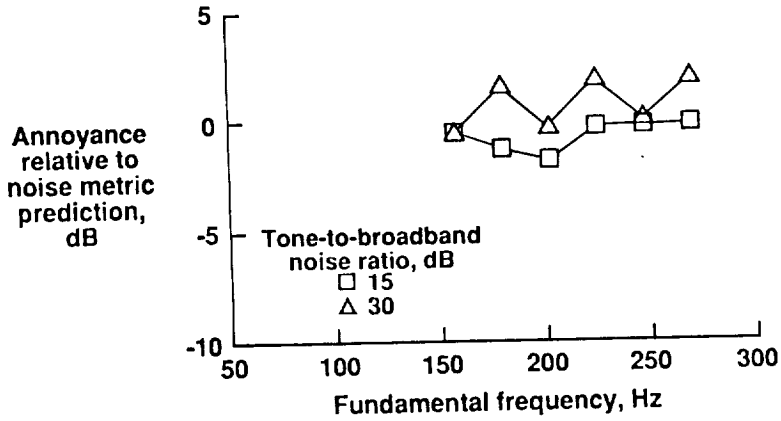

(d) Duration-corrected L_A.

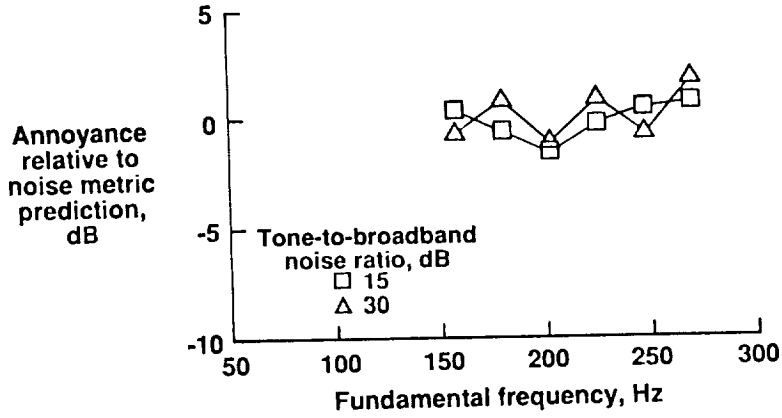

(e) Duration-corrected L_A with T_1 tone correction.

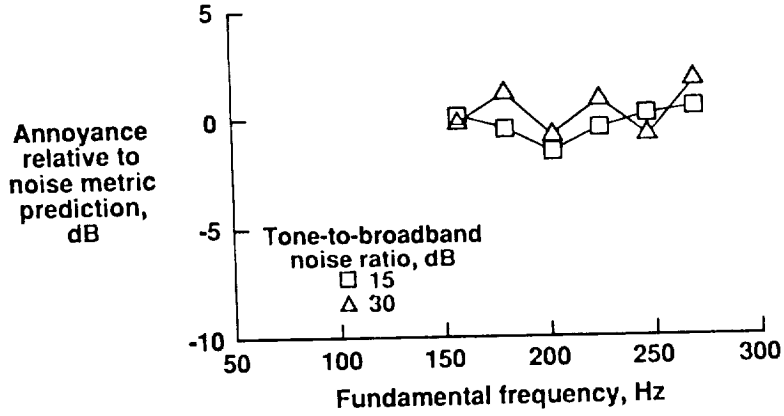

(f) Duration-corrected L_A with T_2 tone correction.

Figure 23. Continued.

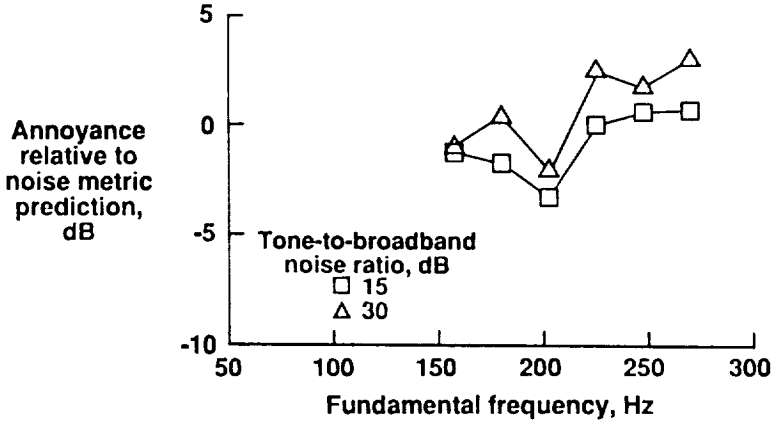

(g) PNL.

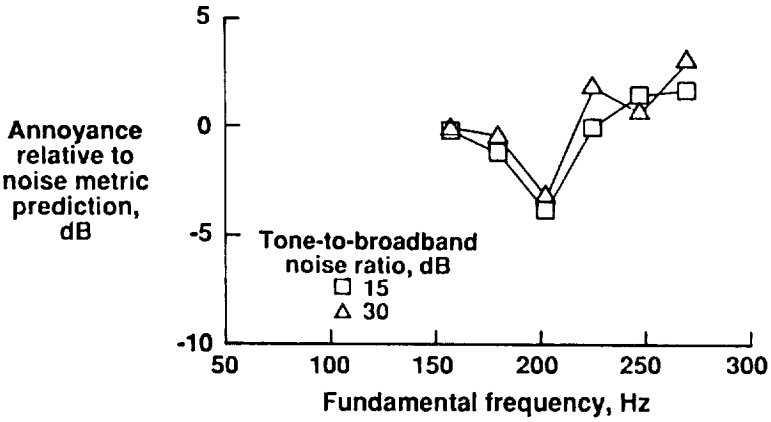

(h) PNL with T_1 tone correction.

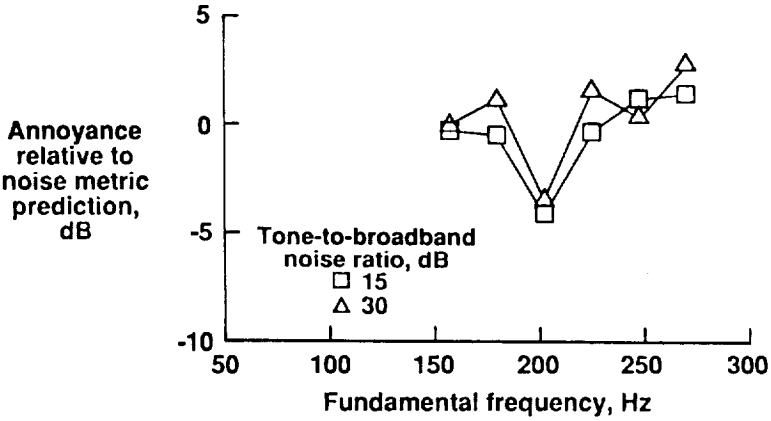

(i) PNL with T_2 tone correction.

Figure 23. Continued.

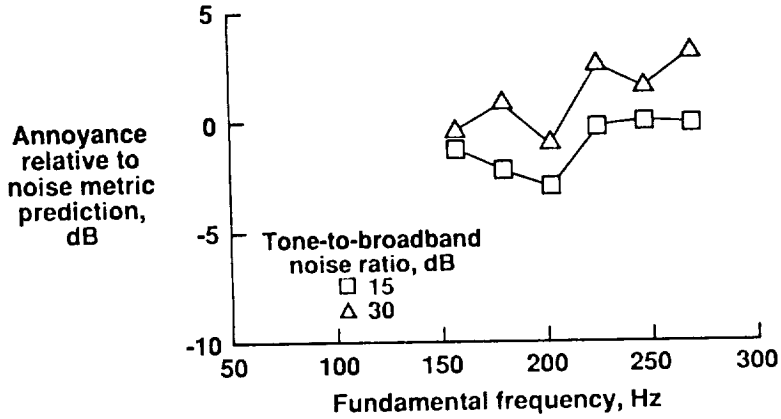

(j) Duration-corrected PNL.

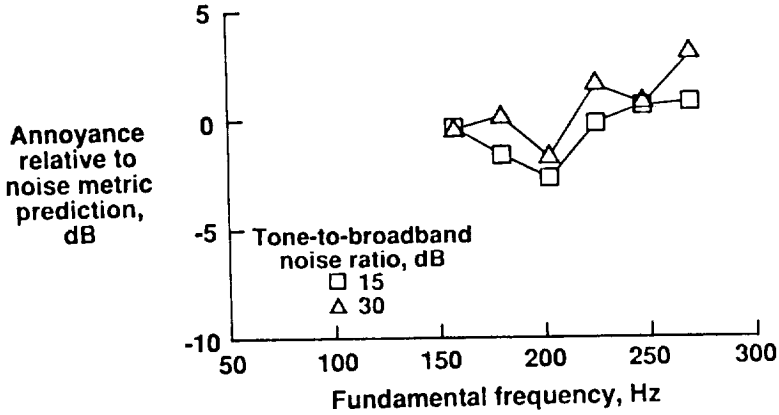

(k) Duration-corrected PNL with T_1 tone correction.

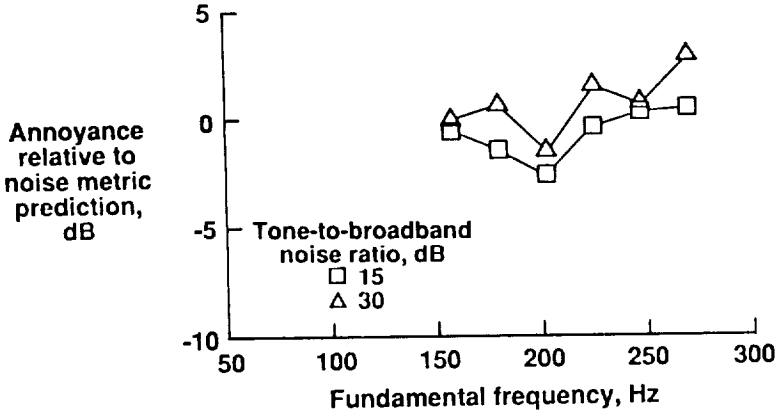

(l) Duration-corrected PNL with T_2 tone correction.

Figure 23. Continued.

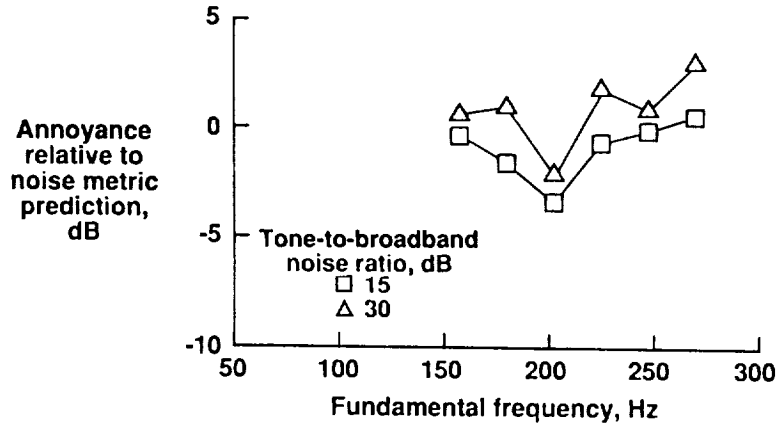

(m) LL_Z.

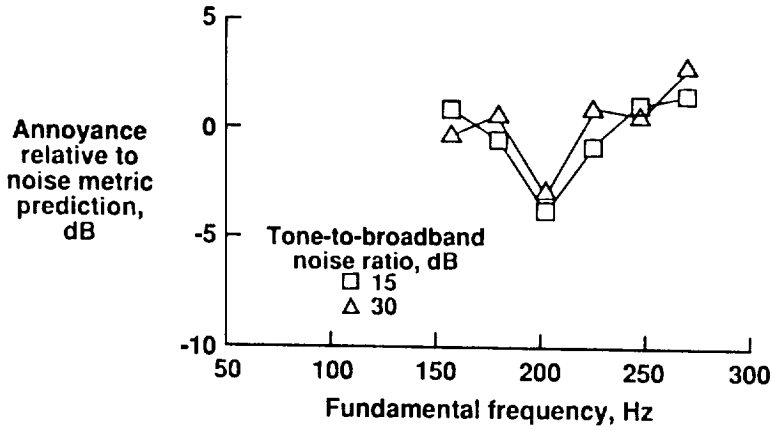

(n) LL_Z with T_1 tone correction.

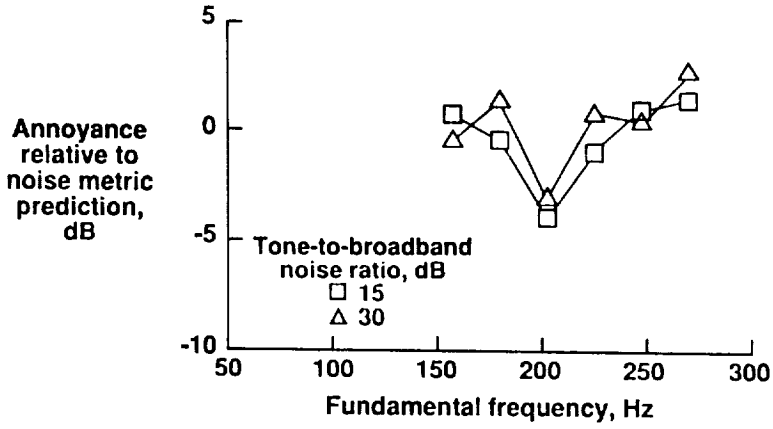

(o) LL_Z with T_2 tone correction.

Figure 23. Continued.

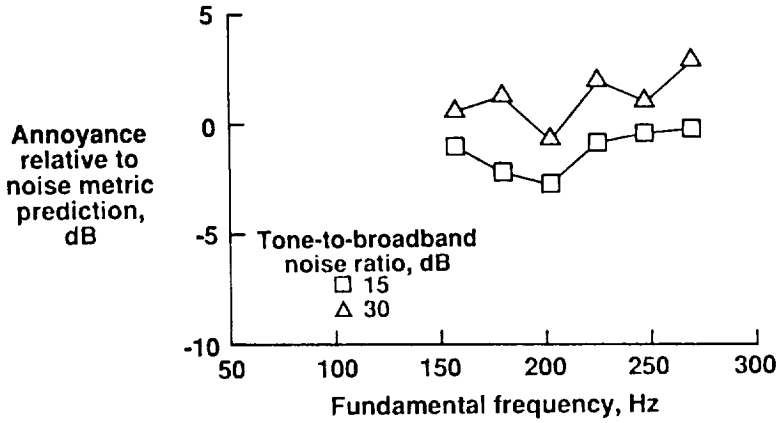

(p) Duration-corrected LL_Z.

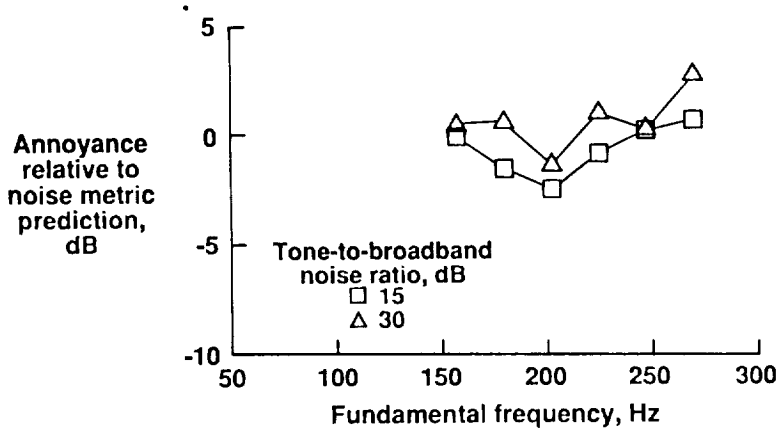

(q) Duration-corrected LL_Z with T_1 tone correction.

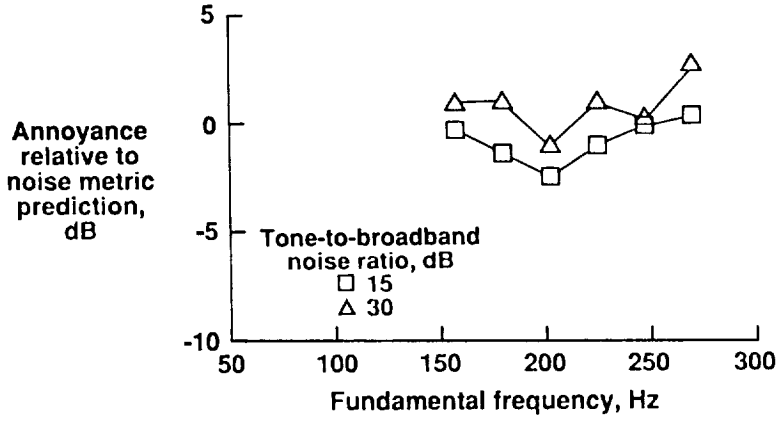

(r) Duration-corrected LL_Z with T_2 tone correction.

Figure 23. Concluded.

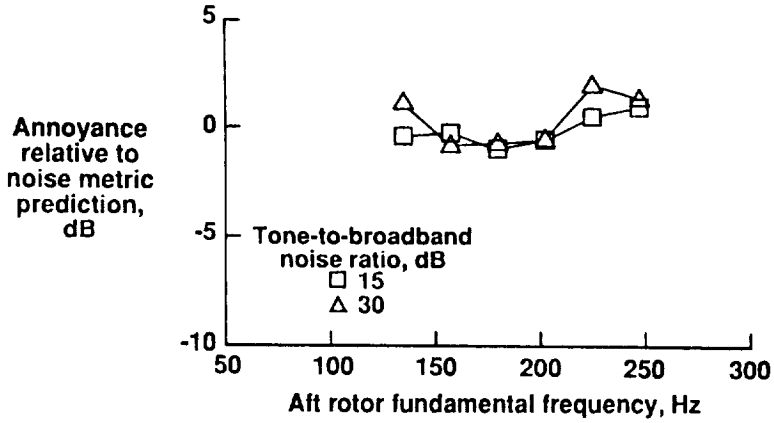

(a) L_A.

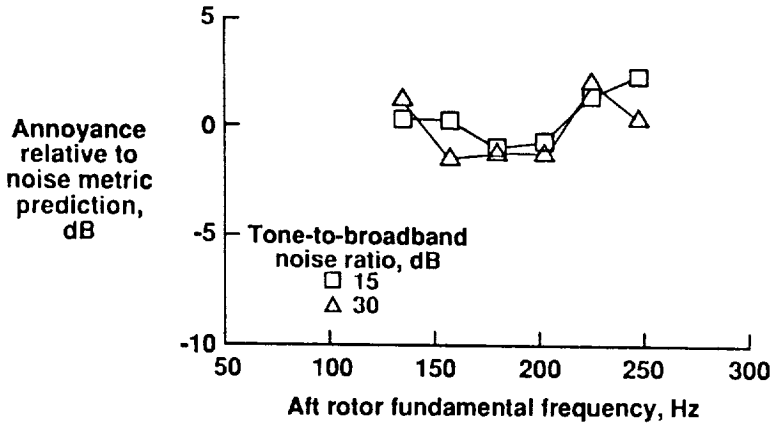

(b) L_A with T_1 tone correction.

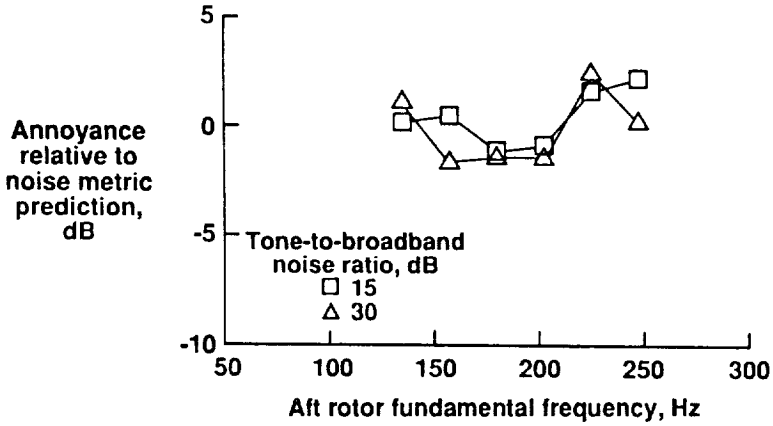

(c) L_A with T_2 tone correction.

Figure 24. Effect of interaction of aft rotor fundamental frequency with tone-to-broadband noise ratio on annoyance prediction in terms of different noise metrics for $n \times m$ CRP advanced turboprop stimuli.

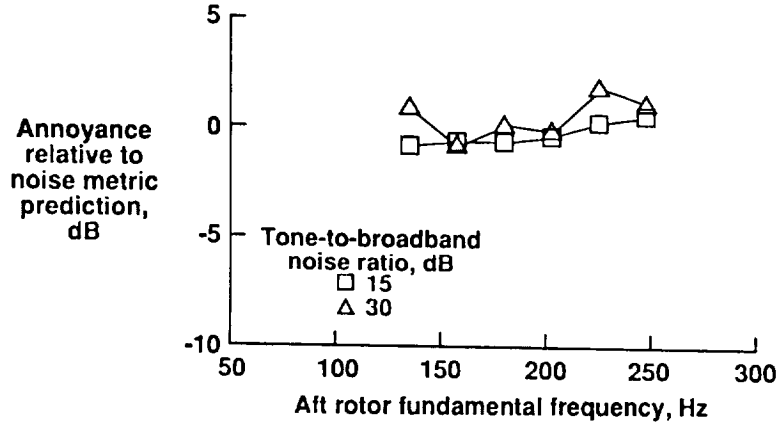

(d) Duration-corrected L_A.

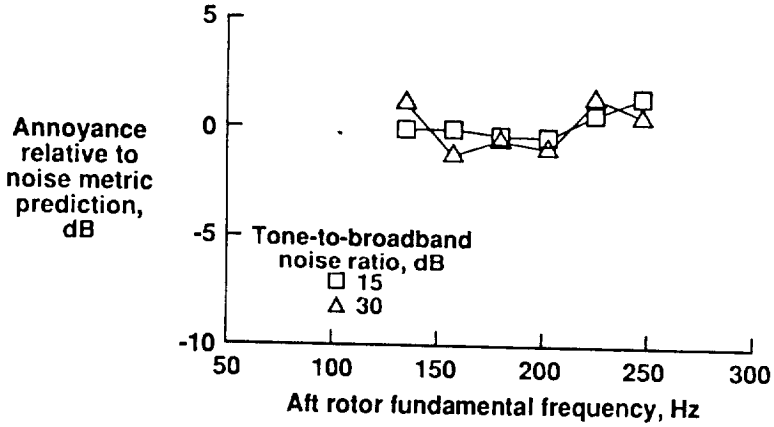

(e) Duration-corrected L_A with T_1 tone correction.

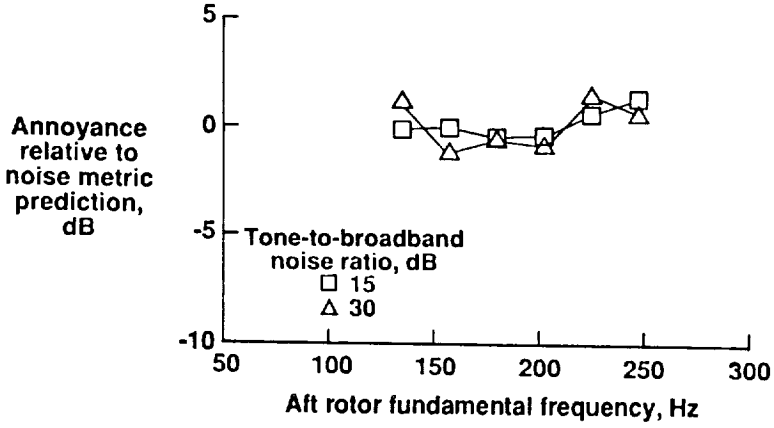

(f) Duration-corrected L_A with T_2 tone correction.

Figure 24. Continued.

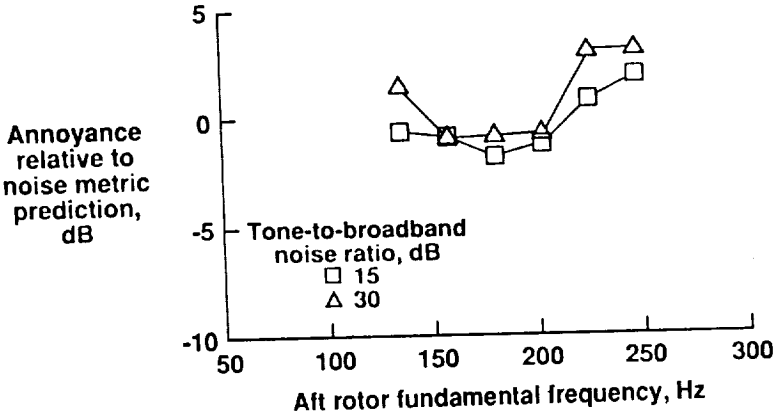

(g) PNL.

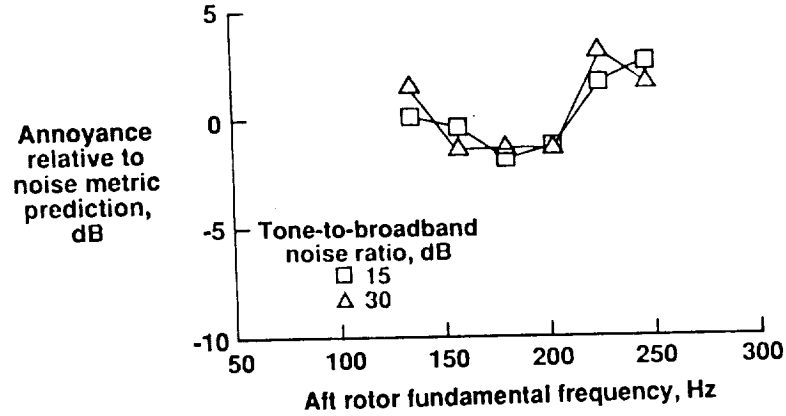

(h) PNL with T_1 tone correction.

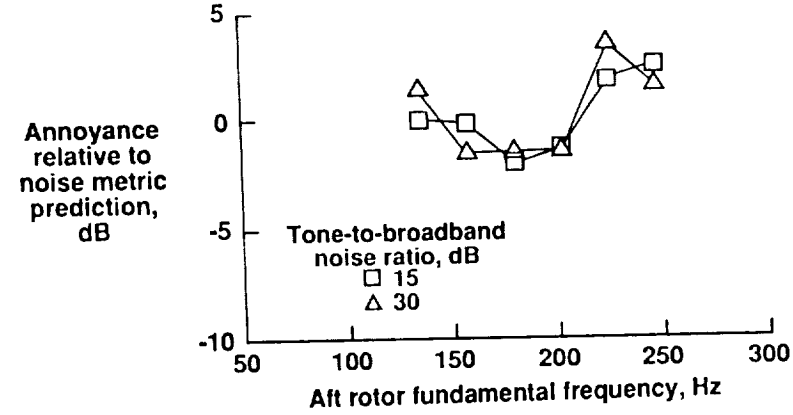

(i) PNL with T_2 tone correction.

Figure 24. Continued.

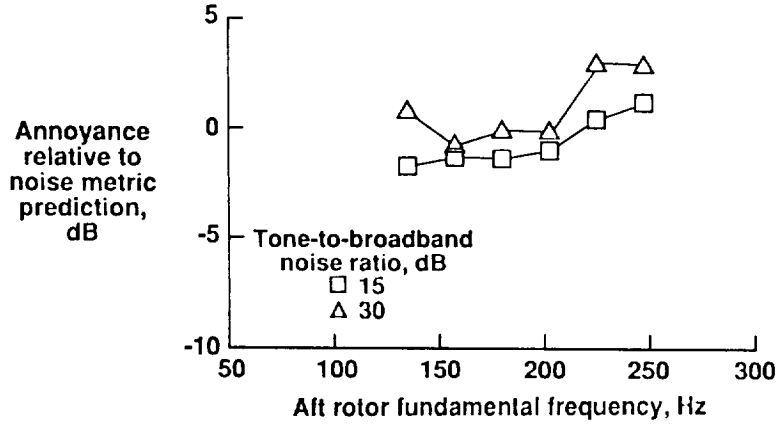

(j) Duration-corrected PNL.

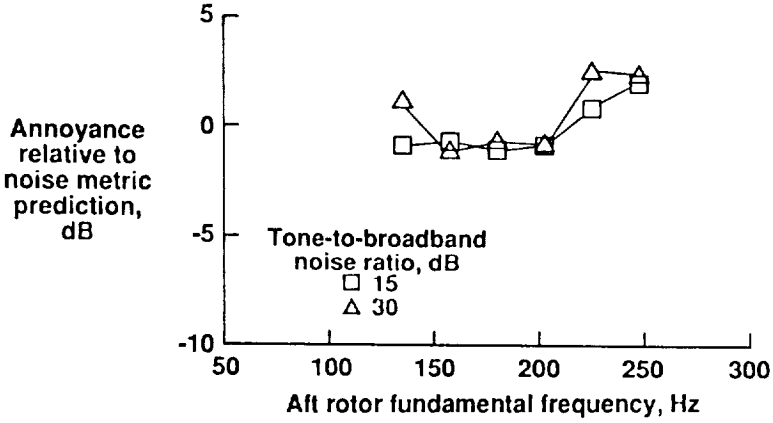

(k) Duration-corrected PNL with T_1 tone correction.

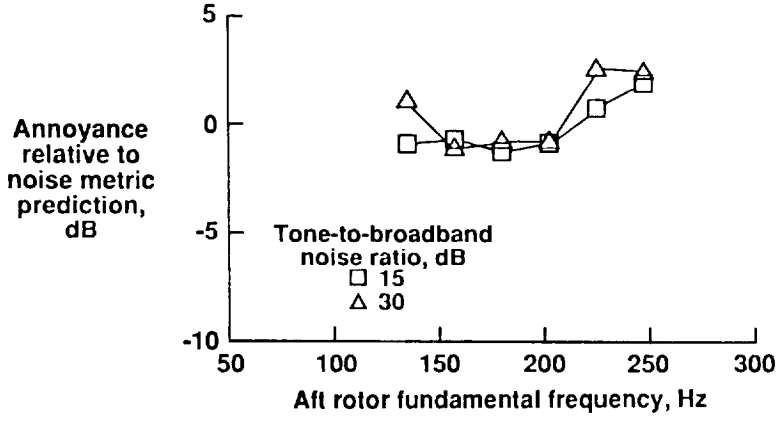

(l) Duration-corrected PNL with T_2 tone correction.

Figure 24. Continued.

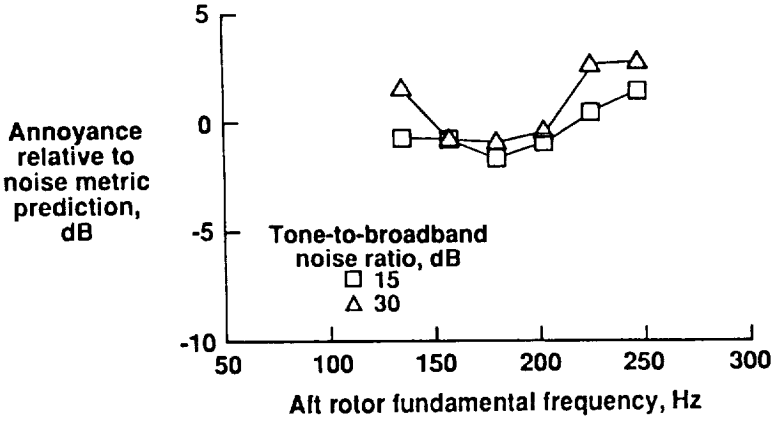

(m) LL_Z.

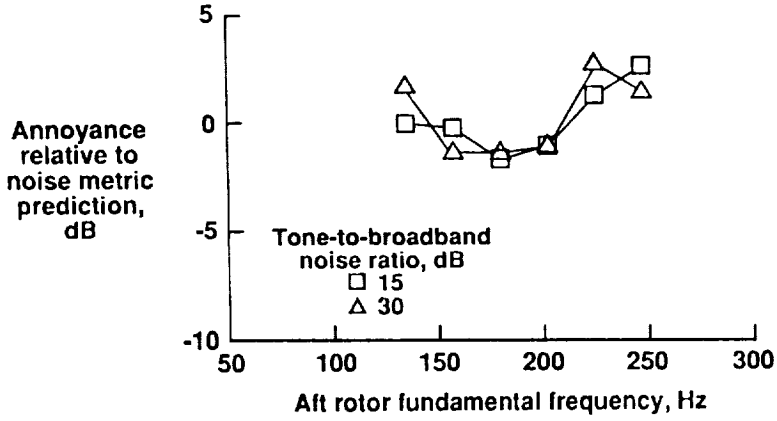

(n) LL_Z with T_1 tone correction.

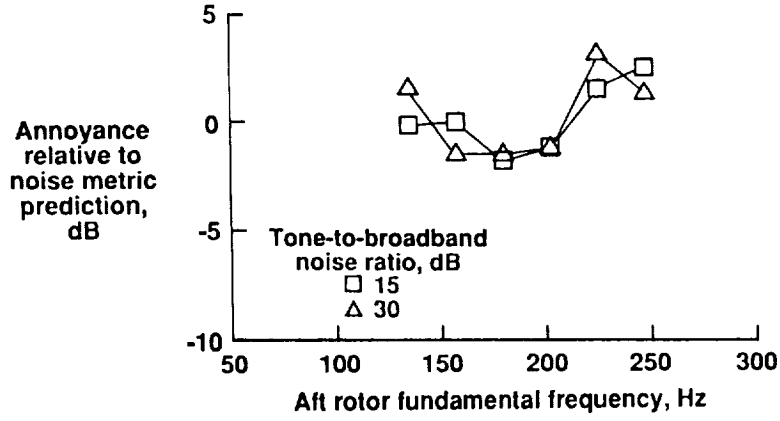

(o) LL_Z with T_2 tone correction.

Figure 24. Continued.

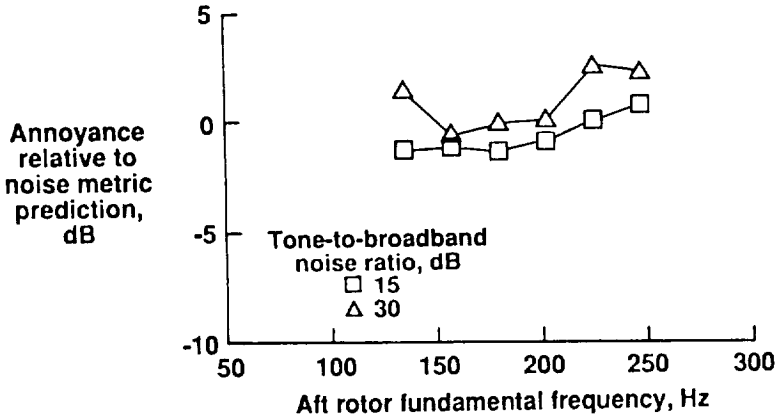

(p) Duration-corrected LL_Z.

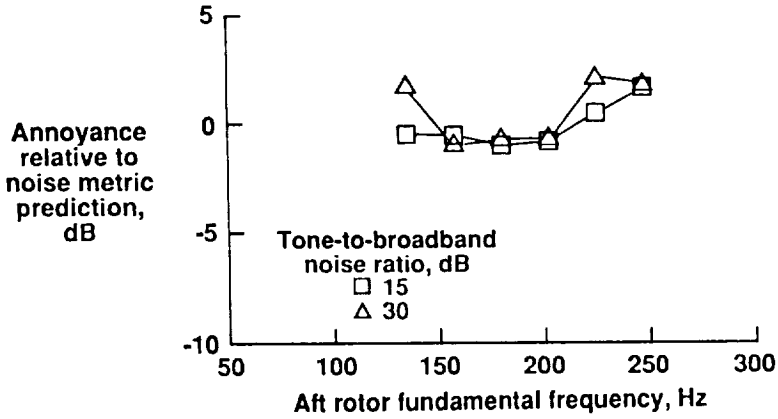

(q) Duration-corrected LL_Z with T_1 tone correction.

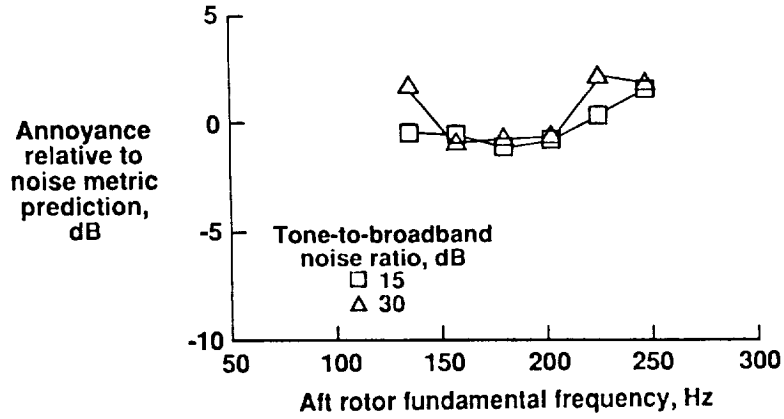

(r) Duration-corrected LL_Z with T_2 tone correction.

Figure 24. Concluded.

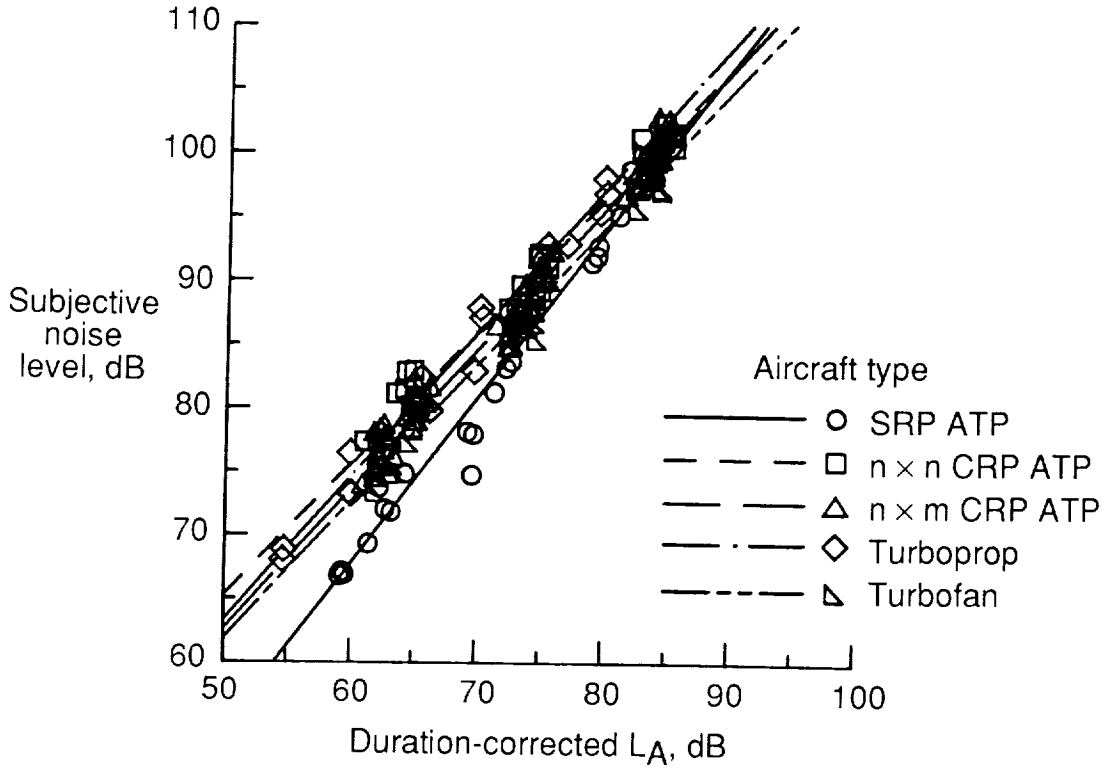

Figure 25. Comparison of annoyance responses using duration-corrected L_A.

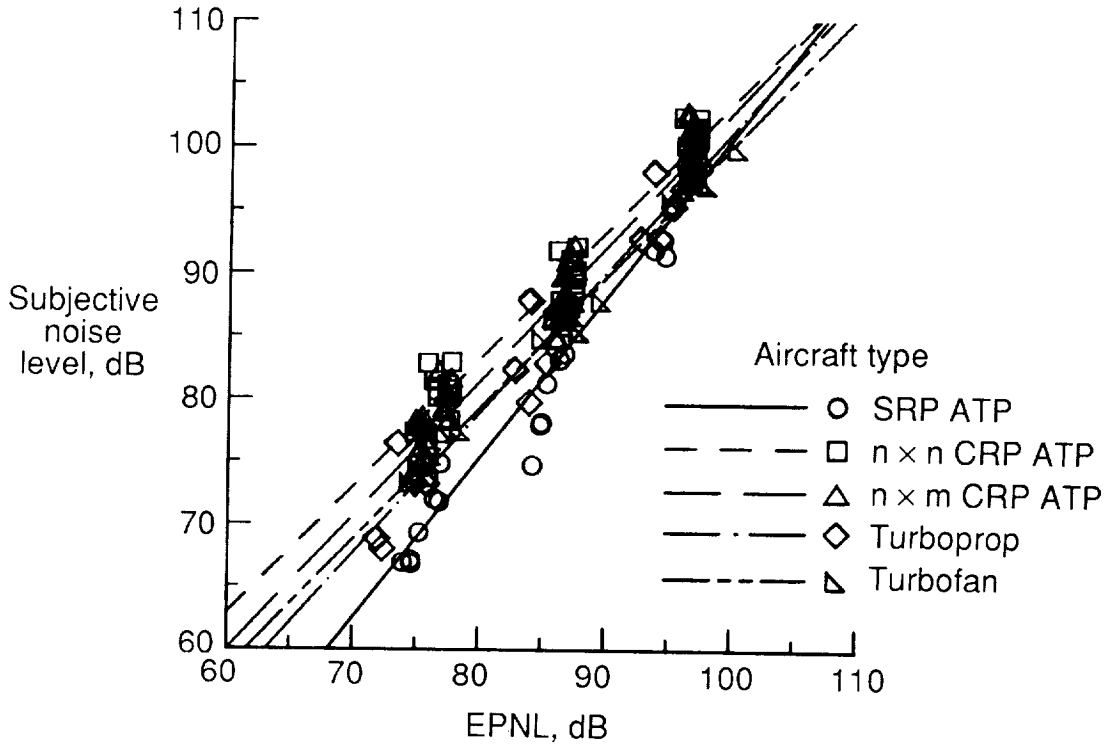

Figure 26. Comparison of annoyance responses using EPNL.

NASA
National Aeronautics and Space Administration

Report Documentation Page

1. Report No.	2. Government Accession No.	3. Recipient's Catalog No.
NASA TP-3104		

4. Title and Subtitle	5. Report Date
Annoyance Caused by Advanced Turboprop Aircraft Flyover Noise *Comparison of Different Propeller Configurations*	October 1991
	6. Performing Organization Code
7. Author(s)	8. Performing Organization Report No.
David A. McCurdy	L-16850
	10. Work Unit No.
9. Performing Organization Name and Address	505-63-51-09
NASA Langley Research Center Hampton, VA 23665-5225	11. Contract or Grant No.
	13. Type of Report and Period Covered
12. Sponsoring Agency Name and Address	Technical Paper
National Aeronautics and Space Administration Washington, DC 20546-0001	14. Sponsoring Agency Code

15. Supplementary Notes

16. Abstract

A laboratory experiment was conducted to compare the annoyance of flyover noise from advanced turboprop aircraft having different propeller configurations with the annoyance of conventional turboprop and turbofan aircraft flyover noise. A computer synthesis system was used to generate 40 realistic, time-varying simulations of advanced turboprop takeoff noise. Of the 40 noises, 8 represented single-rotating propeller configurations, 12 represented counter-rotating propeller configurations with an equal number of blades on each rotor, and 20 represented counter-rotating propeller configurations with an unequal number of blades on each rotor. Sixty-four subjects judged the annoyance of the advanced turboprop takeoffs along with recordings of 10 conventional turboprop and turbofan takeoffs. Each noise was presented at three sound pressure levels to the subjects in an anechoic listening room. Analyses of the judgments found that advanced turboprops with single-rotating propellers were, on average, slightly less annoying than the other aircraft. Fundamental frequency and tone-to-broadband noise ratio affected annoyance response to advanced turboprops but the effects varied with propeller configuration and noise metric. The addition of duration corrections and corrections for tones above 500 Hz to the noise measurement procedures improved annoyance prediction ability.

17. Key Words (Suggested by Author(s))	18. Distribution Statement
Advanced turboprop noise Propfan noise Propeller noise Subjective acoustics Psychoacoustics	Unclassified—Unlimited Subject Category 71

19. Security Classif. (of this report)	20. Security Classif. (of this page)	21. No. of Pages	22. Price
Unclassified	Unclassified	67	A04

NASA-Langley, 1991

NASA FORM 1626 OCT 86

For sale by the National Technical Information Service, Springfield, Virginia 22161-2171

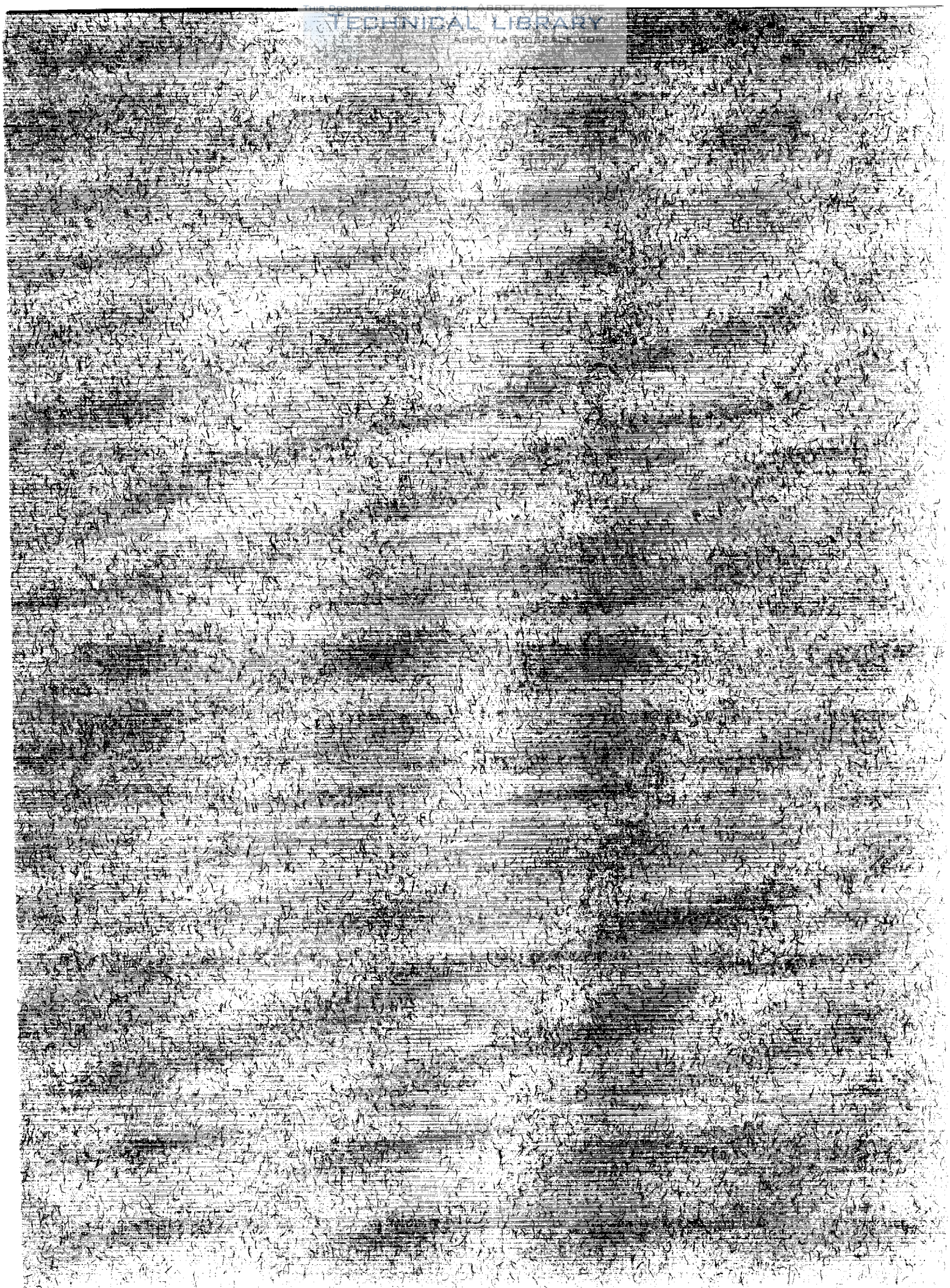

National Aeronautics and
Space Administration
Code NTT-4

Washington, D.C.
20546-0001

Official Business
Penalty for Private Use, $300

BULK RATE
POSTAGE & FEES PAID
NASA
Permit No. G-27

NASA

POSTMASTER: If Undeliverable (Section 158 Postal Manual) Do Not Return